

**QUANTUM CHEMICAL STUDIES OF THE ADDITION OF TRANSITION METAL
OXIDES OF THE TYPE LMO_3 ($L = O^-, Cl^-, NPH_3, CH_3, OCH_3, Cp$) TO ETHYLENE**

**A thesis submitted to the Department of Chemistry, College of Science, Kwame Nkrumah
University of Science and Technology, Kumasi**

in partial fulfillment of the requirements for the degree of

MASTER OF SCIENCE

In Physical Chemistry

By:

Albert Aniagyei, B.Sc. (Hons.)

June, 2012

DECLARATION

I hereby declare that this thesis is my own work towards the M.Sc. and that, to the best of my knowledge and belief, it contain no materials that has been accepted for the award of any other degree in any educational institution nor material previously published or written by another person, except where due reference is made in the text of the thesis.

Albert Aniagyei
.....(Candidate) Signature
Date

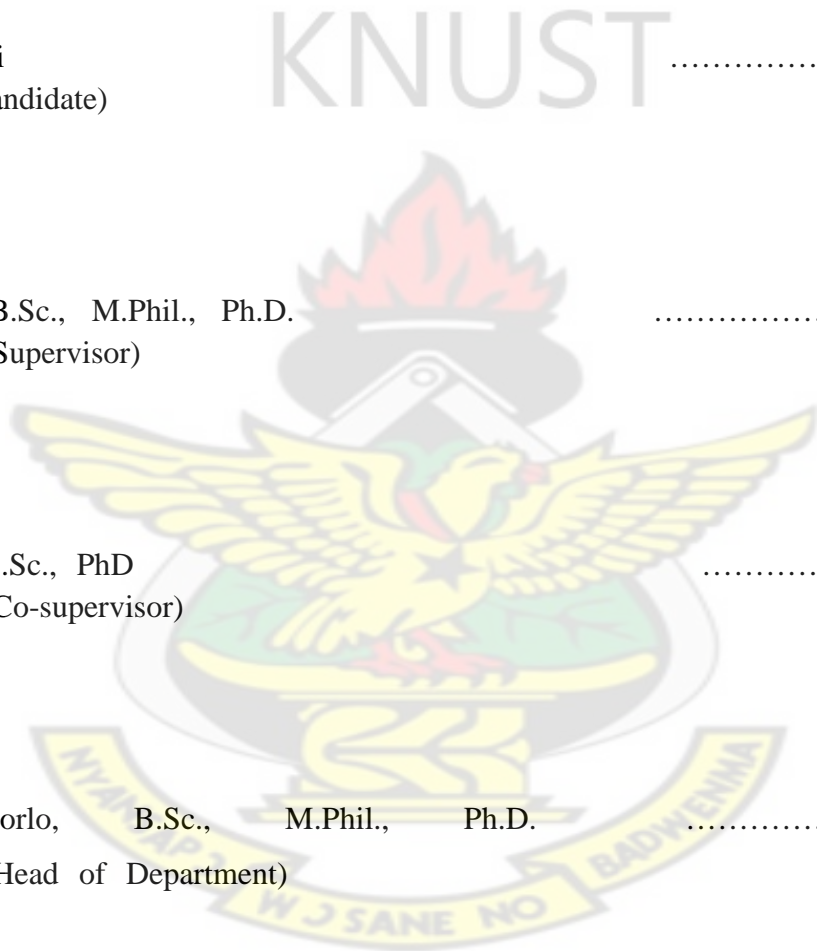
Certified by:

Evans Adei, B.Sc., M.Phil., Ph.D.
.....(Supervisor) Signature
Date

Richard Tia, B.Sc., PhD
.....(Co-supervisor) Signature
Date

And

Ray Voegborlo, B.Sc., M.Phil., Ph.D.
.....(Head of Department) Signature
Date



DEDICATION

This piece of work is dedicated to the entire congregation of Christ Compassion Ministry International and the whole Aniagyei family.



ACKNOWLEDGEMENTS

Firstly, thanks to the Almighty Lord for His Grace, Compassion and Strength He has shown me through my stay on KNUST Campus and for seeing me throughout this period of study and research.

My sincere thanks goes to my supervisors, to Dr. Evans Adei and Dr. Richard Tia for their guidance in my academic pursuits, fatherly and brotherly love and most importantly, training on becoming a critical and good scientist.

Thanks to other members of the lab especially Dr. John. K. Mensah for their constructive criticisms and support during group presentations and seminars, Mrs. Doris Acheampong, my fellow M.Sc. student in the group for helpful suggestion to the project and being a mother especially when the going became tough during the early days in graduate school.

I am very grateful to the National Council for Tertiary Education (NCTE), Ghana, for financial assistance under the Teaching and Learning Innovation Fund (TALIF- KNUST/3/008/2005) to establish a Computational Quantum Chemistry Laboratory at the Department of Chemistry, KNUST, Kumasi, Ghana, where the project was carried out.

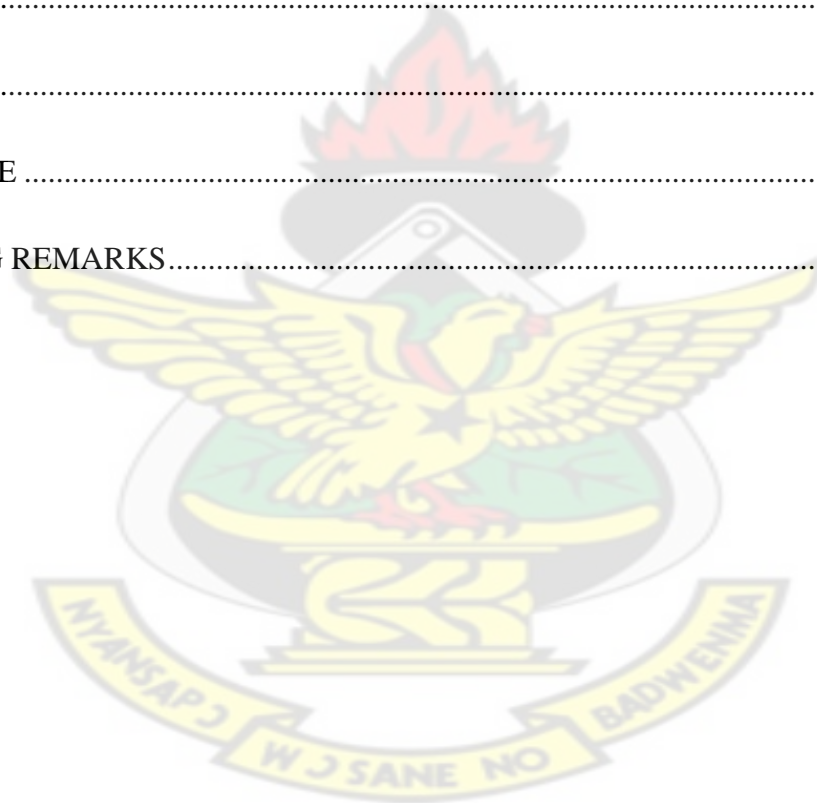
My greatest appreciation goes to my family for their constant support, prayers and love during the entire duration of the programme. I am forever grateful and the Good Lord bless them according to his riches in glory.

TABLE OF CONTENTS

DECLARATION	i
DEDICATION	ii
ACKNOWLEDGEMENTS	iii
TABLE OF CONTENTS	iv
LIST OF FIGURES	Error! Bookmark not defined.
LIST OF SCHEME	x
ABSTRACT	xi
CHAPTER ONE	1
1.1 INTRODUCTION	1
REFERENCES	7
CHAPTER TWO	13
2.1 INTRODUCTION	13
2.2 DETAILS OF CALCULATIONS	16
2.3 RESULTS AND DISCUSSION	18
2.3.1 Reaction of MnO_4^- with ethylene	18
2.3.2 Reaction of MnO_3Cl with ethylene	23
2.3.3 Reaction of $\text{MnO}_3(\text{NPH}_3)$ with ethylene	29

2.3.4 Reaction of $\text{MnO}_3(\text{CH}_3)$ with ethylene	36
2.3.5 Reaction of $\text{MnO}_3(\text{OCH}_3)$ with ethylene	42
2.3.6 Reaction of MnO_3Cp with ethylene	46
2.4 Conclusion	52
REFERENCES	55
CHAPTER THREE	60
3.1 INTRODUCTION	60
3.2 DETAILS OF CALCULATION	64
3.3 Results and Discussion	65
3.3.1 Reaction of TcO_4^- with ethylene	65
3.3.2 Reaction of TcO_3Cl with ethylene	70
3.3.3 Reaction of $\text{TcO}_3(\text{NPH}_3)$ with ethylene	77
3.3.4 Reaction of $\text{TcO}_3(\text{CH}_3)$ with ethylene.....	84
3.3.5 Reaction of $\text{TcO}_3(\text{OCH}_3)$ with ethylene.....	90
3.3.6 Reaction of TcO_3Cp with ethylene	95
REFERENCES	103
CHAPTER FOUR.....	107
4.1 INTRODUCTION	107
4.2 DETAILS OF CALCULATION	111
4.3 RESULTS AND DISCUSSION.....	112

4.3.1 Reaction of ReO_4^- with Ethylene.....	112
4.3.2 Reaction of ReO_3Cl with ethylene	117
4.3.3 Reaction of $\text{ReO}_3(\text{NPH}_3)$ with ethylene.....	125
4.3.4 Reaction of $\text{ReO}_3(\text{CH}_3)$ with ethylene	135
4.3.5 Reaction of $\text{ReO}_3(\text{OCH}_3)$ with ethylene.....	142
4.3.6 Reaction of ReO_3Cp with ethylene	148
4.4 Conclusion	153
REFERENCES	157
CHAPTER FIVE	162
CONCLUDING REMARKS.....	162

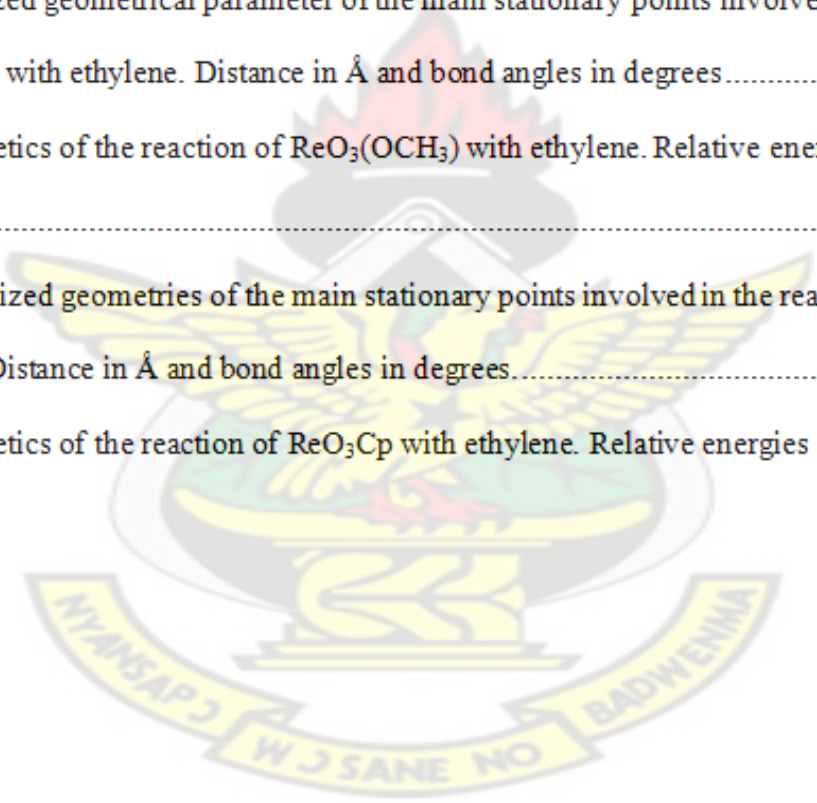


LIST OF FIGURES

Fig 2.1: Optimized geometries of the main stationary points involved in the reaction of MnO_4^- with ethylene. Distance in Å.....	21
Fig 2.2: Energetics of the reaction of MnO_4^- with ethylene. Relative energies in kcal/mol.....	22
Fig 2.3: Optimized geometries of the main stationary points involved in the reaction of MnO_3Cl with ethylene. Distance in Å.....	27
2.4: Energetics of the reaction of MnO_3Cl with ethylene. Relative energies in kcal/mol.....	28
Fig 2.5 Cont'd: Optimized geometrical parameters of the main stationary points involved in the reaction of $\text{MnO}_3(\text{NPH}_3)$ with ethylene. Distance in Å and bond angles in degrees.....	34
Fig 2.6: Energetics of the reaction of $\text{MnO}_3(\text{NPH}_3)$ with ethylene. Relative energies in kcal/m.....	35
Fig 2.7: Optimized geometries of the main stationary points involved in the reaction of $\text{MnO}_3(\text{CH}_3)$ with ethylene. Distance in Å and bond angles in degrees.....	40
Fig 2.8: Energetics of the reaction of $\text{MnO}_3(\text{CH}_3)$ with ethylene. Relative energies in kcal/mol.....	41
Fig 2.9: Optimized geometries of the main stationary points involved in the reaction of $\text{MnO}_3(\text{OCH}_3)$ with ethylene. Distance in Å and bond angles in degrees.....	45
Fig 2.10: Energetics of the reaction of $\text{MnO}_3(\text{OCH}_3)$ with ethylene. Relative energies in kcal/mol.....	46
Fig 2.11: Optimized geometries of the main stationary points involved in the reaction of MnO_3Cp with ethylene. Distance in Å and angles in degrees.....	51
Fig 2.12: Energetics of the reaction of MnO_3Cp with ethylene. Relative energies in kcal/mol.....	52
Figure 3.1: Optimized geometries parameters of the main stationary points involved in the reaction between TcO_4^- and ethylene. Bond distances in Å and angles in degrees.....	69
Figure 3.2: Energetics of the reaction of ReO_4^- and ethylene. Relative energies in kcal/mol.....	70

Figure 3.3: Optimized geometries parameters of the main stationary points involved in the reaction of TcO_3Cl with ethylene. Distance in Å.....	76
Fig 3.4: Energetics of the reaction of TcO_3Cl with ethylene. Relative energies in kcal/mol.....	77
Figure 3.5: Optimized geometrical parameters of the main stationary points involved in the reaction of $TcO_3(NPH_3)$ with ethylene. Distance in Å and angles in degrees	83
Fig 3.6: Energetics of the reaction of $TcO_3(NPH_3)$ with ethylene. Relative energies in kcal/mol.....	84
Fig 3.7: Optimized geometrical parameters of the main stationary points involved in the reaction of $TcO_3(CH_3)$ with ethylene. Distance in Å and angles in degrees.....	89
Fig 3.8: Energetics of the reaction of $TcO_3(CH_3)$ with ethylene. Relative energies in kcal/mol.....	90
Figure 3.9: Optimized geometrical parameter of the main stationary points involved in the reaction of $TcO_3(OCH_3)$ with ethylene. Distance in Å and bond angles in degrees	94
Fig 3.10: Energetics of the reaction of $TcO_3(OCH_3)$ with ethylene. Relative energies in kcal/mol	95
Fig 3.11: Optimized geometries of the main stationary points involved in the reaction of TcO_3Cp with ethylene. Distance in Å and bond angles in degrees.....	99
Fig 3.12: Energetics of the reaction of TcO_3Cp with ethylene. Relative energies in kcal/mol.....	100
Figure 4.1: Optimized geometries parameters of the main stationary points involved in the reaction between ReO_4^- and ethylene. Bond distances in Å and angles in degrees.....	116
Figure 4.2: Energetics of the reaction of ReO_4^- and ethylene. Relative energies in kcal/mol.....	117
Figure 4.3: Optimized geometries parameters of the main stationary points involved in the reaction of ReO_3Cl with ethylene. Distance in Å and bond angles in degrees	124
Fig 4.4: Energetics of the reaction of ReO_3Cl with ethylene. Relative energies in kcal/mol.....	125

Figure 4.5: Optimized geometrical parameters of the main stationary points involved in the reaction of $\text{ReO}_3(\text{NPH}_3)$ with ethylene. Distance in Å and angles in degrees.....	134
Figure 4.6: Energetics of the reaction of $\text{ReO}_3(\text{NPH}_3)$ with ethylene. Relative energies in kcal/mol.....	135
Fig 4.7: Optimized geometrical parameters of the main stationary points involved in the reaction of $\text{ReO}_3(\text{CH}_3)$ with ethylene. Distance in Å and angles in degrees.....	141
Fig 4.8: Energetics of the reaction of $\text{ReO}_3(\text{CH}_3)$ with ethylene. Relative energies in kcal/mol.....	142
Fig 4.9: Optimized geometrical parameter of the main stationary points involved in the reaction of $\text{ReO}_3(\text{OCH}_3)$ with ethylene. Distance in Å and bond angles in degrees.....	147
Fig 4.10: Energetics of the reaction of $\text{ReO}_3(\text{OCH}_3)$ with ethylene. Relative energies in kcal/mol.....	148
Fig 4.11: Optimized geometries of the main stationary points involved in the reaction of ReO_3Cp with ethylene. Distance in Å and bond angles in degrees.....	152
Fig 4.12: Energetics of the reaction of ReO_3Cp with ethylene. Relative energies in kcal/mol..	153



LIST OF SCHEME

Scheme 2.1: Possible pathways for the reaction of LMO_3 ($M=Mn$, $L= O-, Cp, CH_3, OCH_3, NPH_3, Cl$) with ethylene.	17
Scheme 3.1: Proposed pathway for the reaction of LMO_3 with ethylene	63
Scheme 4.1: Proposed pathway for the reaction of LMO_3 ($M=Re$) with ethylene	110

KNUST



ABSTRACT

The oxo complexes of group VII (Mn, Tc, and Re) are of great interest for their potential toward epoxidation and dihydroxylation. In this work, the mechanisms of oxidation of ethylene by the group VII transition metal-oxo complexes of the type LMO_3 ($M = Mn, Tc, Re$ and $L = O^-, Cl, CH_3, OCH_3, Cp$) are explored at the B3LYP/LACVP* level of theory. The activation and reaction energies for the stepwise and concerted addition pathways along spin states other than the singlet which could ultimately lead to exploration of the extent of the two state reactivity was also investigated. In the reaction of $LMnO_3$ ($L = Cp, CH_3$), $LTcO_3$ ($L = O^-, Cl, Cp, OCH_3$) and $LReO_3$ ($L = Cp, O^-$) with ethylene, it was found that the direct [3+2] addition pathway on the doublet potential energy surfaces leading to the formation of the dioxylate intermediate is favored kinetically and thermodynamically over the two-step process via the metallaoxetane intermediate to form the dioxylate. However, in the CH_3TcO_3 system, the formation of the doublet epoxide precursor is kinetically the most favorable pathway. The [2+2] addition pathway leading to the formation of the four membered metallacycle was found to be the kinetically and thermodynamically most viable reaction path for the NPH_3TcO_3 . The formation of the four membered metallacycle intermediate is kinetically and thermodynamically more favorable than the direct [3+2] addition pathway for $LReO_3$ ($L = CH_3, OCH_3, Cl, NPH_3$) on the doublet surface. However, in the $ReO_3(OCH_3)$ system, the reaction occurs on the doublet potential energy surface. The activation energy for the formation of the dioxylate via the metallaoxetane intermediate and the direct [3+2] addition of the ethylene to the oxo-complex were found to be comparable along the doublet potential energy surface. The formation of the epoxide precursor will not result from the reaction of LMO_3 ($M = Mn, Tc, Re, L = O^-, Cp$) with ethylene on all the surfaces studied.

CHAPTER ONE

1.1 INTRODUCTION

Theoretical chemistry can be seen as a bridge from the real physics of the physicists to the real chemistry of the experimental chemists. The term computational chemistry is used when the mathematical method is sufficiently developed that it can be automated for implementation on a computer (Jensen 2007; Helgaker, *et. al.* 2000; Cramer, 2004; Leach, 2001).

Modern research in the chemical sciences seeks not only to make useful molecules and materials, but to understand, design, and control their properties. Theory is at the very center of this effort, providing the framework for an atomic and molecular level description of chemical structure and reactivity that forms the basis for interpreting experimental data and providing guidance toward new experimental directions.

Traditionally, quantum chemistry has been based on the non-relativistic Schrödinger formulation (Schrödinger, 1926) and the Born-Oppenheimer (clamped-nuclei) approximation. One of the central challenges of computational molecular investigation is the solution of the time-independent, non-relativistic Born-Oppenheimer electronic Schrödinger equation. For a system of n electrons and N nuclei with atomic numbers Z_I and interparticle separation r_{ij} and r_{iI} , the eigenvalue equation in atomic units is

predictions while at the same time requiring modest computational resources such that chemically relevant systems can be investigated. Relativistic contributions, which become non-negligible quantitatively and sometimes even qualitatively for heavy elements and thus cannot be neglected for accurate investigations, require an additional computational effort at the all-electron (AE) level. Within effective core potential (ECP) approaches they are included usually by means of a simple parameterization of a suitably chosen valence-only (VO) model Hamiltonian with respect to relativistic AE reference data.

The electronic Schrödinger equation shown above (eq. 1) is still intractable and further approximations are required. The most obvious is to insist that electrons move independently of each other. In practice, individual electrons are confined to functions termed molecular orbitals, each of which is determined by assuming that the electron is moving within an average field of all the other electrons. The total wavefunction is written in the form of a single determinant (a so-called Slater determinant). This means that it is antisymmetric upon interchange of electron coordinates. Methods resulting from solution of the Roothaan-Hall equations are termed Hartree-Fock models (Roothaan, 1959, 1960). The corresponding energy for an infinite (complete) basis set is termed the Hartree-Fock energy.

The term *ab initio* methods (Hehre *et. al*, 1986; Leach, 2001) is also commonly used to describe Hartree-Fock models arising from “non-empirical” attempts to solve the Schrödinger equation (Helgaker, 2000; Szabo and Ostlund, 1989). Hartree-Fock models are well defined and yield unique properties. They are both size consistent and variational. However, the Hartree Fock approximation can only be used if the electronically excited states are clearly higher in energy than the ground state. This is not always the case for transition-metal compounds, because the

energy levels of the occupied and empty s and p valence orbitals of the main group elements (Davidson, 1989, 1991; Salahub and Zerner, 1989).

Semi-empirical models (Dewaret. *al.*, 1977;Thielet. *al.*, 1992; Stewartset. *al.*, 1985; Pople and Beveridge, 1970) follow directly from Hartree-Fock models. In these models, the size of the problem is reduced by restricting treatment to valence electrons only (electrons associated with the core are ignored or frozen). The basis set is restricted to a minimal valence only representation. For main-group elements, this comprises a single s-type function and a set of p-type functions, e.g., 2s, 2px, 2py, 2pz for a first-row element, and for transition metals, a set of d-type functions, an s function and a set of p functions, e.g., 3dx²-y², 3dz², 3dxy, 3dxz, 3dyz, 4s, 4px, 4py, 4pz for first-row transition metals. The only exception to this is the MNDO/d method for second-row (and heavier) main-group elements, used in conjunction with MNDO for hydrogen and first row elements. This incorporates a set of d-type functions, in direct analogy to 3-21G* used in conjunction with 3-21G.

The central approximation, in terms of reducing overall computation, is to insist that atomic orbitals residing on different atomic centers do not overlap. This is referred to as the Neglect of Diatomic Differential Overlap or NDDO approximation. This reduces the number of electron-electron interaction terms from $O(N^4)$ in the Roothaan-Hall equations to $O(N^2)$, where N is the total number of basis functions. Additional approximations are introduced in order to further simplify the overall calculation, and more importantly to provide a framework for the introduction of empirical parameters. With the exception of models for transition metals, parameterizations are based on reproducing a wide variety of experimental data, including equilibrium geometries, heat of formation, dipole moments and ionization potentials. Parameters for PM3 for transition metals (PM3(tm) or PM3(d)) are based only on reproducing equilibrium geometries. The AM1

(Dewar, *et al.*, 1985) and PM3. (Stewart, *et al.*, 1989) models incorporate essentially the same approximations but differ in their parameterization.

One approach to the treatment of electron correlation which is not accounted for in the Hartree-Fock models as a result of treatment of the motions of individual electrons as independent of one another is by employing the density functional theory. Among the varied and ever-expanding approaches to the electronic structure problem, the rise of approximate density functional theory (DFT) as the method of choice for practical calculations (Parr and Yang, 1989; Koch and Holthausen, 2001). The platform for this varied interest were the seminal works of Hohenberg and Kohn, 1964; Kohn and Sham, 1965; Perdew *et al.*, 1996; Becke *et al.*, 1993; Zhao *et al.* (2006): the establishment of the ground-state energy as a functional of the density by the Hohenberg-Kohn theorems (Hohenberg, Kohn, 1964), the Kohn-Sham reformulation of the problem in terms of self-consistent field (SCF) equations with an approximate exchange-correlation (XC) functional (Kohn and Sham, 1965), and the invention of accurate approximations to the XC functional itself (Perdew *et al.*, 1996; Becke *et al.*, 1993; Zhao *et al.* 2006).

A key difference of Kohn-Sham DFT, compared to *ab initio* methods based on the Hartree-Fock (HF) reference wave function, is the favorable scaling with system size that can be obtained with many popular XC functionals. Thus, approximate DFT accounts for much of the dynamical correlation energy absent in HF theory, but at roughly the cost of a HF calculation (Ziegler *et al.*, 1991). This superior balance of accuracy and low computational cost has spurred much of the growth in popularity of approximate DFT over the last 2 decades.

Density functional models have “at their centre” the electron density, $\rho(\mathbf{r})$, as opposed to the many-electron wavefunction, $\Psi(\mathbf{r}_1, \mathbf{r}_2)$. There are both distinct similarities and

differences between traditional wavefunction-based approaches (Hartree-Fock models) and electron-density-based methods. The density functional theory (Hohenberg and Kohn, 1964; Kohn and Sham, 1965) is based on the fact that the sum of the exchange and correlation energies of a uniform electron gas can be calculated exactly knowing only its density. In the Kohn-Sham formalism, the ground-state electronic energy, E , is written as a sum of the kinetic energy, E_T , the electronuclear interaction energy, E_V , the Coulomb energy, E_J , and the exchange/correlation energy, E_{XC} .

$$E = E_T + E_V + E_J + E_{XC} \dots \dots \dots (2)$$

DFT is now consistently applied together with spectroscopic and electrochemical analyses (Schreckenbach *et al.* 1998; Saladino, 2005) and is invoked in the interpretation of novel organic and organometallic reactivity (Lin *et al.* 2010; Leopoldini *et al.* 2007). The favorable accuracy-to-cost ratio of approximate DFT for large systems has made it suitable for quantum chemical studies of bimolecular systems (Siegbahn *et al.*, 2000; Raugei *et al.*, (2006) and has enabled classical molecular dynamics simulations on high dimensional Born-Oppenheimer potential energy surfaces PES (Riley *et al.*, 2007; Tuckerman *et al.*, 2000).

Although, the DFT has many strengths and diverse applications, the traditional functionals are limited by a number of shortcomings which in many cases lead to qualitatively incorrect predictions of chemical structure and reactivity. Traditional functionals suffer to varying degrees from self-interaction error (SIE), which results in false delocalization of the density with semi-local functionals but can also cause the opposite (localization) error in some hybrids (Vydrov *et al.*, 2007; Cohen *et al.*, 2008). These errors are largely responsible for the failures of traditional functionals for such fundamental properties as barrier heights of chemical reactions (Durant *et al.*, 1996), energies and structures of long-range charge-separated states (Wu *et al.*,

2006) and magnetic exchange couplings (Rudra *et. al.*, 2006). Also, non-covalent van der Waals interactions are generally either absent entirely or treated incompletely by traditional functionals, although progress in addressing this problem has been rapid in recent years (Riley *et. al.*, 2010; Lee *et. al.*, 2010; Grimme *et. al.*, 2010; Vydrov *et. al.*, 2010).

Concern over the enantiomeric purity of pharmacologically active compounds has made asymmetric synthesis one of the grand challenges of chemical research. Two outstanding examples are the asymmetric *cis* dihydroxylation of olefins (Hentges and Sharpless, 1980) and the asymmetric epoxidation of olefins (Katsuki *et. al.*, 1980). Both processes utilize high-valent transition-metal complexes as the catalytic agent and chiral ligands to induce asymmetry in the product and can use hydro peroxides as oxidizing agents. Transition metal-oxo complexes such as OsO₄, MnO₄⁻ and ReO₄⁻ have been applied extensively in reactions in which oxygen is inserted into a C-H bond or undergo addition to an olefinic double bond. For the reaction of these metal-oxo complexes with olefinic bonds, the concerted [3+2] addition is proposed, where the C=C π bond of ethylene add across the O=M=O moiety of the oxo- metal complex and *cis*-dihydroxylation of olefins results.

Although the broad mechanistic framework for the addition of metal-oxo complexes is known, most of the key steps remain unresolved. These description of chemical reactivity are, however based on the paradigm of spin conservation, namely the rate determining step(s) proceed on surfaces with uniform spin multiplicity. The participation of more than a single surface in the reaction pathways has been proposed as a key feature in organometallic chemistry. In organometallic gas phase reactions, more than one spin surface connects reactants to products. This can provide low-energy paths for otherwise difficult processes (Shaik *et al.*, 1995; 1998; Buchachenko *et. al.* 2000).

In this work, the mechanism of oxidation of ethylene by the group VII transition metal-oxo complexes of the type LMO_3 ($M = Mn, Tc, Re$ and $L = O^-, Cl, CH_3, OCH_3, Cp$) is explored at the B3LYP/LACVP* level of theory. The oxo complexes of group VII ($Mn, Tc,$ and Re) are of great interest for their propensity toward epoxidation and dihydroxylation. Rhenium (VII) and its congeners have been shown to be highly active oxygen transfer catalysts (Herrmann *et. al*, 1997; Romao *et. al*, 1997). The reaction along spin states other than the singlet which could ultimately lead to exploration of the extent of the two state reactivity is explored in this work. The mechanistic pathways of LMO_3 with ethylene ($M = Mn, Tc, Re$ and $L = O^-, Cl, CH_3, OCH_3, Cp$) have been studied using hybrid density functional theory (DFT). The hybrid density functional theory method was chosen for use throughout the work based on the dual criteria of efficiency and accuracy (Ziegler, 1991; Parr and Yang, 1989; Koch and Holthausen, 2001). Although DFT calculation may underestimate weak interaction such as van der Waals interactions, they generally give better and more reliable description of the geometries and relative energies for transition metal systems than either Hartree-Fock or MP2 methods (Ziegler, 1991; Parr and Yang, 1989; Koch and Holthausen, 2001). Hybrid and gradient-corrected DFT methods often outperforms MP2 while using less computer time. There are also no difficulties for DFT with the calculation of organometallic and inorganic systems.

In chapter 2-4, the mechanisms of oxidation of LMO_3 with ethylene are studied theoretically by exploring the most favorable reaction routes of these complexes in an attempt to provide insight into the class of oxidation reaction. Chapter 5 draws conclusions and make recommendations for further work on the reaction of LMO_3 with ethylene.

REFERENCES

- Becke, A. D. (1993) Density-functional Thermochemistry. III. The role of exact exchange. *J. Chem. Phys.* 98:5648.
- Buchachenko, A. L. (2000) Recent advances in spin chemistry. *Pure Appl. Chem.* 20: 2243-2258.
- Cohen, A. J.; Mori-Sanchez, P.; Yang, W. (2008) Insights into current limitations of density functional theory. *Science*.321: 792.
- Cramer, C. J. (2004) Essential of Computational Chemistry. Theories and Models, 2nd ed.; John Wiley and Sons, Ltd., Chichester.
- Davidson, E. R.(1989) The Challenge of d and f electrons; Salahub, D. R and Zerner, M. C.(eds.) *ACS Symposium*, Washington, D. C.,157.
- Dewar, M. J. S.; Thiel, W. J. (1977) Ground States of Molecules, 38.The MNDO Method.Approximations and Parameters.*J. Am. Chem. Soc.*99: 4899-4907.
- Dewar, M. J. S.; Zoebisch, E. G.; Healy, E. F.; Stewart, J. J. P. (1985) AM1: A New General Purpose Quantum Mechanical Model. *J. Am. Chem. Soc.* 107:3902-3909.
- Dirac, P. A. M. (1929) Quantum Mechanics of Many-Electrons System. *Proc. Roy. Soc. (London)* 123: 714-733.
- Durant, J. L. (1996) Evaluation of transition state properties by density functional theory. *Chem. Phys. Lett.* 256: 595.
- Grimme, S.; Antony, J.; Ehrlich, S.; Krieg, H. (2010) A consistent and accurate *ab initio*parameterization of density functional dispersion correction (DFT-D) for the 94 elements H-Pu.*J. Chem. Phys.* 132:154104.

Hehre, W. J.; Radom, L.; Schleyer, P. V. R.; Pople, J. A. (1986) *ab Initio* Molecular Orbital Theory, Wiley, New York.

Helgaker, T.; Jorgensen, P.; Olsen, J. (2000) *Molecular Electronic-Structure Theory*; John Wiley and Sons, Ltd., Chichester.

Hentges, S. G.; Sharpless, K. B. (1980) Asymmetric induction in the reaction of osmium tetroxide with olefins. *J. Am. Chem. Soc.* 102, 4263.

Herrmann, W. A.; Kuhn, F. E. (1997) Organorhenium Oxides. *Acc. Chem. Res.* 30, 169-180.

Hohenberg, P.; Kohn, W. (1964) Inhomogeneous Electron Gas. *Phys. Rev.* 136: B864–B871.

Jensen, F. (2007) *Introduction to Computational Chemistry*, 2nd ed.; John Wiley and Sons, Ltd., Chichester.

Katsuki, T.; Sharpless, K. B. (1980) The first practical method for asymmetric epoxidation. *J. Am. Chem. Soc.* 102, 5974.

Koch, W.; Holthausen, M. C. (2001) *A Chemist's Guide to Density Functional Theory*; Wiley-VCH: Weinheim.

Kohn, W.; Sham, L. J. (1965) Self-Consistent Equations Including Exchange and Correlation Effects. *Phys. Rev.* 140: A1133–A1138.

Leach, A. R. (2001) *Molecular Modelling. Principle and Applications*, 2nd ed.; Prentice Hall, Harlow, England.

Lee, K.; Murray, E. D.; Kong, L. Z.; Lundqvist, B. I.; Langreth, D. C. (2010) Higher-accuracy Van der Waals density functional. *Phys. Rev. B.* 82:081101.

Leopoldini, M.; Marino, T.; Michelini, M.; Rivalta, I.; Russo, N.; Sicilia, E.; Toscano, M. (2007) Imido Complexes: Synthesis, Structures, and Applications. *Chem. Rev.* 97, 3197-3246
Theor. Chim. Acta. 117, 765.

- Lewis, G. N. (1993) The Chemical Bond. *J. Chem. Phys.* 1:17.
- Lin, Z. (2010) Interplay between Theory and Experiment: Computational Organometallic and Transition Metal Chemistry. *Acc. Chem. Res.* 43, 602–611.
- Parr, R. G.; Yang, W. (1989) Density-Functional Theory of Atoms and Molecules; Oxford University Press: New York.
- Perdew, J. P.; Burke, K.; Ernzerhof, M. (1996) The extended Perdew-Burke-Ernzerhof functional with improved accuracy for thermodynamic and electronic properties of molecular systems. *Phys. Rev. Lett.* 77: 3865.
- Pople, J. A.; Beveridge, D.A (1970) Approximate Molecular Orbital Theory; McGraw-Hill, New York.
- Pyykkö, P. (1978) Relativistic Theory of Atoms and Molecule. *Adv. Quantum Chem.* 11: 353.
- Pyykkö, P. (1988) Relativistic effects in Structural Chemistry. *Chem. Rev.* 88: 563-594.
- Raugei, S.; Gervasio, F. L.; Carloni, P. (2006) DFT modeling of biological systems. *Physica Status Solidi B-Basic Solid State Physics.* 243:2500-2515.
- Riley, K. E.; Op't Holt, B. T.; Merz, K. M., Jr. (2007) Theoretical and Experimental Analysis of Atomic and Molecular Properties. *J. Chem. Theory Comput.* 3, 407- 433.
- Riley, K. E.; Pitonak, M.; Jurecka, P.; Hobza, P. (2010) Stabilization and Structure Calculations for Noncovalent Interactions in Extended Molecular Systems Based on Wave Function and Density Functional Theories. *Chem. Rev.* 110: 5023-5063.
- Romao, C. C.; Kuhn, F. E.; Herrmann, W. A. (1997) Rhenium(VII) Oxo and
- Roothaan, C. C. J. (1951) New Developments in Molecular Orbital Theory. *Rev. Mod. Phys.* 23:69-89

Roothaan, C. C. J. (1960) Self-Consistent Field Theory of Open Shell for Electronic Systems. *Rev. Mod. Phys.* 32: 179-185.

Rudra, I.; Wu, Q.; Van Voorhis, T. (2006) Accurate magnetic exchange couplings in transition-metal complexes from constrained density-functional theory. *J. Chem. Phys.* 124:024103.

Saladino, A. C.; Larsen, S. C. (2005) DFT Calculations of EPR Parameters of Transition Metal Complexes: Implications for Catalysis. *Catal. Today* 105: 122.

Schreckenbach, G.; Ziegler, T. (1998) Prediction of electron paramagnetic resonance g values using coupled perturbed Hartree-Fock and Kohn-Sham theory. *Theor.Chim. Acta* 99:71.

Schrödinger, E. (1926) Quantisierung als Eigenwertproblem (Erste Mitteilung). *Ann. Phys.* 79:361- 376.

Shaik, S.; Danovich, D.; Fiedler, A.; Schwarz, H. (1995) Two-state reactivity in organometallic gas-phase ion chemistry. *Helv.Chim.Acta.*78, 1393.

Shaik, S.; Filatov, M.; Schroder, D.; Schwarz, H. (1998) Electronic structure makes a difference: Cytochrome P-450 mediated hydroxylation of hydrocarbons as a two-state reactivity paradigm. *Chem. Euro. J.* 4, 193.

Siegbahn, P. E. M.; Blomberg, M. R. A. (2000) Transition-Metal Systems in Biochemistry Studied by High-Accuracy Quantum Chemical Methods. *Chem. Rev.* 100: 421- 438.

Stewart, J. J. P. (1989) Optimization of Parameters for Semi-Empirical Methods I-Method. *J. Comp. Chem.* 10: 209-220.

Szabo, A.; Ostlund, N. S. (1989) Modern Quantum Chemistry. Introduction to Advance Electronic Structure Theory; McGraw- Hill, New York.

Thiel, W.; Voityuk, A. (1992) Extension of the MNDO Formalism to d orbitals: Integral Approximations and Preliminary Numerical Results. *Theor.Chim.Acta*.81:391-404.

Thiel, W.; Voityuk, A. (1992) Extension of the MNDO formalism to *d* orbitals: Integral approximations and preliminary numerical results.*Int. J. Quantum Chem*.44: 807.

Tuckerman, M. E.; Martyna, G. J. (2000) non-Hamiltonian Systems.*J. Phys. Chem. B*. 104: 159.

Vydrov, O. A.; Scuseria, G. E.; Perdew, J. P. (2007) Tests of functionals for systems with fractional electron number. *J. Chem. Phys.* 126:154109.

Vydrov, O. A.; Van Voorhis, T. (2010) Nonlocal van der Waals density functional: The simpler the better. *J. Chem. Phys.* 133: 244103.

Wu, Q.; Van Voorhis, T. (2006) Direct calculation of electron transfer parameters through constrained density functional theory. *J. Phys. Chem. A*. 110, 9212 - 9218.

Zhao, Y.; Schultz, N. E.; Truhlar, D. G. (2006) The M06 suite of density functionals for main group Thermochemistry, thermochemical kinetics, noncovalent interactions, excited states, and transition elements: two new functionals and systematic testing of four M06-class functionals and 12 other functionals. *J. Chem. Theory Comput*.2: 364.

Ziegler, T. (1991) Approximate density functional theory as a practical tool in molecular energetics and dynamics. *Chem. Rev.* 91, 651–667.

CHAPTER TWO

[3+2] VERSUS [2+2] ADDITION OF METAL OXIDES ACROSS C=C BONDS: A THEORETICAL STUDY OF THE MECHANISM OF OXIDATION OF ETHYLENE BY MANGANESE OXIDE COMPLEXES.

2.1 INTRODUCTION

Transition metal-oxo compounds and oxo-halides such as CrO_2Cl_2 , OsO_4 , MnO_4^- , ReO_4^- and RuO_4^- are applied extensively in reaction in which oxygen is inserted into C-H bonds or undergoes addition to an olefinic double bond. The application of such reagents in chemical synthesis has spurred considerable interest in the underlying activation mechanism (Enemark and Young, 1993; Sharpless *et. al.*, 1975; Mijs and de Jonge, 1986; Sono *et. al.*, 1996).

Some transition metal-oxo complexes such as CrO_2Cl_2 react with olefins to form epoxides, chlorohydrins and vicinal dihalides (Jorgensen, 1989; San Filippo *et. al.*, 1977) whereas others such as MnO_4^- and OsO_4^- react to form diols without significant epoxide formation (Schröder, 1980; Wiberg, 1965). Many experimental and theoretical investigations have focused on mechanistic aspects of this type of reaction. Olefin dihydroxylation catalyzed by transition metal oxo species of the type LMO_3 has been the subject of extensive theoretical studies ((Dapprich *et. al.*, 1996; Pidun *et. al.*, 1996; Torrent *et. al.*, 1997; Del Monte *et. al.*, 1997; Nelson *et. al.*, 1997; Corey *et. al.*, 1996; Haller *et. al.*, 1997; Houk *et. al.*, 1999; Torrent *et. al.*, 1998). The mechanism of the oxidation of alkenes by permanganate is believed to be related to the oxidation of alkenes by OsO_4 , even though the reaction rates are influenced differently by donor and acceptor olefins on going from OsO_4 to MnO_4^- due to charge differences (Waters *et. al.*, 1958).

The proposal that, in the initial step of the dihydroxylation reaction catalyzed by transition metal oxo compound MnO_4^- , the olefin reacts directly with a $\text{O}=\text{Mn}=\text{O}$ functionality of MnO_4^- in a [2+3] manner to form a metalladioxolane, a five-membered metallacycle (Criegee *et. al.*, 1936; 1942) (structure **2** in Scheme 2.1) was generally favored, until a suggestion was made for a stepwise mechanism involving a metallaoxetane intermediate in the chromyl chloride oxidation by (Sharpless *et. al.*, 1977). However, the intermediacy of a metallaoxetane (structure **4** in Scheme 2.1) arising from the [2+2] addition pathway as suggested by Sharpless (Sharpless *et. al.*, 1977) for chromyl chloride oxidation was ruled out, at least for MnO_4^- , by density functional theory (DFT) calculations (Houk *et. al.*, 1999) and corroborated by experimental kinetic isotope effects studies (Del Monte *et. al.*, 1997; Rouhi *et. al.*, 1997).

For tetramethylethylene (TME) addition to MnO_3Cl , Limberg and Wistuba (2001) reported the [3+2] addition of TME to the MnO_2 moiety of MnO_3Cl to be thermodynamically favored over the direct [2+1] addition (epoxidation) product while the kinetic barriers for both reactions are of comparable height at the B3LYP LANL2DZ/6-311G(d). However, in an experimental investigation of the TME/ MnO_3Cl by means of matrix-isolation techniques, selective formation of the epoxidation product $[\text{ClO}_2\text{MnO}[\text{C}(\text{CH}_3)_2]_2$ was observed. Limberg and Wistuba (2001) did not find a minimum corresponding to the geometry of singlet or triplet metallaoxetane arising from the [2+2] addition pathway.

Strassner and Busold (2004) found that the activation barrier for the [3+2] addition pathway to be lower than the [2+2] addition pathway for permanganate oxidation of substituted alkynes although the lowest lying identified state is a reactive triplet intermediate.

Theoretical calculations focusing on the [3+2] addition pathway was explored for the transition metal-oxo complex of the type CH_3MnO_3 with ethylene by Gisdakis and Rösch (2001).

They found the activation barrier and reaction energy along the [3+2] route to be lower than the corresponding [2+2] addition pathway employing the hybrid B3LYP approach, with effective core potentials and double-zetabasis sets, LanL2DZ, for the transition metal and 6-311G(d,p) basis sets for H, C, O, and F.

Strassner and Busold, (2001) reported density functional calculation at B3LYP/6-31G(d) to strongly favor the [3+2] against the [2+2] addition pathway that proceed through a metallaoxetane intermediate for permanganate oxidation of substituted alkenes. The activation barriers associated with the [2+2] addition pathway are very high (61.5 - 67.3 kcal/mol). The metallaoxetane intermediates are calculated to be endothermic with reaction energies of (+24.7-33.6 kcal/mol). The endothermic formation of the metallaoxetane product via the [2+2] transition state that is on the average 40 kcal/mol higher in energy is not competitive with the [3+2] addition pathway which has a lower activation barrier (10.8 – 14.7 kcal/mol) which leads to a exothermic products.

In this work, the calculated potential energy surfaces for the [3 + 2] and [2 + 2] addition of LMnO_3 (L = O-, Cl, Cp, CH_3 , OCH_3 , NPH_3) to ethylene and for the interconversion of the metallaoxetane to the dioxylates is explored by employing a hybrid density functional theory at the B3LYP/LACVP* level of theory. Also, the mechanistic pathways to the formation of the epoxide precursor are explored for the reaction of LMnO_3 with ethylene. The singlet, doublet, triplet and quartet electronic states of each species are explored where possible.

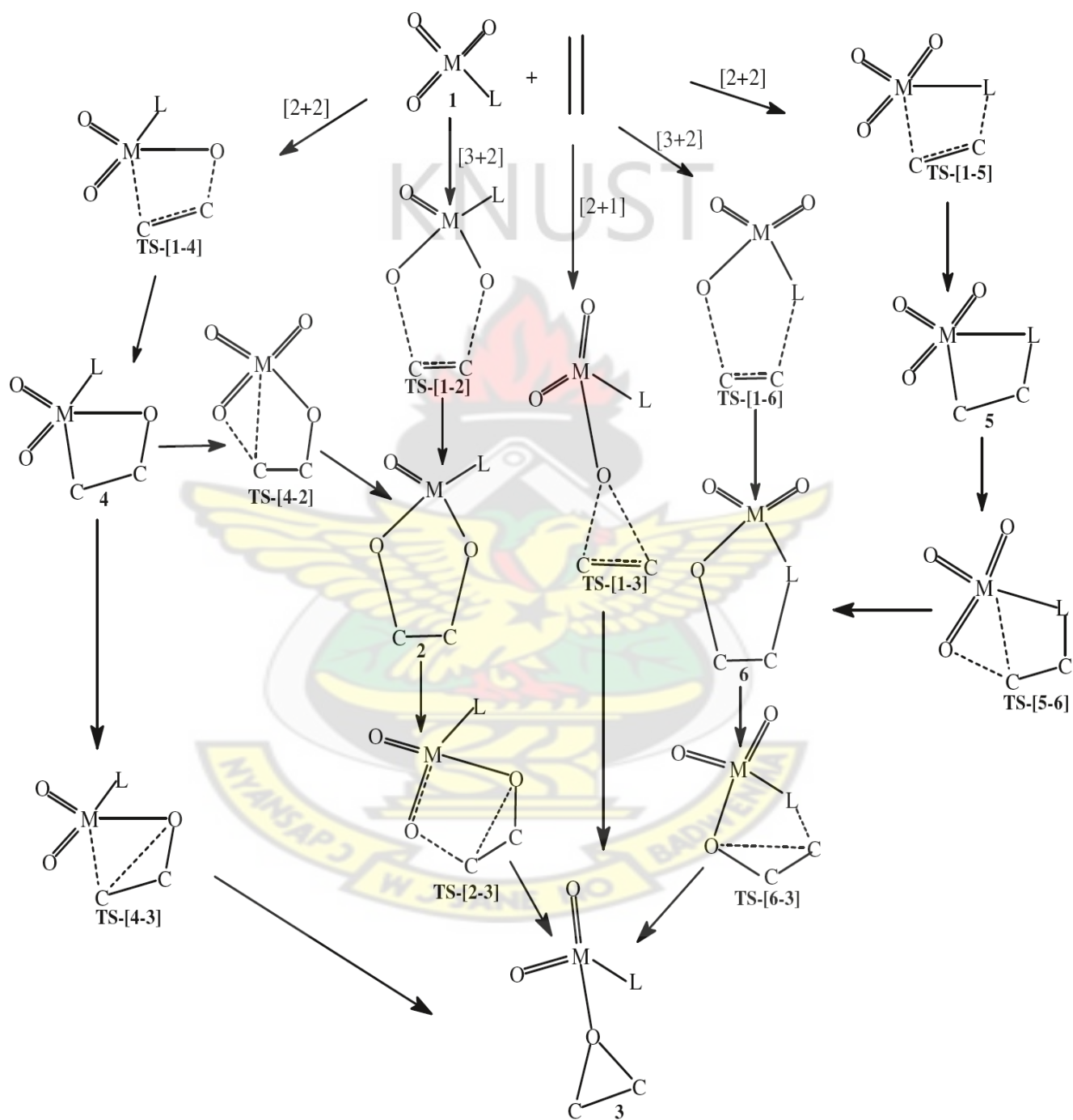
2.2 DETAILS OF CALCULATIONS

All calculation were carried out with Spartan'08 V1.2.0 and Spartan '10 V1.1.0 Molecular Modeling programs (Wavefunction, 2008; 2010) at the DFT B3LYP/LACVP* level of theory. The B3LYP functional is a Hartree-Fock DFT hybrid functional. The LACVP* basis set is a relativistic effective core –potential that describes the atoms H-Ar with the 6-31G* basis while heavier atoms are modeled with the LANL2DZ basis set which uses the all-electron valence double zeta basis set (D95V), developed by Dunning, for first row elements (Dunning and Hay, 1976) and the Alamos ECP plus double zeta basis set developed by Wadt and Hay for the atoms Na-La, Hf-Bi (Hay and Wadt, 1985a; 1985b; Wadt and Hay, 1985).

The starting geometries of the molecular systems were constructed using Spartan's graphical model builder and minimized interactively using the sybyl force field (Clark's *et. al.*, 1989). All geometries were fully optimized without any symmetry constraints. A normal mode analysis was performed to verify the nature of the stationery point. Equilibrium geometries were characterized by the absence of imaginary frequencies.

The transition state structures were located by a series of constrained geometry optimization in which the forming-and breaking–bonds are fixed at various lengths whiles the remaining internal coordinates were optimized. The approximate stationary points located from such a procedure were then fully optimized using the standard transition state optimization procedure in Spartan. All first–order saddle- point were shown to have a Hessian matrix with a single negative eigenvalue, characterized by an imaginary vibrational frequency along the reaction coordinate. All computations were performed on Dell precision T3400 Workstation computer

Scheme 2.1: Possible pathways for the reaction of LMO_3 ($\text{M}=\text{Mn}$, $\text{L}=\text{O}^-$, Cp , CH_3 , OCH_3 , NPH_3 , Cl) with ethylene.



2.3 RESULTS AND DISCUSSION

2.3.1 Reaction of MnO_4^- with ethylene

The optimized geometries and relative energies of the main stationary points involved in the reaction between MnO_4^- and ethylene are shown in Fig.2.1 and Fig.2.2 respectively. The density functional theory (DFT) geometry optimization of MnO_4^- (**A1/s**) on a singlet potential energy surface (PES) has all the Mn-O bonds at 1.60 Å. The computed bond lengths are in agreement with experimentally determined X-ray data on permanganate (Palenik *et al.* 1967).

A triplet permanganate reactant (**A1/t**) has been computed to be 22.41 kcal/mol less stable in relation to the singlet structure. A doublet and quartet reactant **A1/d** and **A1/q** have been computed to be 105.14 and 128.32 kcal/mol less stable than the singlet reactant **A1/s**. Thus the singlet reactant is the most stable.

The [3+2] addition of the $\text{C}=\text{C}\pi$ bond of ethylene across the $\text{O}=\text{Mn}=\text{O}$ bonds through a singlet transition state **TS-[A1-A2]/s** to form dioxomangana-2,5-dioxolane **A2/s** has an activation barrier of 9.14 kcal/mol and exothermicity of 47.60 kcal/mol, in agreement with the works of Houk *et. al.*, (1999) computed the barrier for this route to be 9.20 kcal/mol and exothermicity of 47.20 kcal/mol. The calculated transition state structures in this work are highly symmetrical and synchronous with respect to the newly forming C-O bonds (2.06 Å) of the cyclic ester intermediate and are comparable with results by Houk *et. al.*(1999).

The transition state structure for the [3+2] addition of the $\text{C}=\text{C}$ bond of ethylene across $\text{O}=\text{Mn}=\text{O}$ bonds to form the five-membered cyclic ester intermediate could not be located on the triplet PES. However, a triplet product **A2/t** was located and found to be 2.06 kcal/mol more stable than the singlet dioxylate **A2/s** and 2 kcal/mol more stable than the dioxylate computed by

Houk *et al.*, (1999). In the singlet product, the two Mn=O bonds to the 'spectator' oxygen atoms (the oxygen atom which is not part of the ring) are equal (1.58 Å) and those to the oxygen atom involved in the ring are also equal (1.83 Å), which agrees with the results of Houk *et al.*, (1999) who found the two Mn=O bonds to the 'spectator' oxygen atoms (the oxygen atom which is not part of the ring) are equal (1.58 Å) and those to the oxygen atom involved in the ring are also equal (1.83 Å). The triplet product, has the two Mn=O bonds to the 'spectator' oxygen atoms (the oxygen atom not part of the ring) equal (1.61 Å) and those to the oxygen atom involved in the ring are also equal (1.84 Å); 0.01 Å less in the singlet structure (**fig2.1**) and the dioxylate structure computed by Houk *et al.*, (1999). The quartet dioxylate species **A2/q** has reaction energy of -93.35 kcal/mol. No doublet dioxylate product could be located on the reaction surface. No [3+2] transition state connecting the reactants to the products was located on the quartet surface.

In a related work on the osmium tetroxide reaction with ethylene, Tia and Adei, (2011) found the activation barrier for the [3+2] addition to form the osmadioxylate ester intermediate to be very low (3.97 kcal/mol). Earlier works of Frenking *et al.*, (1996), Ziegler *et al.*, (1997), Morokuma *et al.*, (1996) made similar findings. The calculated barrier for the [3+2] addition of the C=C bond of ethylene across the O=Os=O bonds of OsO₄ is much lower than the barrier calculated for the MnO₄⁻ (9.14 kcal/mol) in this work, an analogous reaction of isoelectronic OsO₄ in this work.

The formation of the singlet manganooxetane **A3/s** by [2+2] addition of the C=C bond of ethylene across M=O bond of the permanganate complex **A1** is 18.45 kcal/mol endothermic, in agreement with the reported value by work of Houk *et al.*, (1999).

A triplet metallaoxetane **A3/t** was located and found to be 7.12 kcal/mol less stable than the singlet **A3/s**. The Mn-O and C-O bond lengths of 2.01 and 1.39 Å in the singlet metallaoxetane **A3/s** are in agreement with the Mn-O and C-O bond lengths reported by Houk *et. al.*, (1999).

In the triplet metallaoxetane **A3/t**, the Mn-O bond is 0.13 Å shorter than in **A3/s**. However, the C-O bond is 0.07 Å longer in the triplet metallaoxetane. The doublet **A3/d** and quartet **A3/q** metallaoxetane species have reaction energies of -16.92 and -31.42 kcal/mol respectively.

The re-arrangement of the manganooxetane to the dioxylate (**TS-[4-2]** in Scheme 2.1) as suggested by Sharpless *et. al.* (1977) for the chromyl chloride oxidation of olefins was also explored for the reaction of permanganate with ethylene. The activation barrier for the re-arrangement of the singlet manganooxetane to the dioxylate through transition state **TS-[A3-A2]/s** is +46.59 kcal/mol. No transition state was located for the re-arrangement of the triplet manganooxetane to the dioxylate. Thus, the overall activation barrier for the re-arrangement of the singlet manganooxetane to the dioxylate is 26.33 kcal/mol, which is higher than the activation barrier for the direct [3+2] addition of ethylene across the two oxygen atoms of singlet MnO_4^- .

The potential energy surface of the reaction of permanganate with ethylene was further explored in an attempt to locate an epoxide precursor ($\text{O}_3\text{-Mn-OC}_2\text{H}_4$) (**3** in Scheme 4.1), but no such minimum was found on the reaction surface.

From the work of Ziegler *et al.*(1999), Tia and Adei (2010) and the epoxide precursor could arise from three pathways:

- a) A two-step process involving the formation of a metallaoxetane, followed by re-arrangement.

- b) A two-step process involving the formation of the five membered metallacycle, followed by re-arrangement.
- c) A direct one-step addition of the C=C bond across one oxygen atom of MnO_4^- .

In addition, attempts were made to find a transition state for the formation of an epoxide precursor from re-arrangement of the four-membered metallaoxetane (**TS [4-3]** in Scheme 4.1) and five-membered metallacycle (**TS[2-3]** in Scheme 4.1) or from direct addition of the C=C bond of ethylene to one oxygen atom of MnO_4^- (**TS[1-3]** in Scheme 4.1). All these are indication that the reaction of permanganate with ethylene does not lead to the formation of an epoxide precursor.

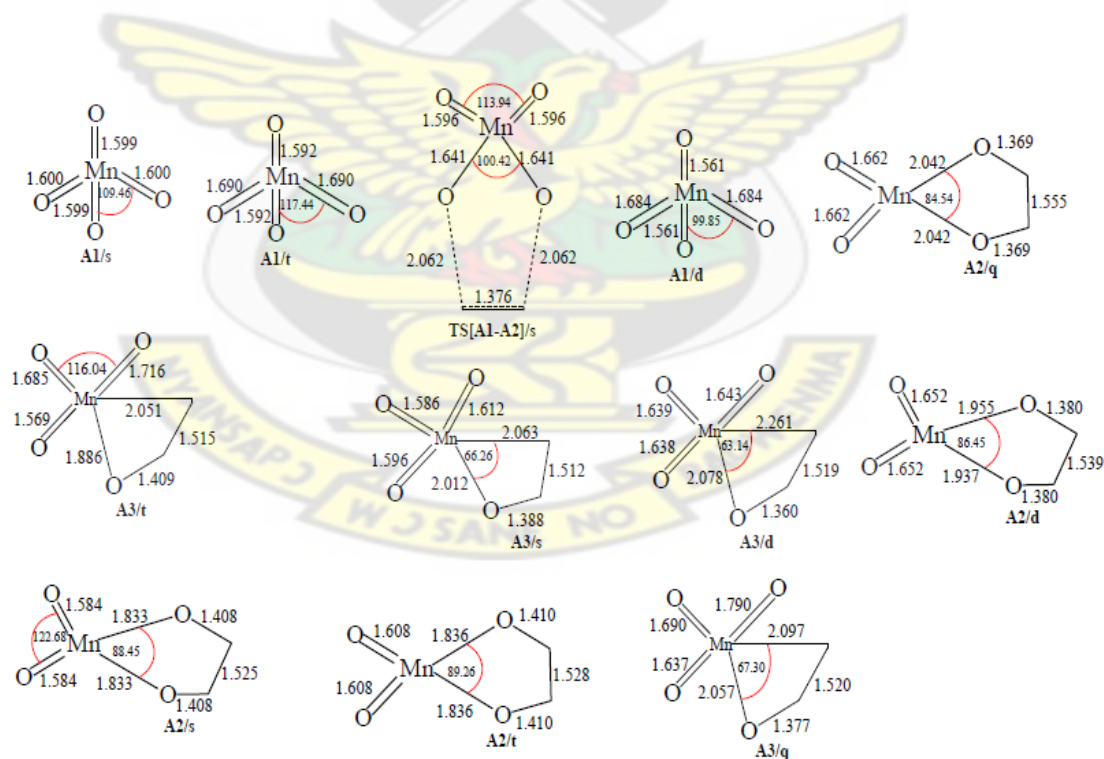


Fig 2.1: Optimized geometrical parameters of the main stationary points involved in the reaction of MnO_4^- with ethylene. Distance in Å and bond angles in degrees.

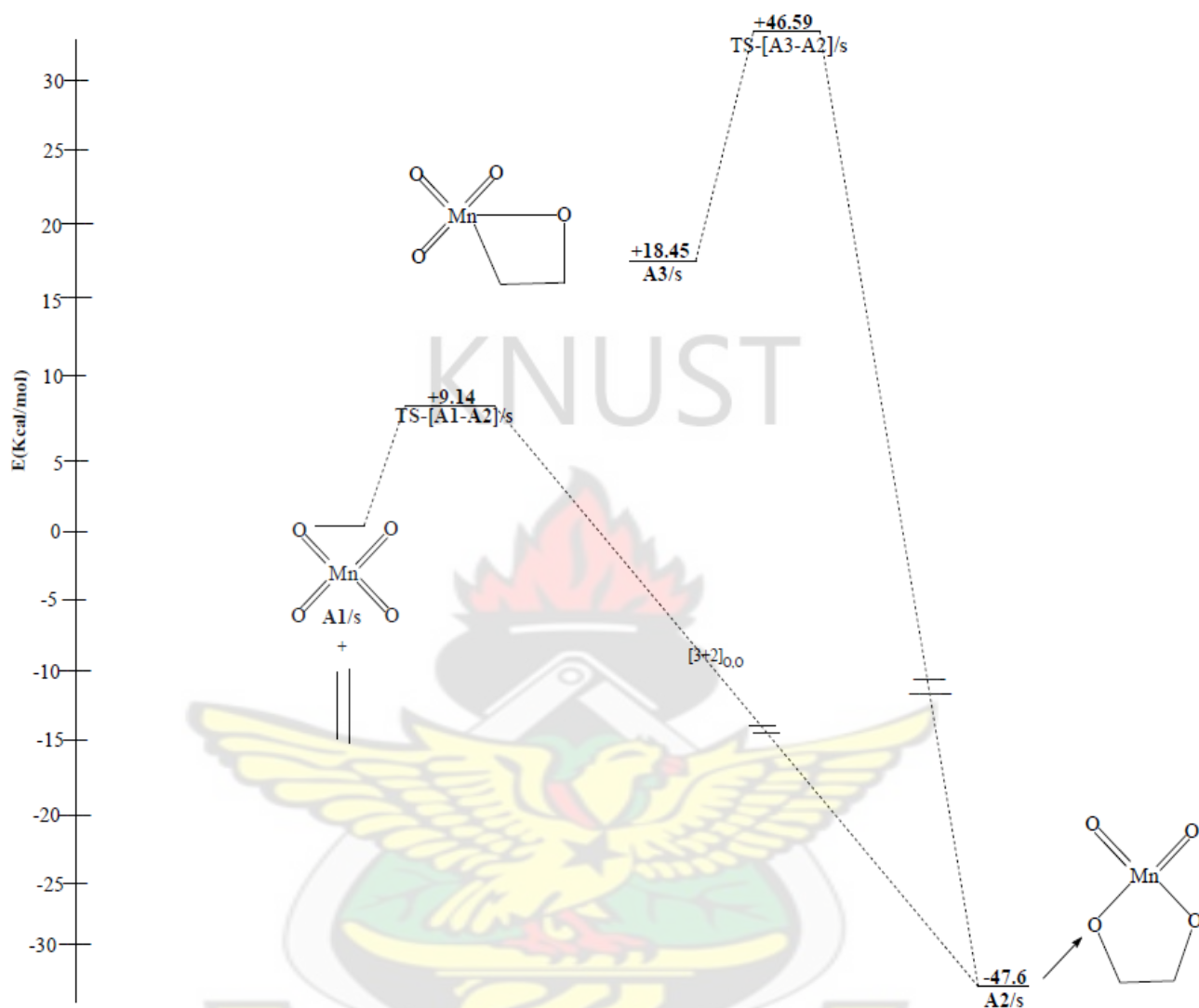


Fig 2.2: Energetics of the reaction of MnO_4^- with ethylene. Relative energies in kcal/mol

2.3.2 Reaction of MnO₃Cl with ethylene

Figures 2.3 and 2.4 show respectively the optimized geometries and relative energies of the main stationary points involved in the reaction between MnO₃Cl and ethylene. The DFT geometry optimization of MnO₃Cl on a singlet potential energy surface (PES) yielded two minima: **R1-A4** of C_{3v} symmetry in which the three Mn=O double bonds are each 1.56 Å long and the Mn-Cl is 2.13 Å long. The other minimum is **R2-A4** of C_s symmetry in which the Mn-Cl bond is broken and the chloro is bonded to one of the oxo ligands.

The singlet **R1-A4** has been computed to be 36.63 kcal/mol more stable in relation to **R2-A4**. A doublet reactant **R1-A4/d** has been computed and found to be 85.09 kcal/mol more stable in relation to the singlet reactant **R1-A4** and 109.49 kcal/mol more stable in relation to the triplet reactant **R1-A4/t**. In the doublet reactant **R1-A4/d**, the Mn-Cl bonds are 0.10 Å longer than those in the singlet structure **R1-A4** and in the triplet structure **R1-A4/t**.

A quartet reactant **A4/q** has been computed to be 17.83 kcal/mol less stable than the doublet. With respect to the singlet reactant **R1-A4** and triplet reactants **R1-A4/t**, the quartet reactant is 67.27 and 91.67 kcal/mol more stable.

On the doublet surface, the [3+2] addition of C=C π bond of ethylene across the O=Mn=O bonds of doublet MnO₃Cl was found to either follow the concerted or stepwise addition pathways. On the concerted pathway, the activation barrier for the formation of the dioxylate species **A5/d** is 8.91 kcal/mol. The dioxylate species **A5/d** has exothermicity of 44.18 kcal/mol.

Along the stepwise pathway, one of the C=C π bonds of ethylene attacks an oxo-ligand of MnO₃Cl to form the organometallic intermediate **X/d**. The activation barrier for the formation of the intermediate **X/d** is +15.69 kcal/mol. The intermediate has exothermicity of 0.64 kcal/mol.

The intermediate can then re-arrange through transition state **TS-[X-A5]/d** to form the dioxylate **A5/d** with activation barrier of +0.72 kcal/mol.

No [3+2] transition state connecting the reactants to the products could be located on the triplet surface. The triplet dioxylate product **A5/t** is 96.58 kcal/mol exothermic. A quartet species **A5/q** has been computed to be 28.04 kcal/mol stable than the doublet product **A5/d**.

The activation barrier for the direct [3+2] addition of C=C bond of ethylene across the O=Mn=O bonds of singlet MnO₃Cl through the singlet transition state **TS-[A4-A5]/s** has an activation barrier of -3.44 kcal/mol and reaction energy of -59.74 kcal/mol in agreement with a related work of Boehme *et. al.*, (1999) who reported the activation barrier for the singlet [3+2] ethylene addition pathway to be lowered by +13.70 kcal/mol when an oxo group in ReO₄ is replaced with a chloro ligand at the DFT level of theory (B3LYP) using relativistic effective core potential for the metals and valence basis set of DZ+P quality.

In this work, the activation barrier for the direct [3+2] addition of ethylene across the two oxygen atoms of MnO₃Cl on the singlet surface is barrierless, while on the doublet surface the activation barrier is 8.91 kcal/mol. The barriers computed on the singlet and doublet surfaces are lower in comparison with the activation barrier reported by Houk *et. al.* (1999) in the reaction of ethylene and MnO₄⁻, the parent from which substitution was made.

On the singlet surface, the [3+2] addition of the C=C π bond of ethylene across the O=Mn-Cl bonds of MnO₃Cl through a transition state **TS-[A4-A6]/s** has activation barrier of +0.64 kcal/mol and reaction energy of -32.83 kcal/mol.

The five membered metallacycle **A6/d** could be formed from the organometallic intermediate **X/d**. However, the transition state linking the intermediate to the **A6/d** could not be located. Also

attempts to form **A6/d** from the direct addition pathway were unsuccessful. The doublet **A6/d**, triplet **A6/t** and quartet **A6/q** metallacyclic intermediate has been computed to have reaction energies of 4.13, 66.23 and 28.33 kcal/mol exothermic. An exhaustive search on these surfaces for the [3+2] transition states connecting the reactants to the product yielded no positive results.

The formation of the singlet and doublet manganooxetane **A7/s** and **A7/d** through the [2+2] addition of the C=C bond of ethylene across the Mn=O bond of singlet and doublet permanganyl chloride complex **R1-A4** has reaction energies of 1.45 and -6.38 kcal/mol. A quartet metallaioxetane-like species **A7/q** but with an elongated metal-carbon bond has an exothermicity of 18.13 kcal/mol. The formation of the metallaioxetane **A7** could potentially have come from intermediate **X/d** and **A7/q**, however attempts at locating the relevant transition states linking the intermediate to the metallaioxetane was not successful. No triplet metallaioxetane intermediate **A7/t** was located on the triplet reaction surface.

The energy required to re-arrange the metallaioxetane **A7/s** through **TS-[A7-A5]/s** was found to be +5.33 kcal/mol in contrast to the barrierless direct [3+2] formation of the dioxylate.

An epoxide precursor formation was explored for the reaction of MnO_3Cl with ethylene; this was unsuccessful in the case of MnO_4^- . No doublet, triplet and quartet epoxide precursor were located on the reaction surfaces.

The transition state **TS-[A6-E]/s** for the re-arrangement of the singlet five-membered metallacycle (**TS-[1-6]** in Scheme 2.1) to the epoxide precursor has activation barrier of +27.84 kcal/mol and endothermicity of +3.25 kcal/mol. Also, the activation barrier and reaction energy for the singlet direct one-step addition of the C=C bond across one oxygen atom of MnO_3Cl are +8.23 and -28.94 kcal/mol.

The most plausible pathway for the formation of the epoxide if it is to form at all is by direct [3+2] addition of ethylene across the oxygen and chlorine atom followed by re-arrangement to the epoxide precursor.

Thus in the reaction of MnO_3Cl with ethylene, even though the formation of the dioxylate is the most favorable reaction both on the singlet and doublet surfaces, kinetic and thermodynamic consideration favor preferentially the doublet pathway.

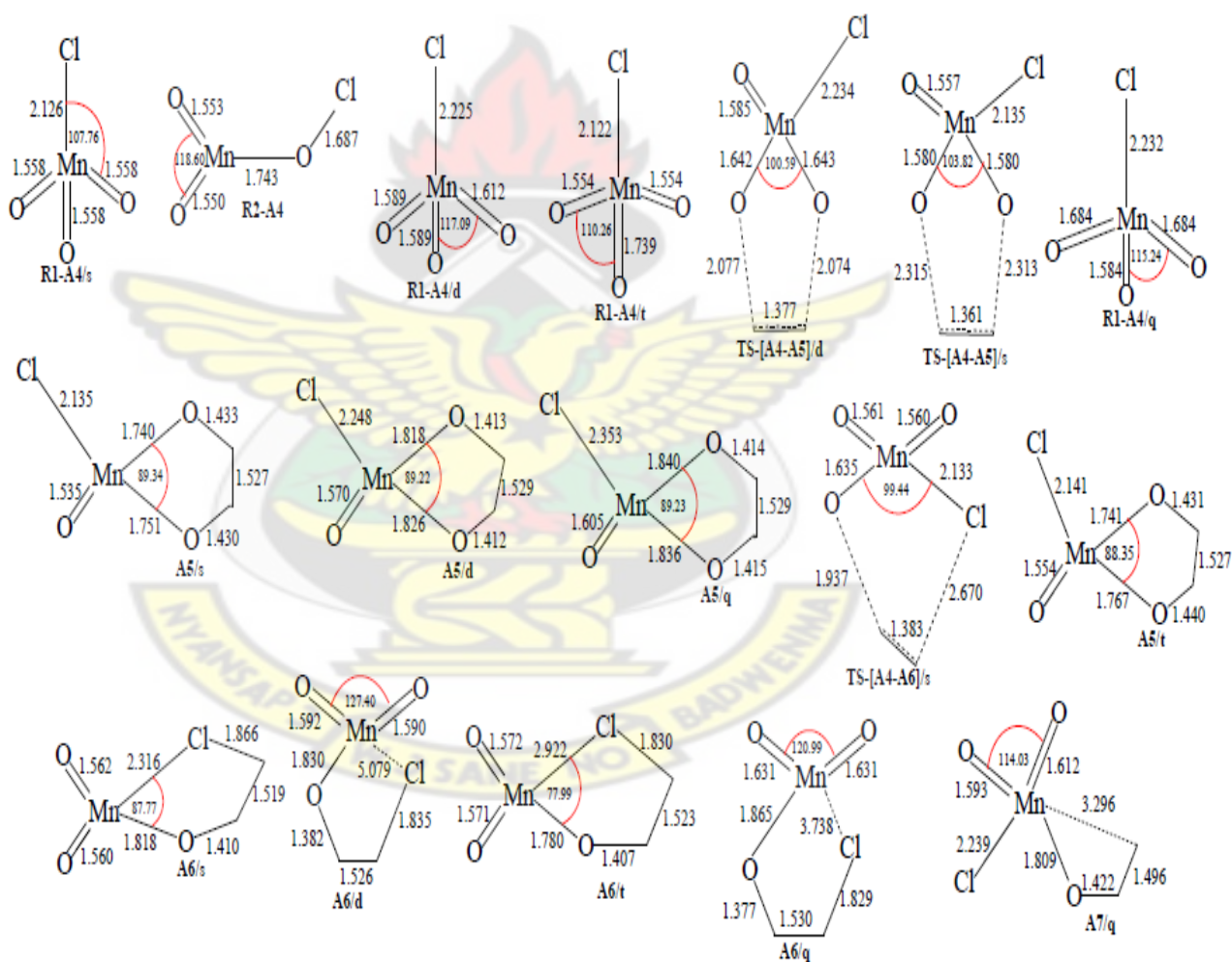


Fig 2.3 : Optimized geometrical parameters of the main stationary points involved in the reaction of MnO_3Cl with ethylene. Distance in Å and bond angles in degrees.

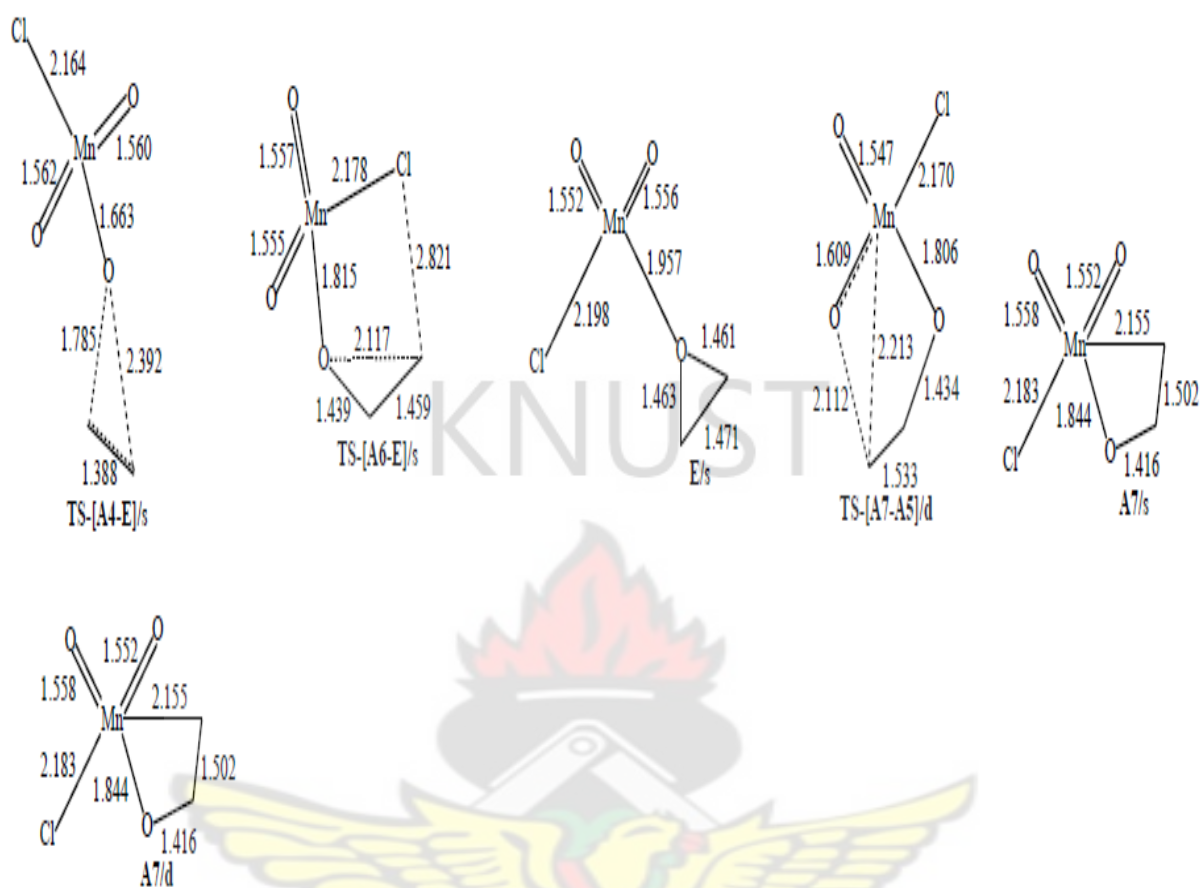


Fig 2.3: Optimized geometrical parameters of the main stationary points involved in the reaction of MnO_3Cl with ethylene. Distance in Å and bond angles in degrees

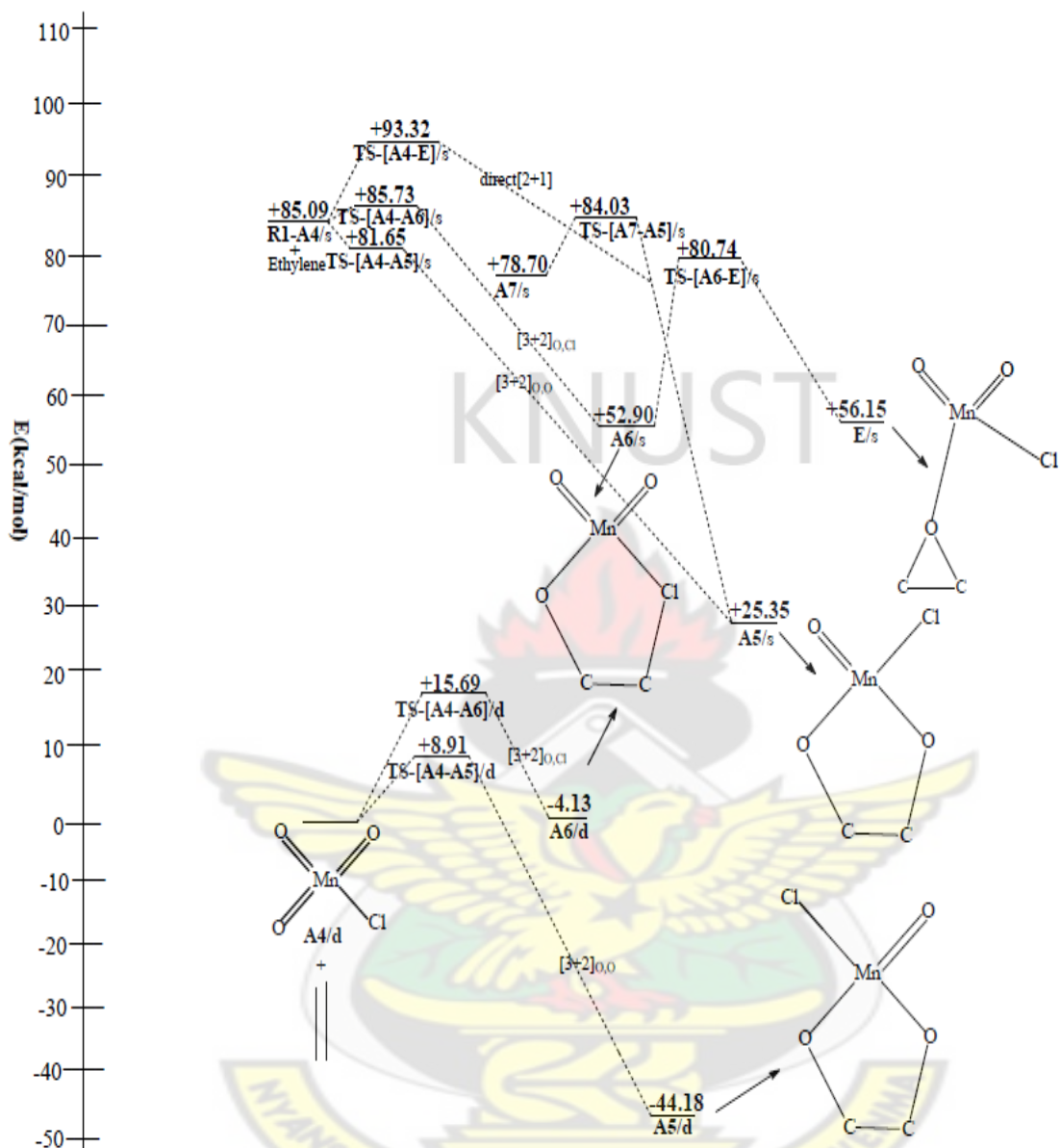


Fig 2.4: Energetics of the reaction of MnO₃Cl with ethylene. Relative energies in kcal/mol (s=singlet, d=doublet)

2.3.3 Reaction of $\text{MnO}_3(\text{NPH}_3)$ with ethylene

Figures 2.5 and 2.6 show respectively the optimized geometries and relative energies of the main stationary points involved in the reaction between $\text{MnO}_3(\text{NPH}_3)$ and ethylene. The singlet $\text{MnO}_3(\text{NPH}_3)$ reactant **A7/s** has the Mn=N bond length of 1.77 Å. The Mn=O bond lengths are 1.565, 1.575 and 1.577 Å. The N-P bond distance is 1.60 Å. A triplet $\text{MnO}_3(\text{NPH}_3)$ **A7/t** has been computed to be 11.80 kcal/mol less stable than the singlet structure. The Mn=N and N-P bonds are 1.75 Å and 1.61 Å respectively.

In the doublet **A7/d** and quartet reactants **A7/q**, the phosphorus atom in the complex $\text{MnO}_3(\text{NPH}_3)$ attaches itself to one of the oxo ligands to form a four-membered ring. The O-P bonds are 1.84 and 1.75 Å in the doublet and quartet reactants.

The [3+2] addition of the C=C bond of ethylene across the O=Mn=O bonds of singlet $\text{MnO}_3(\text{NPH}_3)$ through a singlet transition state **TS-[A7-A8]/s** to form the dioxylate intermediate **A8/s** has an activation barrier of -5.38 kcal/mol and an exothermicity of 60.42 kcal/mol. The transition state **TS-[A7-A8]/s** is a synchronous one, with respect to the newly forming C-O bonds. No corresponding transition state linking the reactants to the products could be located on the doublet PES. However, a doublet dioxylate product **A8/d** was found to be +27.42 kcal/mol less stable than the singlet **A8/s**. A triplet and quartet dioxylate product **A8/t** and **A8/q** has been computed to have reaction energies of -83.28 and -65.30 kcal/mol.

On the quartet PES, a seven-membered metallacyclic intermediate **A8/q** is formed in which one of the oxo-ligand on the metal centre (Mn) forms a new bond with the phosphine moiety (O-P = 1.74 Å) attached to nitrogen (**fig 2.5**). Thus, the newly-formed O-P bond in the triplet **A8/t** and

quartet **A8/q** dioxylate have a remarkable effect on the stabilities of the product formed. In the singlet and doublet dioxylate species, there is no bond formed between the O-P moieties.

The [3+2] addition of the C=C bond of ethylene across the O=Mn=N bonds of singlet MnO₃(NPH₃) through a singlet transition state **TS-[A7-A9]/s** has an activation barrier of -4.23 kcal/mol and an exothermicity of 65.30 kcal/mol.

A doublet seven-membered metallacyclic intermediate **A9/d** in which one of the oxo ligand at the metal centre (Mn) bonds with phosphine (1.71 Å) attached to the nitrogen in the five-membered ring (**fig 2.5**), has been computed to be 67.58 kcal/mol exothermic; 2.28 kcal/mol more stable than the singlet product **A9/s** and 16.51 kcal/mol less stable than the triplet **A9/t**. A quartet metallacyclic intermediate **A9/q** has an exothermicity of 63.20 kcal/mol; 4.38 kcal/mol less stable than the doublet intermediate **A9/d**.

The [3+2] addition of the C=C bond of ethylene across the O=Mn=N bonds of triplet MnO₃(NPH₃) through the triplet transition state **TS-[A7-A9]/t** results in a product **A9/t** in which one of the oxo ligands bonded to the metal centre forms a new bond with phosphine (PH₃) ligand (1.85 Å) attached to nitrogen in the five-membered ring (**fig 2.5**). In the quartet product, the newly formed O-P bond is at 1.72 Å; 0.01 Å longer in the quartet structure **A9/q**.

The formation of the singlet metallaoxetane **A11/s** by [2+2] addition of the C=C bond of ethylene across the Mn=O bond of the singlet MnO₃(NPH₃) has a reaction energy of -13.66 kcal/mol. A doublet **A11/d** and triplet **A11/t** metallaoxetane intermediate have reaction energies of -16.86 and -24.25 kcal/mol. No transition states for [2+2] were located on the singlet, doublet, triplet and quartet potential energy surfaces. A quartet metallaoxetane-like species but with

elongated metal - carbon bond intermediate **A11/q** has been located to be 9.62 kcal/mol exothermic.

The formation of a singlet four-membered metallacyclic intermediate **A10/s** through the transition state **TS-[A7-A10]/s** by [2+2] addition of the C=C π bond of ethylene across Mn=N bond of the singlet MnO₃(NPH₃) has an activation barrier of +17.55 kcal/mol and leads to a six-membered product in which one of the oxo group on the metal centre bonds with phosphine (PH₃) attached to the nitrogen (1.78 Å). The singlet product has an exothermicity of 27.39 kcal/mol. A triplet species **A10/t** has reaction energy of -14.66 kcal/mol.

In the quartet product **A10/q**, the newly formed (O-P) bond is at 1.72 Å; 0.06 Å shorter in the singlet structure **A10/s**. The reaction energy of the quartet species is -24.42 kcal/mol. In the triplet product, there is a new bond formed between P-O (1.90 Å) as observed in the singlet product. No [2+2] transition states were located on the quartet, doublet and triplet potential energy surfaces. A doublet product **A10/d** has been computed to be -33.96 kcal/mol exothermic.

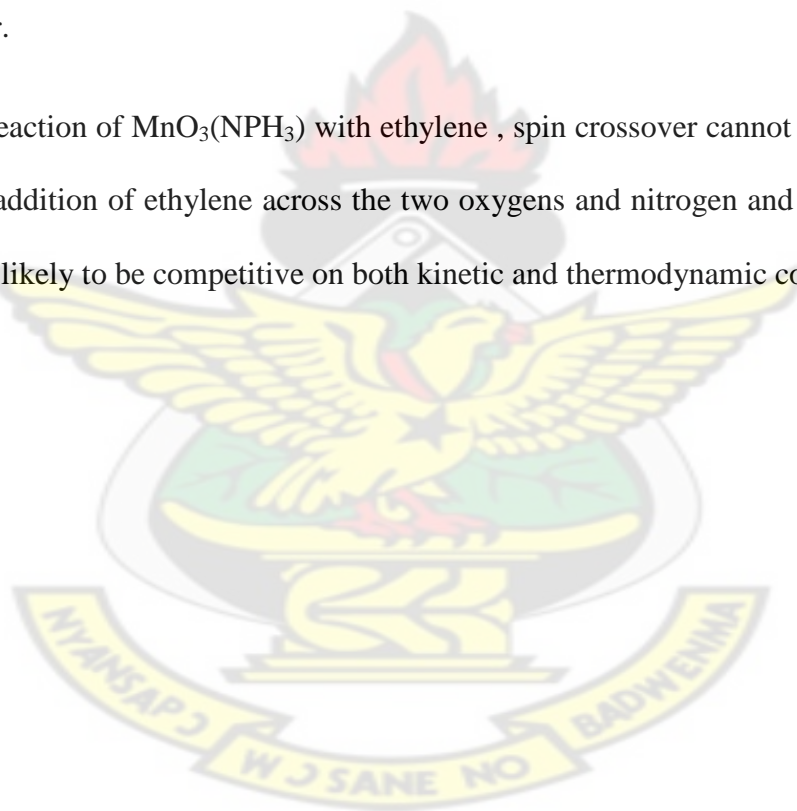
A search on the surfaces for the re-arrangement of the four membered metallacycle metallaioxetane to the five membered metallacycle was unsuccessful.

The reaction of MnO₃(NPH₃) with ethylene was explored for the possibility of formation of an epoxide precursor. The transition state **TS-[A9-E]/s** for the re-arrangement of the singlet five-membered metallacycle (**TS-[1-6]** in Scheme 2.1) to the epoxide precursor is very high energy species resulting in activation barrier of +63.06 kcal/mol and forming a very unstable species of endothermicity of +41.24 kcal/mol. Also the re-arrangement of the singlet five-membered metallacycle (**TS-[2-3]** in Scheme 2.1) through transition state **TS-[A8-E]/s** to the epoxide precursor has an activation barrier of +70.67 kcal/mol and endothermicity of +36.36 kcal/mol.

The transition state (**TS-[4-3]**/s in Scheme 2.1) for the rearrangement of the singlet four-membered metallaoxetane to the epoxide precursor through transition state **TS-[A11-E]**/s has a barrier of +23.88 kcal/mol and exothermicity of 10.40 kcal/mol. However since the activation energy required to form the metallaoxetane is not known, no conclusion could be drawn on the formation of the epoxide precursor for the metallaoxetane.

The most plausible pathway for the formation of the epoxide precursor if it is to form at all is by initial [3+2] addition to form the dioxylate intermediate followed by re-arrangement to the epoxide precursor.

Considering the reaction of $\text{MnO}_3(\text{NPH}_3)$ with ethylene, spin crossover cannot be ruled out. The two direct [3+2] addition of ethylene across the two oxygens and nitrogen and oxygen atoms of $\text{MnO}_3(\text{NPH}_3)$ are likely to be competitive on both kinetic and thermodynamic consideration.



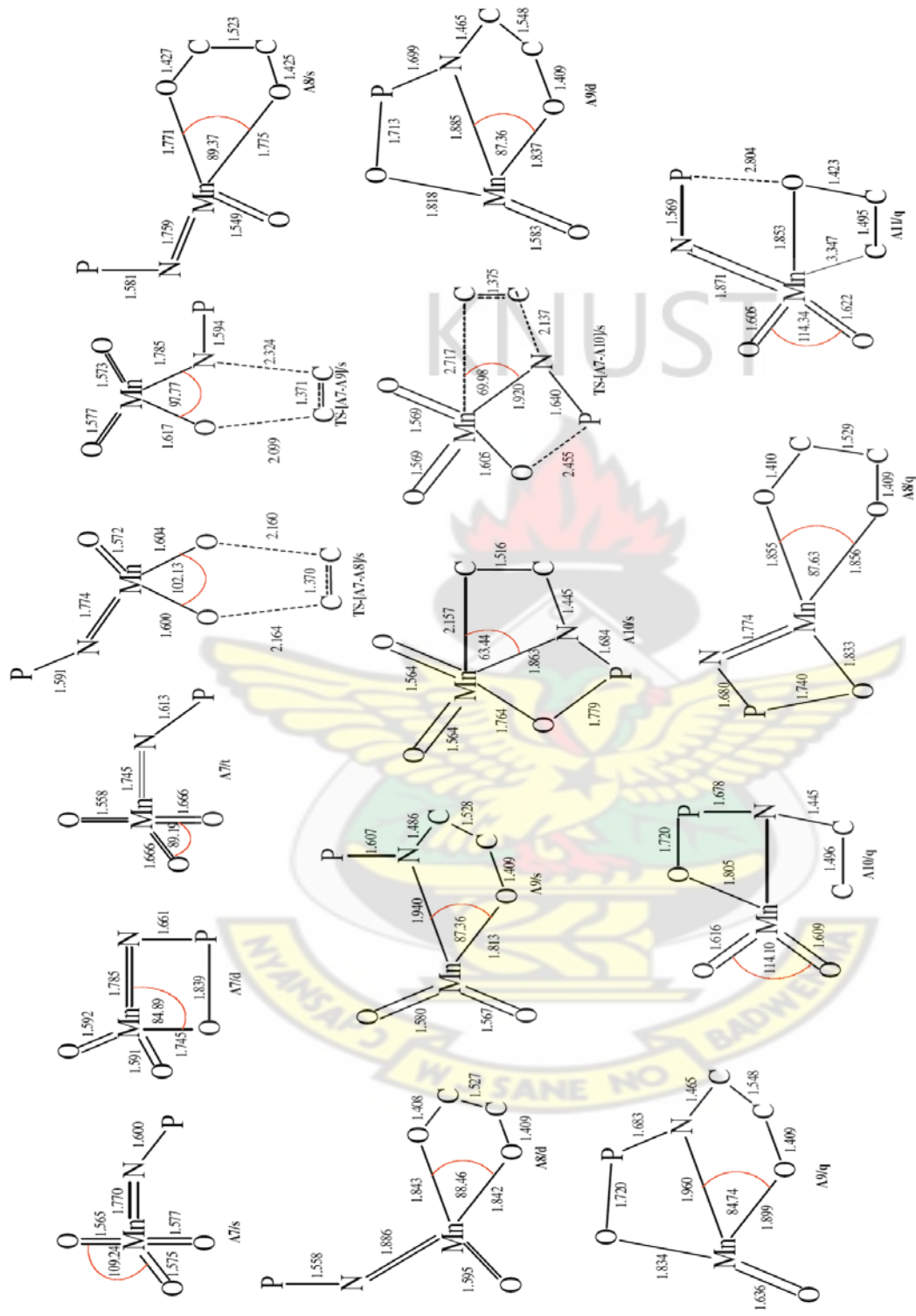


Figure 2.5: Optimized geometrical parameters of the main stationary points involved in the reaction of $\text{MnO}_3(\text{NPH}_3)$ with ethylene. Distances in Å and angles in degrees.

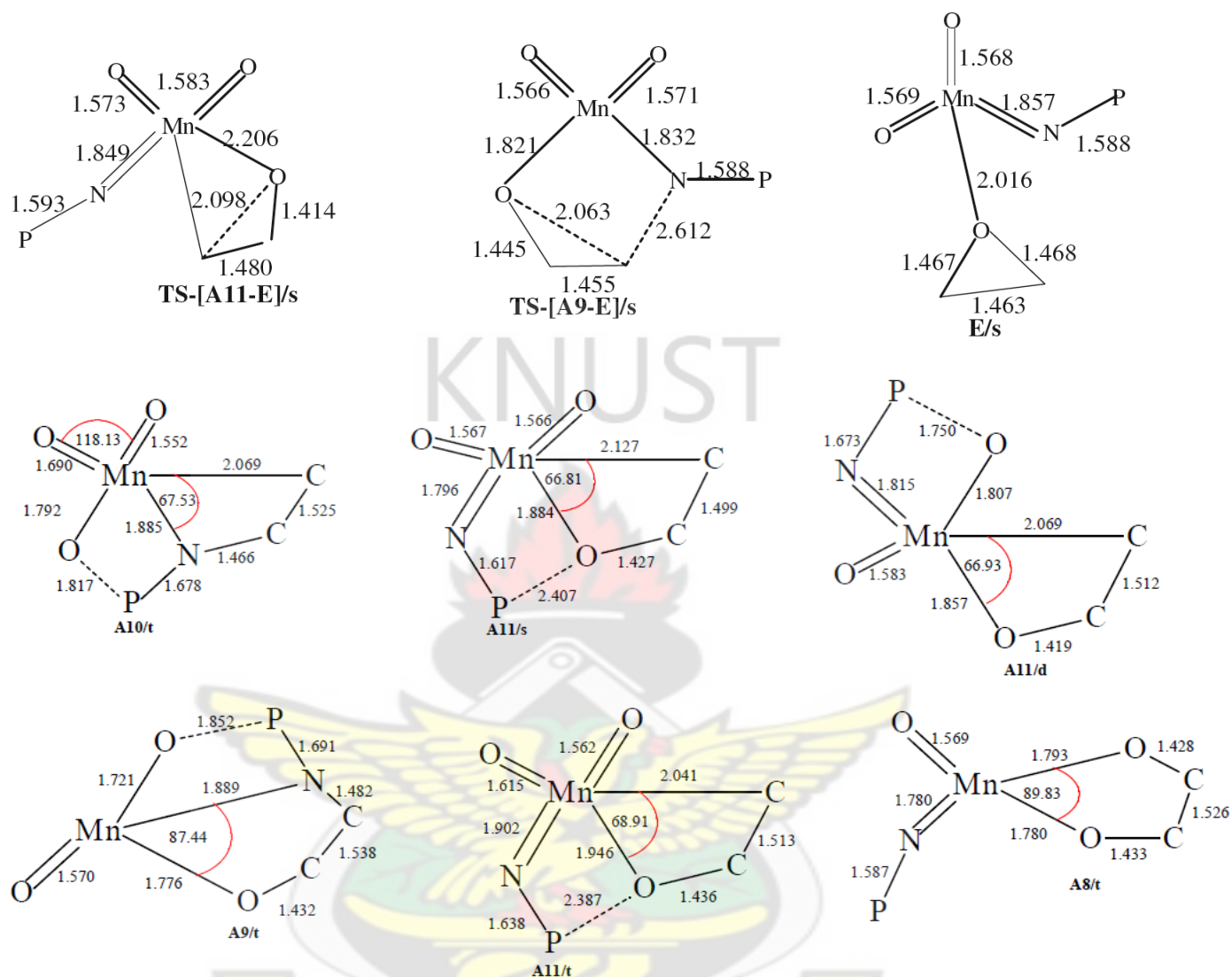


Figure 2.5cont'd: Optimized geometrical parameters of the main stationary points involved in the reaction of $\text{MnO}_3(\text{NPH}_3)$ with ethylene. Distances in Å and angles in degrees

*Hydrogen omitted from phosphorus atom

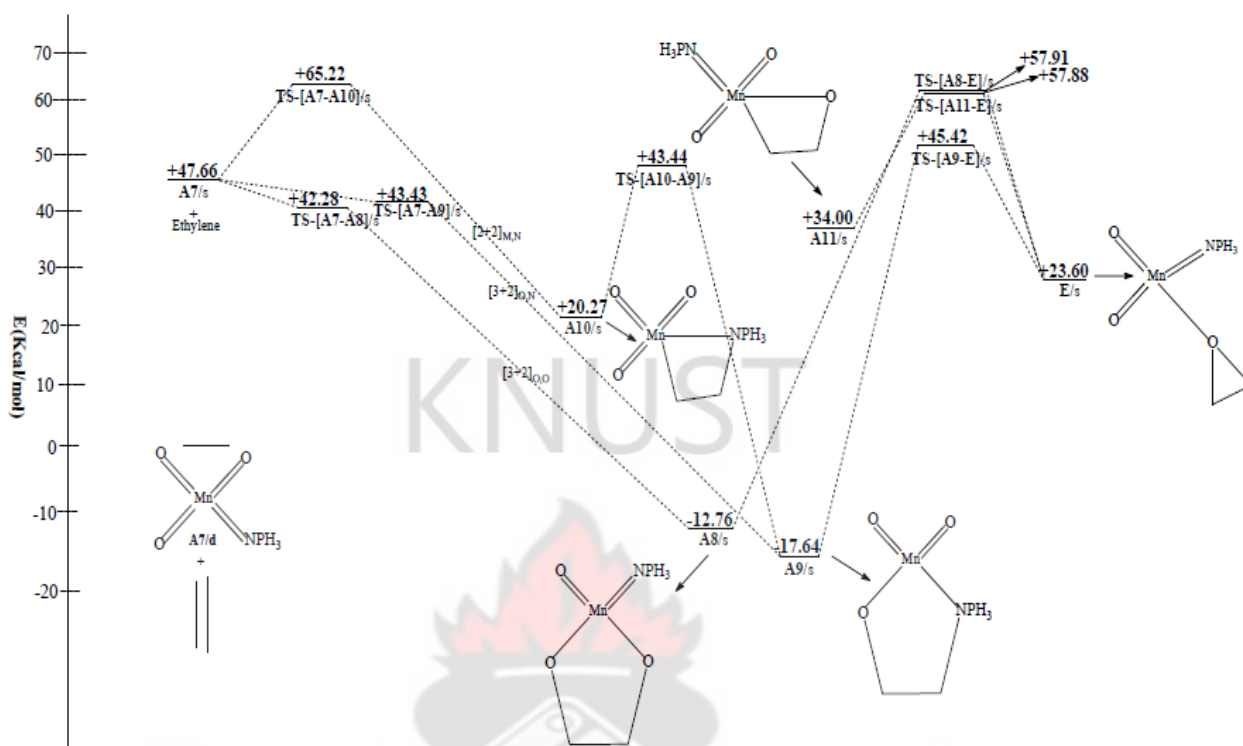


Fig 2.6: Energetics of the reaction of $\text{MnO}_3(\text{NPH}_3)$ with ethylene. Relative energies in kcal/mol

2.3.4 Reaction of $\text{MnO}_3(\text{CH}_3)$ with ethylene

Figures 2.7 and 2.8 shows the optimized geometries and relative energies of the main stationary points involved in the reaction between $\text{MnO}_3(\text{CH}_3)$ and ethylene respectively. The DFT geometry optimization of $\text{MnO}_3(\text{CH}_3)$ on a singlet potential energy surface [PES] yielded two minima: **R1-A12** of C_{3V} symmetry in which the three Mn=O bonds are each 1.56 Å long and the Mn-C bond is 1.99 Å long. The other minimum **R2-A12** of C_1 symmetry in which the methyl ligand break from the metal centre and forms a new bond with one of the oxo-ligands.

The minimum **R1-A12** has been computed to be 11.81 kcal/mol less stable than **R2-A12**. A doublet reactant **A12/d** has been computed and found to be 49.41 kcal/mol more stable than singlet **R2-A12** and 61.22 kcal/mol more stable than the singlet **R1-A12**. In the doublet reactant **A12/d**, the Mn-C bond is 0.004 Å longer than that in the singlet structure **R1-A12** and 0.02 Å longer than that in the triplet structure **A13/t**. A quartet reactant **A12/q** has been computed to be 25.99 kcal/mol less stable than the doublet reactant **A12/d**.

The [3+2] addition of the C=C π bond of ethylene across the O=Mn=O bonds of doublet $\text{MnO}_3(\text{CH}_3)$ through a doublet transition state **TS- [A12-A13]/d** to form the dioxylate **A13/d** has an activation barrier of 15.90 kcal/mol and exothermicity 29.67 kcal/mol, in disagreement with the work of Gisdakis and Rösch, (2001) who calculated the activation barrier along this route to be 8.9 kcal/mol at the B3LYP//LANL2DZ/6-311G(d,p). The doublet transition state is symmetrical with respect to the forming C-O bonds (1.99 Å). The Mn-C bond distance (1.99 Å) in the doublet transition state is the same as in the doublet reactant. The reaction energy of the triplet product **A13/t** has been computed to be -84.02 kcal/mol.

The activation barrier for the [3+2] addition of the C=C π bond of ethylene across the O=Mn=O bonds of singlet MnO₃(CH₃) through a singlet transition state **TS-[A12-A13]/s** has an activation barrier of 20.29 kcal/mol and reaction energy of -25.85 kcal/mol.

A quartet dioxylate **A13/q** is 36.66 kcal/mol more stable than the doublet product **A13/d**. In the singlet product, the Mn=O bonds to the 'spectator' oxygen atoms (the oxygen atom which is not part of the ring) is 1.54 Å and those to the oxygen atoms involved in the ring are 1.74 and 1.77 Å respectively.

The formation of the doublet manganooxetane **A14/d** through doublet transition state **TS-[A12-A14]/d** by [2+2] addition of the C=C bond of ethylene across the Mn=O bond of the doublet MnO₃(CH₃) has activation barrier of +18.38 kcal/mol and reaction energy of +13.92 kcal/mol endothermic. A triplet metallaoxetane product **A14/t** has been computed to be 43.60 and 38.8 kcal/mol more stable than the doublet **A14/d** and singlet **A14/s** metallaoxetane intermediates.

The formation of singlet manganooxetane **A14/s** through the singlet transition state **TS-[A12-A14]/s** has activation barrier of +51.36 kcal/mol. A quartet metallaoxetane species **A14/q** has been computed to be 34.83 kcal/mol more stable than the doublet metallaoxetane intermediate. No triplet and quartet transition state could be located on the reaction surface.

The re-arrangement of the singlet metallaoxetane to the singlet dioxylate through transition state **TS-[A14-A13]/s** has activation barrier of +18.77 kcal/mol. Thus the overall activation barrier for the re-arrangement of the singlet metallaoxetane to the dioxylate (+18.77 kcal/mol) is lower than the activation barrier for the direct [3+2] addition of C=C π of ethylene across O=Mn=O of singlet and doublet MnO₃(CH₃). However, since the first-step of the reaction involves a higher

activation barrier, the dioxylate would proceed from the direct [3+2] addition pathway and not from the metallaoxetane through the [2+2] addition pathway and subsequent re-arrangement.

The formation of an epoxide precursor was explored from the reaction of $\text{MnO}_3(\text{CH}_3)$ with ethylene. The transition state **TS [A14-E]/s** for the rearrangement of the singlet four-membered metallaoxetane to the epoxide precursor has activation barrier and reaction energy of +22.52 and -7.32 kcal/mol respectively. Also, the activation energy for the formation of the singlet epoxide precursor from direct attack of the C=C bond across the oxygen atom of $\text{MnO}_3(\text{CH}_3)$ has been computed to be +29.45 kcal/mol and reaction energy has endothermicity of +1.8 kcal/mol. On the doublet, triplet, and quartet surfaces, the reaction energies are +4.58, -40.61 and -21.50 kcal/mol respectively. The most plausible pathway for the formation of the epoxide precursor is by direct [2+1] addition pathway.

For the reaction of $\text{MnO}_3(\text{CH}_3)$ with ethylene, even though formation of the dioxylate is the most favorable reaction both on the singlet and doublet surfaces, kinetic and thermodynamic factors favors the occurrence of the reaction preferentially on the doublet surface.

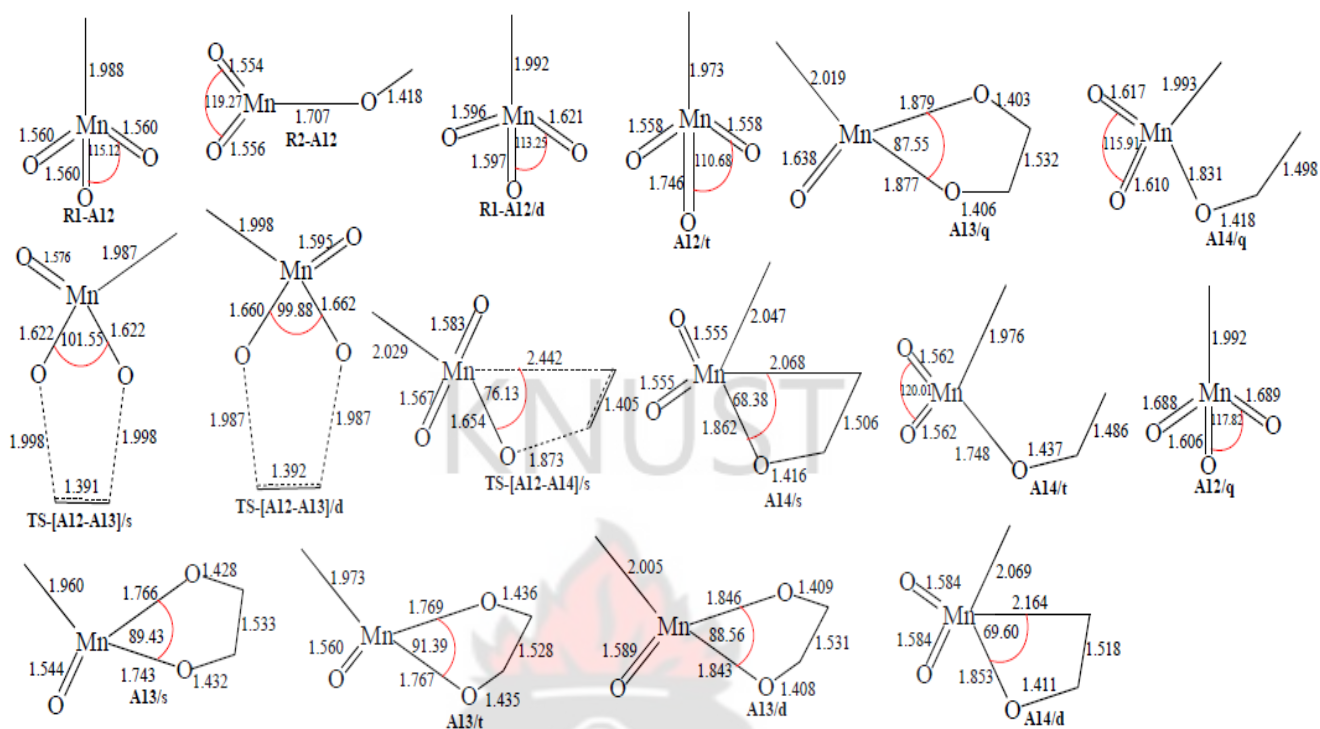


Fig 2.7: Optimized geometries of the main stationary points involved in the reaction of $\text{MnO}_3(\text{CH}_3)$ with ethylene. Distance in Å.

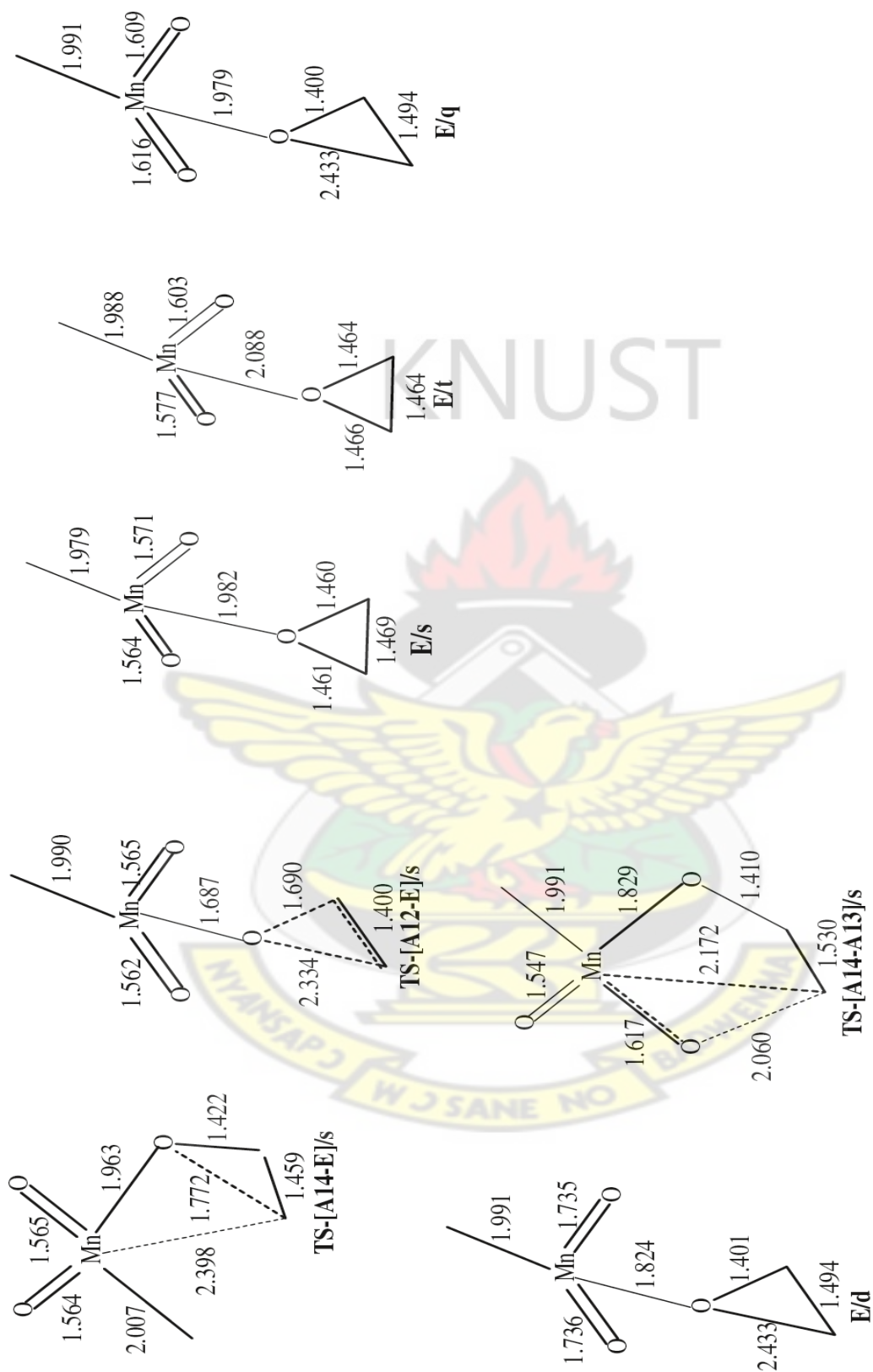


Fig 2.7 Cont'd: Optimized geometrical parameters of the main stationary points involved in the reaction of $\text{MnO}_3(\text{CH}_3)$ with ethylene. Distance in Å

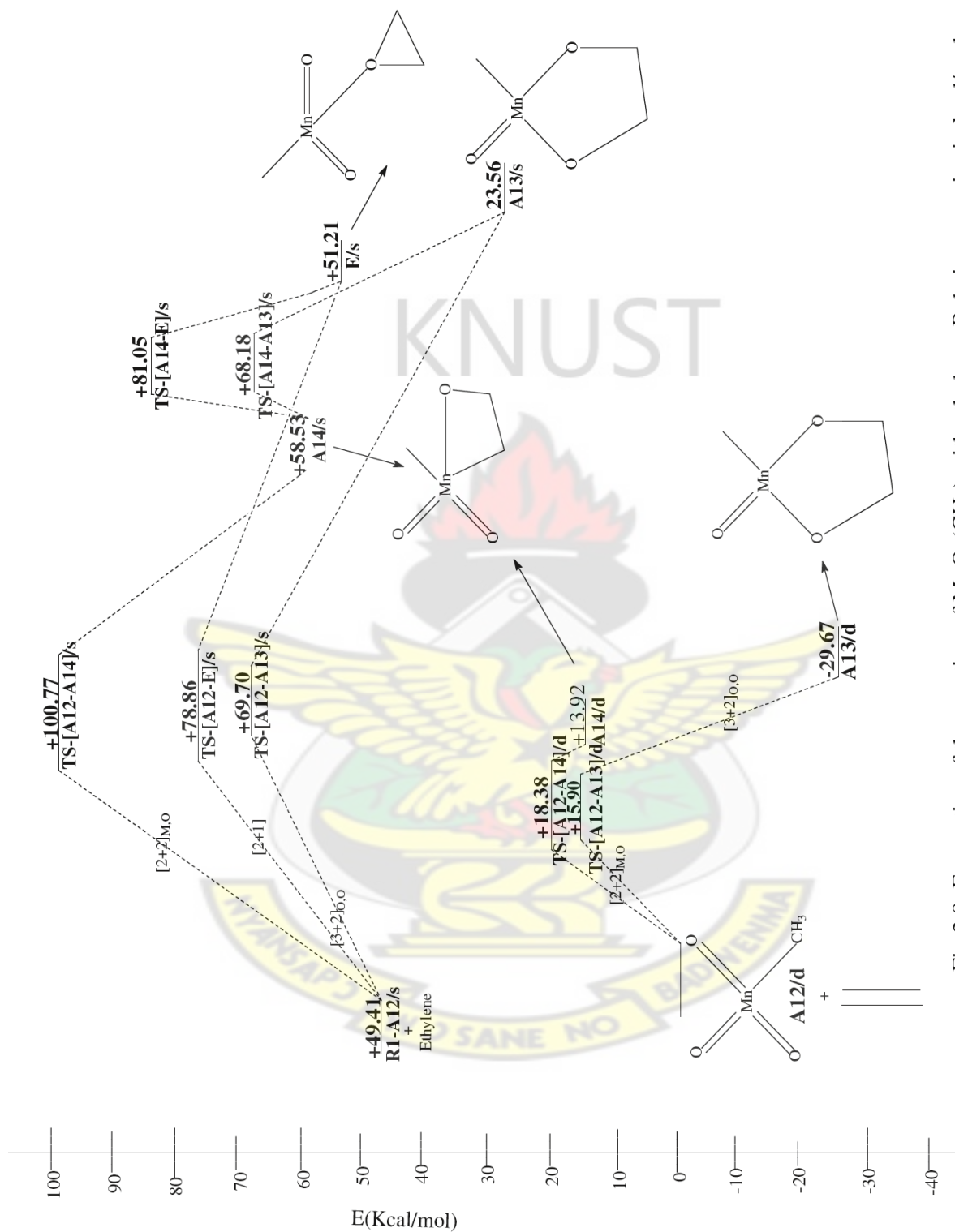


Fig 2.8: Energetics of the reaction of $\text{MnO}_3(\text{CH}_3)$ with ethylene. Relative energies in kcal/mol.

2.3.5 Reaction of $\text{MnO}_3(\text{OCH}_3)$ with ethylene

Figures 2.9 and 2.10 show respectively the optimized geometries and relative energies of the main stationary points involved in the reaction between $\text{MnO}_3(\text{OCH}_3)$ and ethylene. A singlet, doublet, triplet and quartet species have been optimized for the reactant $\text{MnO}_3(\text{OCH}_3)$. The singlet reactant **A15/s** has two of the Mn=O bonds at 1.57 Å and the other Mn=O at 1.56 Å long. The Mn-O bond is 1.74 Å long.

A doublet reactant **A15/d** has been computed to be 69.05 kcal/mol more stable in relation to the singlet reactant **A15/s** and 90.21 kcal/mol more stable in relation to the triplet reactant **A15/t**. A quartet reactant **A15/q** of C_s symmetry is 20.24 kcal/mol less stable in relation to the doublet **A15/d**. The quartet reactant is 48.81 and 69.96 kcal/mol more stable with respect to the singlet and triplet ground state reactants.

On the doublet surface, there is a stepwise attack of one of the C=C π of ethylene on an oxo-ligand of $\text{MnO}_3(\text{OCH}_3)$ to form an organometallic intermediate **X/d** through transition state **TS-[A15-X]/d**. The activation barrier along this route is +3.28 kcal/mol. The intermediate **X/d** has an endothermicity of +0.63 kcal/mol. The intermediate **X/d** can re-arrange through transition state **TS-[X-A16]/d** to form the dioxylate intermediate **A16/d**. The activation barrier for the formation of the dioxylate intermediate **A16/d** is +6.26 kcal/mol. The dioxylate intermediate has reaction energy of -39.80 kcal/mol.

The triplet transition state linking the reactants to the products could not be located; however a triplet dioxylate product **A16/t** was located and found to be 34.27 kcal/mol more stable than the singlet dioxylate product **A16/s**. A quartet product **A16/q** has been computed to have a reaction energy of +26.48 kcal/mol.

The activation barrier for the direct [3+2] addition of ethylene across the O=Mn=O bonds of singlet $\text{MnO}_3(\text{OCH}_3)$ through a singlet transition state **TS-[A15-A16]/s** is 1.58 kcal/mol. The reaction energy of the dioxylate intermediate **A16/s** has been computed to have reaction energy of -54.08 kcal/mol.

Attempts at locating the manganooxetane product which is expected to result from the [2+2] addition of ethylene to the Mn=O bonds of singlet and doublet $\text{MnO}_3(\text{OCH}_3)$ proved unsuccessful. This was the case for the singlet, doublet, triplet and quartet surfaces.

The reaction of $\text{MnO}_3(\text{OCH}_3)$ with ethylene was explored for the formation of the epoxide precursor. No doublet, triplet and quartet epoxide precursors were found on the reaction surfaces.

The transition state (**TS-[2-3]** in Scheme 2.1) for the re-arrangement of the five-membered dioxylate through transition state **TS-[A16-E]/s** to the epoxide precursor has activation barrier of +64.28 kcal/mol and endothermicity of +29.07 kcal/mol.

The most plausible pathway for the formation of the epoxide precursor, is by initial [3+2] addition across the two oxygen atoms of singlet $\text{MnO}_3(\text{OCH}_3)$ followed by re-arrangement to the epoxide precursor.

Thus in the reaction of $\text{MnO}_3(\text{OCH}_3)$ with ethylene, the reaction will preferentially take place on the doublet surface and the [3+2] addition of ethylene across the two oxygen atoms of $\text{MnO}_3(\text{OCH}_3)$ to form the dioxylate intermediate **A16/d** is likely to be the only product.

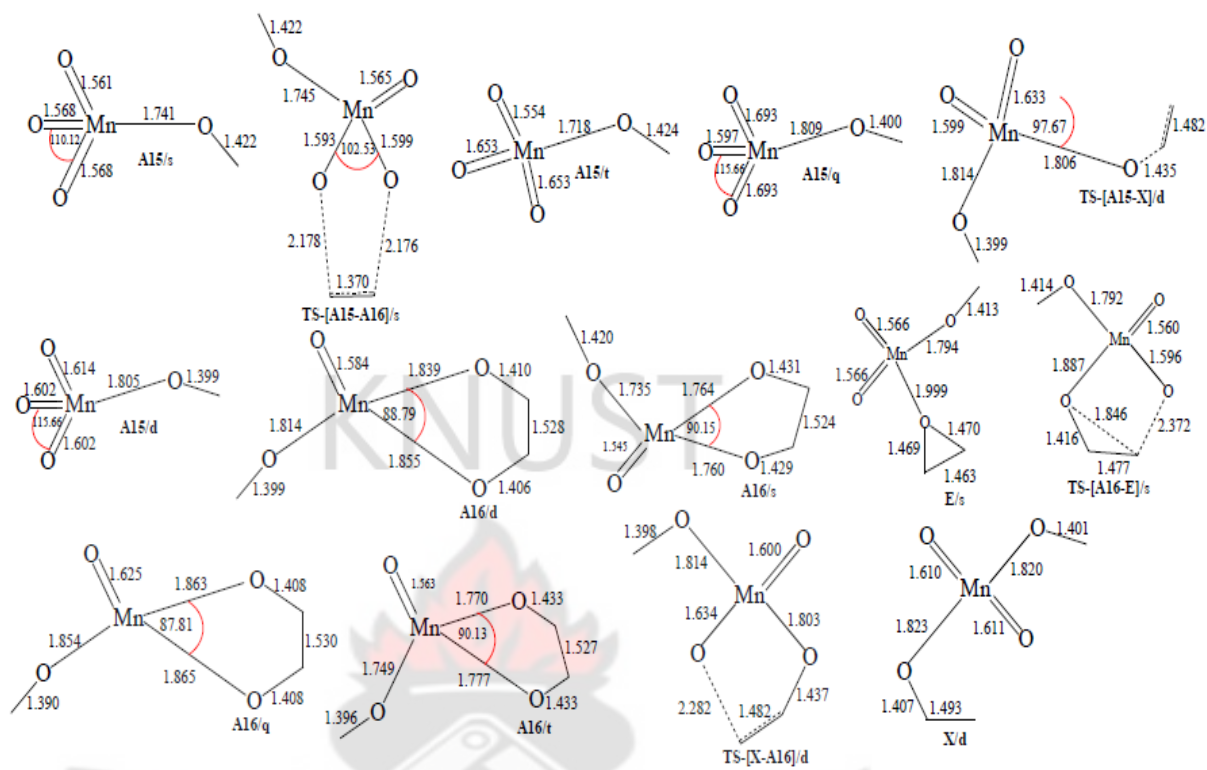


Fig 2.9: Optimized geometrical parameters of the main stationary points involved in the reaction of $\text{MnO}_3(\text{OCH}_3)$ with ethylene. Distance in Å and bond angles in degree.

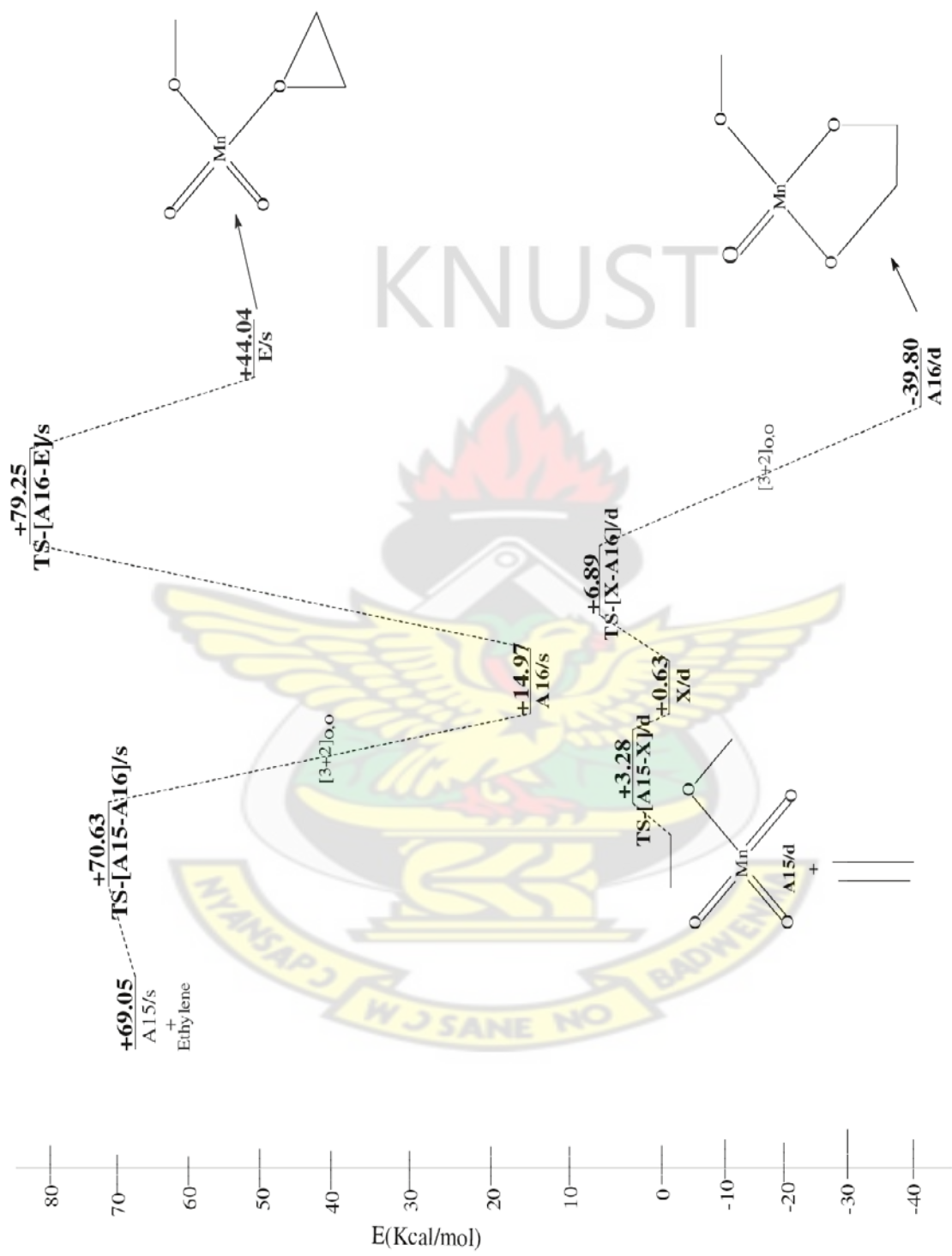


Fig 2.10: Energetics of the reaction of $\text{MnO}_3(\text{OCH}_3)_3$ with ethylene. Relative energies in kcal/mol

2.3.6 Reaction of MnO₃Cp with ethylene

The optimized geometries and relative energies of the main stationary points involved in the reaction between MnO₃Cp and ethylene are shown in Fig.2.11 and Fig.2.12, respectively. The DFT geometry optimization of MnO₃Cp **A17** on a singlet potential energy surface has two of the Mn=O bonds at 1.57 Å and the other Mn=O is 1.56 Å long. The cyclopentadienyl ligand Cp is bonded in a η^3 fashion in the singlet reactant, i.e. Mn-C (Cp) = 2.018, 2.838 and 2.830 Å. However, Gisdakis and Rösch, (2001) reported the Cp ligand to be bonded in a η^1 fashion to the metal centre at B3LYP//LANL2DZ/6-311G (d, p) level of theory.

A doublet reactant **A17/d** has been computed to be 65.53 kcal/mol more stable than the singlet. The cyclopentadienyl ligand Cp is bonded in a η^3 fashion in the doublet reactant, i.e. Mn-C (Cp) = 2.04, 2.90 and 2.92 Å. In the triplet reactant **A17/t**, the cyclopentadienyl ligand is bonded to the manganese centre in a η^5 fashion i.e. Mn-C (Cp) = 2.21, 2.26, 2.46, 2.46 and 2.26 Å. The triplet reactant **A17/t** is 91.58 kcal/mol less stable than doublet reactant **A17/d**. A quartet **A17/q** has been computed to be 24.24 kcal/mol less stable than the doublet reactant. The cyclopentadienyl ligand Cp is bonded in a η^3 fashion to the Mn i.e. (Mn-C (Cp) = 2.05, 2.84, 2.89 Å.

It has been found that the formation of the cyclic ester intermediate through the [3+2] addition pathway can proceed from a doublet as well as a singlet transition state. The activation barrier through the doublet transition state **TS-[A17-A18]/d** is 14.15 kcal/mol. The activation barrier along the singlet transition state is +6.57 kcal/mol.

A triplet dioxylate species **A18/t** (-85.84 kcal/mol) and a singlet dioxylate product **A18/s** (-57.62 kcal/mol) is located. A doublet dioxylate species **A18/d** has reaction energy of -35.11 kcal/mol.

The Cp ligand in the singlet MnO₃Cp-dioxylate **A18/s** shows η^5 -bonding fashion to the Mn centre (Mn-C (Cp) =2.22, 2.22 and 2.33, 2.36, 2.26 Å) contrary to the η^3 -bonded mode expressed in the singlet reactant. A η^5 -bonding fashion (Mn-C (Cp) =2.24, 2.27 and 2.29, 2.36, 2.34 Å) is also expressed in the triplet product **A18/t**. A quartet dioxylate intermediate **A18/q** has been computed to have reaction energy of -70.69 kcal/mol. The Cp ligand in quartet MnO₃Cp-dioxylate **A18/q** shows η^4 -bonding fashion to the Mn centre (Mn-C (Cp) =2.34, 2.33 and 2.82, 2.84 Å) contrary to the η^3 -bonded mode expressed in the quartet reactant.

In a related work on a rhenium system, Boehme *et. al.*, (1999) found out that replacing an oxo ligand with a cyclopentadienyl ring lowers the activation barrier for the [3+2] and [2+2] addition pathways ((i.e. ReO₄⁻ + C₂H₄: TS [3+2] = 37.7 Kcal/mol, TS[2+2] = 47.2Kcal/mol: CpReO₄ + C₂H₄; TS [3+2] = 14.10 kcal/mol, TS [2+2] = 25.40 kcal/mol).

The activation barrier (14.1 kcal/mol) for the [3+2] addition of ethylene across the O=Re=O bonds of CpReO₃ reported by Boehme *et. al.*, (1999) is comparable to the activation barrier (14.50 kcal/mol) for the [3+2] addition of the C=C π bond of ethylene across the O=Mn=O moiety of doublet MnO₃Cp. This is not surprising, since manganese and rhenium are members of the same Group.

The formation of the singlet manganooxetane **A19/s** from the [2+2] addition of ethylene across the Mn=O bond of singlet MnO₃Cp gives an activation barrier of 40.92 kcal/mol through a singlet transition state **TS-[A17-A19]/s**. The manganooxetane has reaction energy of -5.53 kcal/mol. The Cp ligand in the singlet MnO₃Cp-oxetane **A19/s** shows η^3 -bonding mode to the Mn centre, (Mn-C (Cp) =2.122, 2.892 and 2.957Å) in conformity with η^3 -bonding mode in the singlet reactant.

A quartet metallaoxetane **A19/q** has been computed to be -0.16 kcal/mol. The Cp ligand in the quartet MnO₃Cp-oxetane **A19/q** shows η^3 -bonding mode to the Mn centre, (Mn-C (Cp) = 2.094, 2.905 and 2.962 Å). A triplet metallaoxetane intermediate **A19/t** has been computed to have reaction energy of -67.50 kcal/mol.

These findings are in disagreement with a related work of Rappe et al [40], who used qualitative molecular orbital diagram to assert that, strong π -bonding ligands such as Cp thermodynamically favor dioxylate formation because of π -bond strain relief. In this work, the dioxylate and metallaoxetane intermediate formed on the singlet, doublet, triplet and quartet PES are all exothermic.

The re-arrangement of the singlet, doublet, and triplet and quartet metallaoxetane to the dioxylate were explored for the reaction of MnO₃Cp with ethylene (**TS-[4-2]** in Scheme 2.1). The re-arrangement of the singlet metallaoxetane to the dioxylate through transition state **TS-[A19-A18]/s** has activation barrier of +14.02 kcal/mol. No doublet, triplet and quartet re-arrangement of the metallaoxetane intermediate to the dioxylate was located on the reaction surface. This rules out the re-arrangement of the metallaoxetane to the dioxylate as a possible pathway to the formation of the dioxylate intermediate on the singlet surface.

The potential energy surface of the reaction of MnO₃Cp with ethylene was further explored in an attempt to locate an epoxide precursor [(Cp)O₂-Mn-OC₂H₄] (**3** in Scheme 1), but no such minimum was found on these reaction surfaces in agreement with a related findings of Burrell *et al.*, 1995; Herrmann *et al.*, (1984), Klahn-olive *et al.*, (1984) and Kühn *et al.*, (1994) who reported that CpReO₃ reacts with olefins to predominately form dioxylates (**2** in Scheme 2.1).

The energetics in Fig 2.12 suggest that in the addition of ethylene to CpMnO_3 , the only favorable reaction which is the direct [3+2] addition to form the dioxylate intermediate is likely to exclusively occur on the doublet PES.

KNUST



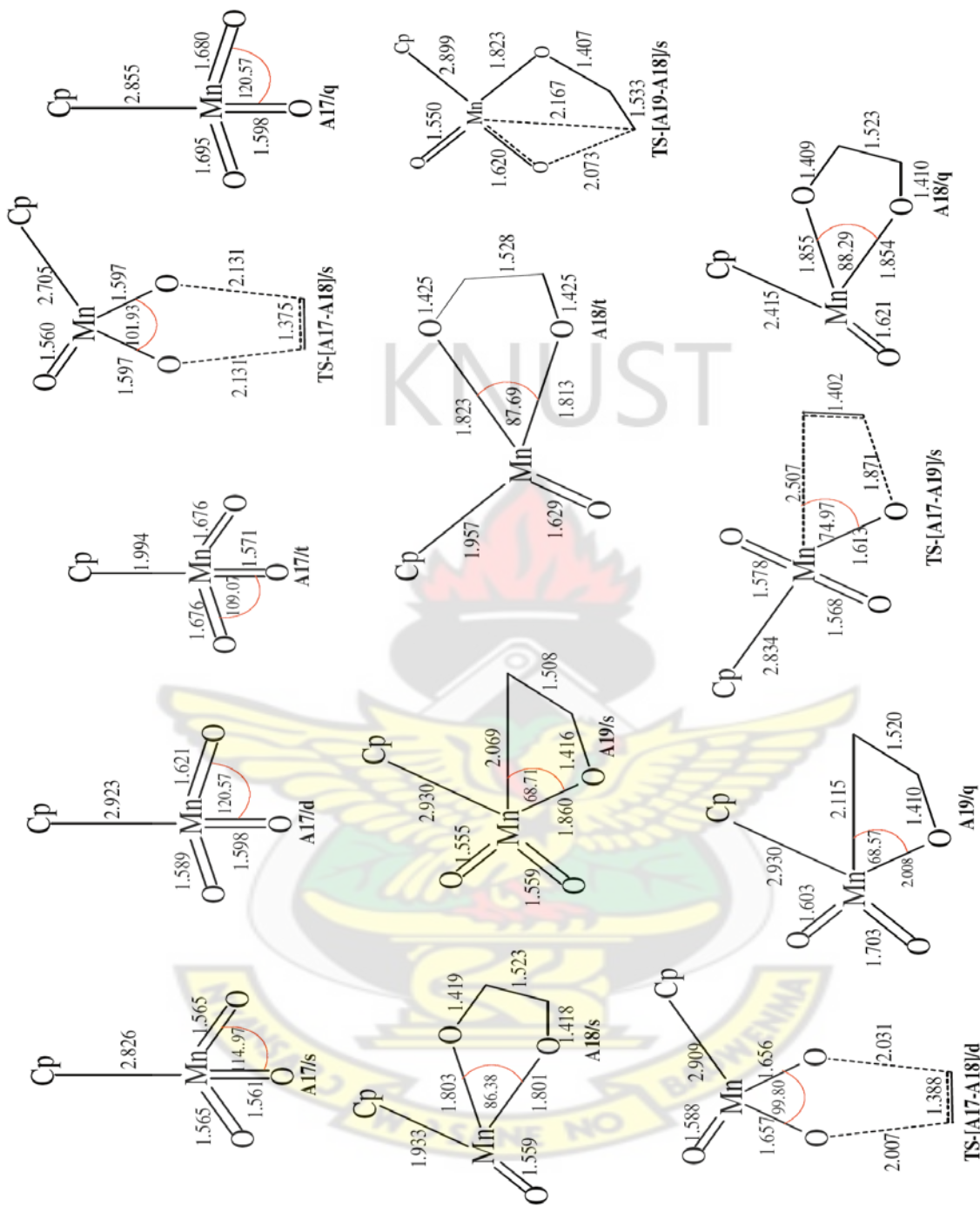


Fig 2.11: Optimized geometrical parameters of the main stationary points involved in the reaction of MnO_3Cp with ethylene. Distance in Å and bond angles in degrees.

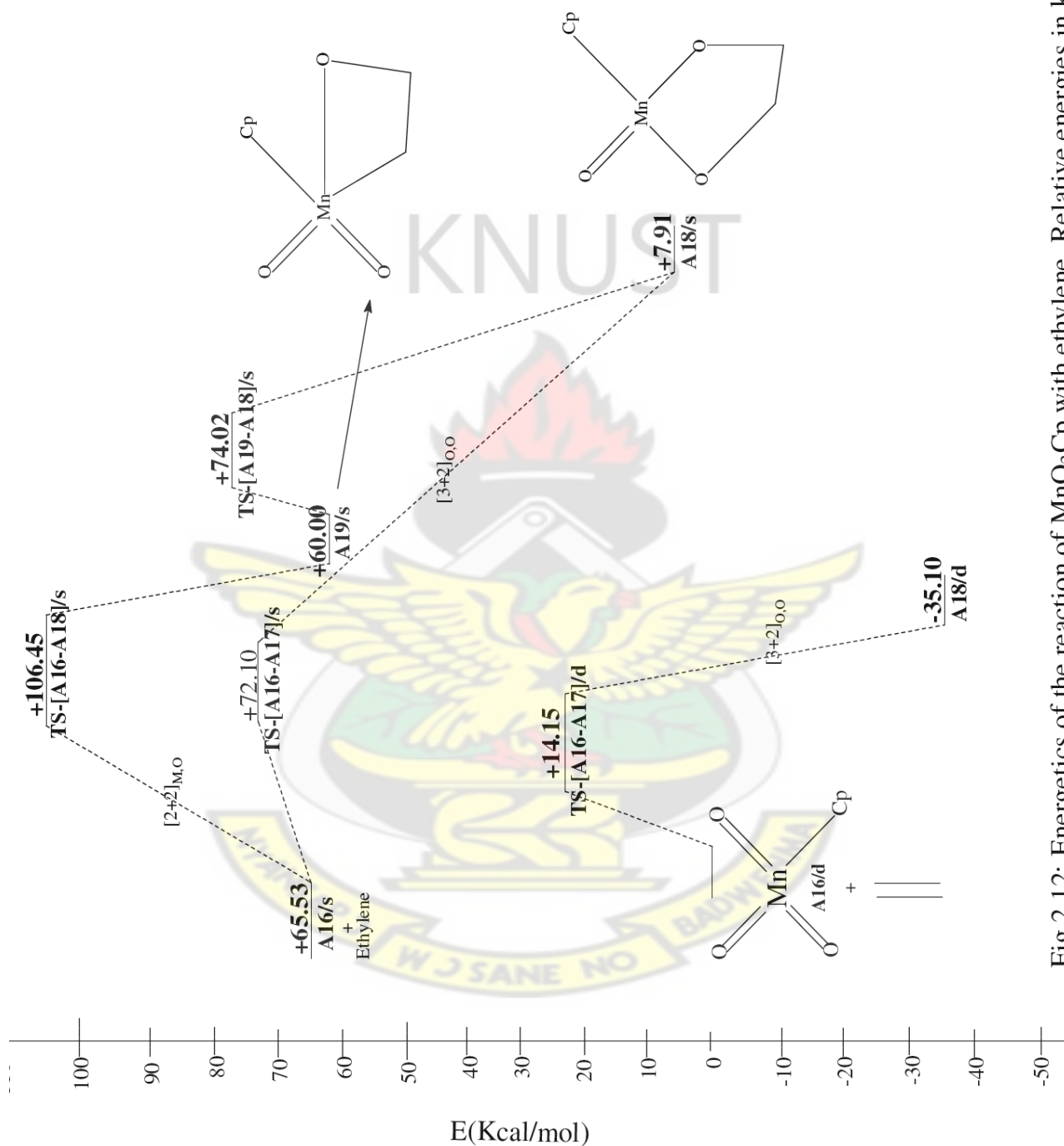


Fig 2.12: Energetics of the reaction of MnO_3Cp with ethylene. Relative energies in kcal/mo.

2.4 Conclusion

1. In the oxidation reaction between ethylene and permanganate (MnO_4^-), the direct [3+2] addition of the C=C bond of ethylene across the O=Mn=O bond of MnO_4^- to form the five-membered metallacycle intermediate is more stable than the [2+2] addition of the C=C bond of ethylene across the M=O bond to form the metallaioxetane in a agreement with the work of Houk *et. al.*, (1999). The suggested re-arrangement of the metallaioxetane intermediate to the dioxylate by Sharpless *et. al.* (1977) has a higher activation barrier than the direct [3+2] addition of ethylene across the two oxygen atoms of singlet MnO_4^- . The reaction between permanganate and ethylene would not result in the formation of the epoxide precursor.
2. In the reaction of ethylene with MnO_3Cl , the direct [3+2] addition of the C=C bond of ethylene across O=Mn=O moiety of doublet MnO_3Cl to form the dioxylate intermediate has a lower activation barrier intermediate than the direct and stepwise [3+2] addition of ethylene across the Cl-Mn=O and O=Mn=O bonds of singlet and doublet MnO_3Cl to form the five-membered metallacyclic intermediate. The most plausible pathway that leads to the epoxide precursor which is an unfavorable reaction will result from direct attack of the C=C bond of ethylene on one of the oxo-ligand of singlet MnO_3Cl . The dioxylate intermediate (structure **2** in Scheme 2.1) is more stable than the five-membered metallacycle (structure **6** in Scheme 2.1) and the metallaioxetane intermediate (structure **4** in Scheme 2.1). Thus in the reaction of MnO_3Cl with ethylene, the direct [3+2] addition to form the dioxylate intermediate on the doublet surface is thermodynamically and kinetically favorable.

3. In the reaction between $\text{MnO}_3(\text{CH}_3)$ and ethylene, the direct[3+2] addition of the C=C bond of ethylene across the O=Mn=O bond of doublet $\text{MnO}_3(\text{CH}_3)$ to form the dioxylate intermediate has a lower activation barrier than the [2+2] addition of ethylene across the Mn=O bond of $\text{MnO}_3(\text{CH}_3)$ to form the metallaoxetane intermediate and subsequent re-arrangement of the metallaoxetane intermediate to the dioxylate. The most plausible pathway to the formation of the epoxide precursor is by direct attack of the C=C bond of ethylene on one of the oxo-ligand of singlet $\text{MnO}_3(\text{CH}_3)$ which is an unfavorable reaction relative to the doublet starting reactant. Thus in the reaction of $\text{MnO}_3(\text{CH}_3)$ with ethylene, the [3+2] addition pathway is kinetically and thermodynamically favorable than the [2+2] addition pathway.
4. In the oxidation of ethylene by MnO_3Cp , the direct [3+2] addition of the C=C bond of ethylene across O=Mn=O moiety of doublet MnO_3Cp to form the dioxylate intermediate has a lower activation barrier than the two-step process via, the [2+2] addition across Mn=O bond to form the metallaoxetane and the subsequent re-arrangement of the metallaoxetane to the dioxylate intermediate. The dioxylate intermediate formed is more stable than the metallaoxetane intermediate. The reaction of MnO_3Cp with ethylene would not result in the formation of an epoxide precursor. Thus the [3+2] addition pathway is kinetically and thermodynamically favorable than the [2+2] addition pathway leading to the metallaoxetane intermediate for ethylene addition to MnO_3Cp .
5. In the reaction of $\text{MnO}_3(\text{OCH}_3)$ with ethylene, the initial attack of ethylene on one of the oxo-ligands of **A15/d** to form the intermediate **X/d** and subsequent re-arrangement to the dioxylate intermediate **A16/d** has a lower activation barrier than the direct [3+2] addition of the C=C bond of ethylene across the O=Mn=O bond of singlet $\text{MnO}_3(\text{OCH}_3)$ to form

the dioxylate intermediate **A15/s**. The most plausible pathway for the formation of the epoxide precursor is by the direct [3+2] addition of ethylene across the two oxygen atoms of singlet $\text{MnO}_3(\text{OCH}_3)$ followed by re-arrangement. The reaction of $\text{MnO}_3(\text{OCH}_3)$ with ethylene would not lead to the formation of the metallaioxetane intermediate. The [3+2] addition pathway on the doublet surface is kinetically and thermodynamically favorable for ethylene addition to $\text{MnO}_3(\text{OCH}_3)$

6. In the oxidation of ethylene by $\text{MnO}_3(\text{NPH}_3)$, the direct [3+2] addition of the C=C bond of ethylene across the O=Mn=O bond of singlet $\text{MnO}_3(\text{NPH}_3)$ to form the dioxylate intermediate will be competitive with the direct [3+2] addition across O=Mn=N and the [2+2] addition across the M=N bond of singlet $\text{MnO}_3(\text{NPH}_3)$ leading to the formation of four-membered metallacycle. The five-membered metallacycle (structure **6** in Scheme 2.1) formed from the [3+2] addition pathway is the most stable. The most plausible pathway to the formation of the epoxide precursor is by initial [3+2] addition. Thus in the reaction of ethylene with $\text{MnO}_3(\text{NPH}_3)$, the direct [3+2] addition of ethylene across the two oxygen atoms of singlet $\text{MnO}_3(\text{NPH}_3)$ is kinetically favorable and the [3+2] addition across the nitrogen and oxygen atom is thermodynamically favorable.
7. Generally, in the reaction of ethylene with LMnO_3 , the [3+2] addition pathway is favored kinetically and thermodynamically when (L= O^- , Cp, OCH_3 , Cl, CH_3 , NPH_3).

REFERENCES

- Burrell, A. K.; Cotton, F. A.; Daniels, L. M.; Petricek, V. (1995) Structure of Crystalline $(C_5Me_5)ReO_3$ and Implied Nonexistence of $(C_5Me_5)Tc_2O_3$. *Inorg.Chem.*34: 4253
- Clark, M.; Cramer, R. D.; Opdenbosch, N. V. (1989) Validation of the general purpose tripos5.2 force field.*J. Comp. Chem.* 10: 982-1012.
- Corey, E. J.; Noe, M. C. (1997) Kinetic Investigations Provide Additional Evidence That an Enzyme-like Binding Pocket Is Crucial for High Enantioselectivity in the Bis-Cinchona Alkaloid Catalyzed Asymmetric Dihydroxylation of Olefins. *J. Am. Chem. Soc.* 118: 319 - 329.
- Criegee, R. (1936) Osmiumsäure-ester als Zwischenprodukte bei Oxydationen. *Justus Liebigs Ann. Chem.* 522:75-96.
- Criegee, R.; Marchand, B.; Wannowius, H. (1942) Zur Kenntnis der organischen Osmium-Verbindungen. II. Mitteilung. *Justus Liebigs Ann. Chem.* 550:99-133.
- Dapprich, S.; Ujaque, G.; Maseras, F.; Lledos, A.; Musaev, D.G.; Morokuma, K. (1996) Theory Does Not Support an Osmaoxetane Intermediate in the Osmium-Catalyzed Dihydroxylation of Olefins. *J. Am. Chem. Soc.* 118: 11660 - 11661.
- Del Monte, A. J.; J. Haller, J.; Houk, K. N.; Sharpless, K. B.; Singleton, D. A.; Strassner, T.; Thomas, A. A. (1997) Experimental and Theoretical Kinetic Isotope Effects for Asymmetric Dihydroxylation. Evidence Supporting a Rate-Limiting [3+2] Cycloaddition.*J. Am. Chem. Soc.* 119: 9907 - 9908.

Dunning, T. H. Jr.; Hay, P. J. (1976) In: Modern Theoretical Chemistry, H. F. Schaefer, III, Vol.3; Plenum, New York.

Enemark, J. H.; Young, C. G. (1993) Bioinorganic Chemistry of Pterin-Containing Molybdenum and Tungsten Enzymes. *Adv. Inorg. Chem.* 40: 1.

Gisdakis, P.; Rösch, N. (2001) [2+3] Cycloaddition of Ethylene to Transition Metal Oxo Compounds. Analysis of Density Functional Results by Marcus Theory. *J. Am. Chem. Soc.* 123:697 - 701.

Haller, J.; Strassner, T.; Houk, K. N. (1997) Experimental and Theoretical Kinetic Isotope Effects for Asymmetric Dihydroxylation. Evidence Supporting a Rate-Limiting [3+2] Cycloaddition. *J. Am. Chem. Soc.* 119: 8031.

Herrmann, W. A.; Serrano, R.; Bock, H. (1984) *Angew. Chem., Int. Ed. Engl.* 23: 383.

Houk, K. N.; Strassner, T. (1999) Establishing the [3+2] Mechanism for the Permanganate Oxidation of Alkenes by Theory and Kinetic Isotope Effects. *J. Org. Chem.* 64: 800 – 802

Jorgensen, K. A. (1989) Transition-metal-catalyzed epoxidation. *Chem. Rev.* 89:431- 458

K.B. Wiberg (Ed.), Oxidation in Organic Chemistry. Part A, Academic Press, New York, 1965, pp.1-68.

Klahn-Oliva, A. H.; Sutton, D. (1984) (Pentamethylcyclopentadienyl)trioxorhenium, (.eta.⁵-C₅Me₅)ReO₃. *Organometallics*. 3:1313.

Kühn, F. E.; Herrmann, W. A.; Hahn, R.; Elison, M.; Blumel, J.; Herdtweck, E. (1994) *Organometallics*. 13: 1601

M. Rouhi, M. (1997) Charting a path for macromolecules, *Chem. Eng. News* 75: 23.

Mijs, W.; Jonge, C. R. (1986) (Eds.) Organic Synthesis by oxidation with Metal Compound. Plenum, New York, 1986.

Nelson, D. W.; Gypser, A.; Ho, P. T.; Kolb, H. C.; Kondo, T.; Kwong, H.; McGrath, D. V.; Rubin, A. E.; Norrby, P.; Gable, K. P.; Sharpless, K. B. (1997) Toward an Understanding of the High Enantioselectivity in the Osmium-Catalyzed Asymmetric Dihydroxylation. Electronic Effects in Amine-Accelerated Osmylations. *J. Am. Chem. Soc.* 119: 1840.

Palenik, G. J. (1967) Crystal structure of potassium manganate. *Inorg. Chem.* 6:507–511

Pidun, U.; Boehme, C.; Frenking, G. (1996) Theory Rules Out a [2 + 2] Addition of Osmium Tetraoxide to Olefins as Initial Step of the Dihydroxylation Reaction. *Angew. Chem. Int. Ed. Engl.* 35: 2817-2820.

Pietsch, M. A.; Russo, T. V.; Murphy, R. B.; Martin, R. L.; Rappe, A. K. (1998) LReO_3 Epoxidizes, *cis*-Dihydroxylates, and Cleaves Alkenes as Well as Alkenylates Aldehydes: Toward an Understanding of Why. *Organometallics* 17: 2716.

San Filippo, J.; Chern, C. (1977) chemisorbed chromyl chloride as a selective oxidant *J. Org. Chem.* 42: 2182.

Schröder, M. (1980) Osmium tetraoxide *cis*-hydroxylation of unsaturated substrates. *Chem. Rev.* 80: 187 - 213.

Sharpless, K. B.; Akashi, K. (1975) Oxidation of alcohols to Aldehydes by reagents derived from chromyl chloride. *J. Am. Chem. Soc.* 97: 5927.

Sharpless, K. B.; Teranishi, A. Y.; Bäckvall, J. E. (1977) Chromyl chloride oxidations of olefins. Possible role of organometallic intermediates in the oxidations of olefins by oxo transition metal species. *J. Am. Chem. Soc.* 99: 3120.

Sono, M.; Roach, M. P.; Coulter, E. D.; Dawson, H. E. (1996) Heme-Containing Oxygenases. *Chem Rev.* 96: 2841.

Spartan, Waefunction, Inc.; 18401 Von Karman Ave., # 370, Irvine, CA, 92715, USA.

Strassner, T.; Busold, M. (2001) A Density Functional Theory Study on the Mechanism of the Permanganate Oxidation of Substituted Alkenes. *J. Org. Chem.* 66:672-676.

Strassner, T.; Busold, M. (2004) Density Functional Theory Study on the Initial Step of the Permanganate Oxidation of Substituted Alkynes. *J. Phys. Chem. A.* 108:4455- 4458.

Tia, R.; Adei, E. (2009) Density functional theory study of the mechanism of oxidation of ethylene by chromyl chloride. *Inorg. Chem.* 48: 11434-11443.

Tia, R.; Adei, E. (2011) [3+2] versus [2+2] addition of metal oxides across C=C bonds: A theoretical study of the mechanism of oxidation of ethylene by osmium oxide complexes. *Computational and Theoretical Chemistry.* 977: 140 - 147.

Torrent, M.; Deng, L.; Duran, M.; Sola, M.; Ziegler, T. (1997) Density Functional Study of the [2+2] and [2+3] Cycloaddition Mechanisms for the Osmium-Catalyzed Dihydroxylation of Olefins. *Organometallics.* 16: 13-19.

Torrent, M.; Deng, L.; Duran, M.; Sola, M.; Ziegler, T. (1999) Mechanism for the formation of epoxide and chlorine-containing products in the oxidation of ethylene by chromyl chloride: a density functional study. *Can. J. Chem.* 77: 1476 - 1491.

Torrent, M.; Deng, L.; Ziegler, T. (1998) A Density Functional Study of [2+3] versus [2+2] Addition of Ethylene to Chromium–Oxygen Bonds in Chromyl Chloride. *Inorg. Chem.* 37: 1307.

Torrent, M.; Deng, L.; Ziegler, T. (1998) A Density Functional Study of [2+3] versus [2+2] Addition of Ethylene to Chromium–Oxygen Bonds in Chromyl Chloride. *Inorg. Chem.* 37: 1307.

Wadt, W. R.; Hay, P. J. (1985) Ab initio effective core potentials for molecular calculations. Potentials for main group elements Na to Bi. *J. Chem. Phys.* 82: 284.

Wadt, W. R.; Hay, P. J. (1985) Ab initio effective core potentials for molecular calculations. Potentials for K to Au including the outermost core orbitals. *J. Chem. Phys.* 82: 299.

Waters, W. A. (1958) *Quart. Rev.* 12: 29.

Wistuba, T.; Limberg, C. (2001) Reaction of Permanganyl chloride with Olefins: Intermediates and Mechanism as Derived from Matrix-isolation Studies and Density Functional Theory Calculation. *Chem. Euro. J.* 21:4674.

CHAPTER THREE

A DENSITY FUNCTIONAL STUDY OF THE MECHANISMS OF OXIDATION OF ETHYLENE BY TECHNETIUM OXO COMPLEXES

3.1 INTRODUCTION

The development of new catalytic reactions that perform chemical transformations with high selectivity and efficiency is a key objective in chemical research. Many new reactions are discovered serendipitously, but increasing mechanistic knowledge permits the rational design of new reactions of key intermediates.

Although enormous efforts have been made to find out experimentally the mechanism of transition-metal catalyzed processes, most reactions are still little understood in terms of mechanistic details. (Enemark and Young, 1993; Sharpless *et. al.*, 1975; Mijs and de Jonge, 1986; Sono *et. al.*, 1996). Transition-metal-complex-mediated oxygen-transfer reactions are of considerable importance in chemistry, both in the industrial arena and under laboratory conditions. The addition of osmium tetroxide across the C=C double bond of olefins yielding a metallacyclopentane-2,5-dioxolane is the initial step of *cis*-dihydroxylation, one of the most elegant reactions for a 1,2-functionalization of alkenes (Criegee *et. al.*, 1936; 1942; Döbler *et. al.*, 2001; Jonsson *et. al.*, 2001). Some transition metal-oxo complexes such as CrO₂Cl₂ (Jorgensen, 1989; San Filippo *et. al.*, 1977) react with olefins to form epoxides, chlorohydrins and vicinal dihalides whereas others such as MnO₄⁻ and OsO₄⁻ react to form diols without significant epoxide formation (Schröder, 1980; Wiberg, 1965).

The oxo complexes of group VII (Mn, Tc, and Re) are of great interest for their tendency toward epoxidation and dihydroxylation. MnO₄⁻ is commonly used as a dihydroxylation agent

(March, 1985) while the system $\text{CH}_3\text{ReO}_3/\text{H}_2\text{O}_2$ is experimentally known to be efficient epoxidation catalysts (Al-Ajlouni *et. al.*, 1995; 1996; Herrmann *et. al.*, 1993; 1997; Romão *et. al.*, 1997). With allusion to these two types of oxidation reactions, Tc is intermediate (Herrmann *et.al.*, 1990). Electronic and structural properties of Mn (Dickson *et al.*, 1998), Tc (Herrmann *et.al.*, 1990) and Re (Herrmann *et. al.*, 1997; Romão *et. al.*, 1997) compounds have previously been analyzed in various density functional studies. Differences in reactivity between analogous Tc and Re oxo compounds have been attributed to relativistic effects on the Lewis acidity and the polarizability of the MO_3 moiety. Re was found to form a stronger and harder (less polarizable) Lewis acid center than Tc (Herrmann *et. al.*, 1995; 1997; Romão *et. al.*, 1997). CpReO_3 has been shown to react with olefins to predominately form dioxylates (Burrell *et al.*, 1995; Herrmann *et .al.*, 1984; Klahn-olive *et al*, 1984 and Kühnet. *al.*, 1994).

Gisdakis and Rösch (2001) in a theoretical studies of ethylene addition to LTcO_3 (L= Cp, Cl, CH_3 and O⁻) calculated the [3+2] addition pathway to form the dioxylate to have a lower activation barrier than the corresponding [2+2] addition pathway leading ultimately to the formation of the metallaoxetane.

Haunschild *et al.*, (2008) calculated the [2+2] addition pathway to be favored when a transition metal-carbon double bond is present. For ethylene addition to $\text{TcO}_2(\text{CH}_3)(\text{CH}_2)$, the [2+2] addition across the $\text{Tc}=\text{CH}_2$ becomes more favorable than the [3+2] addition pathway across the two oxygen atoms and oxygen and carbon atoms of $\text{TcO}_2(\text{CH}_3)(\text{CH}_2)$.

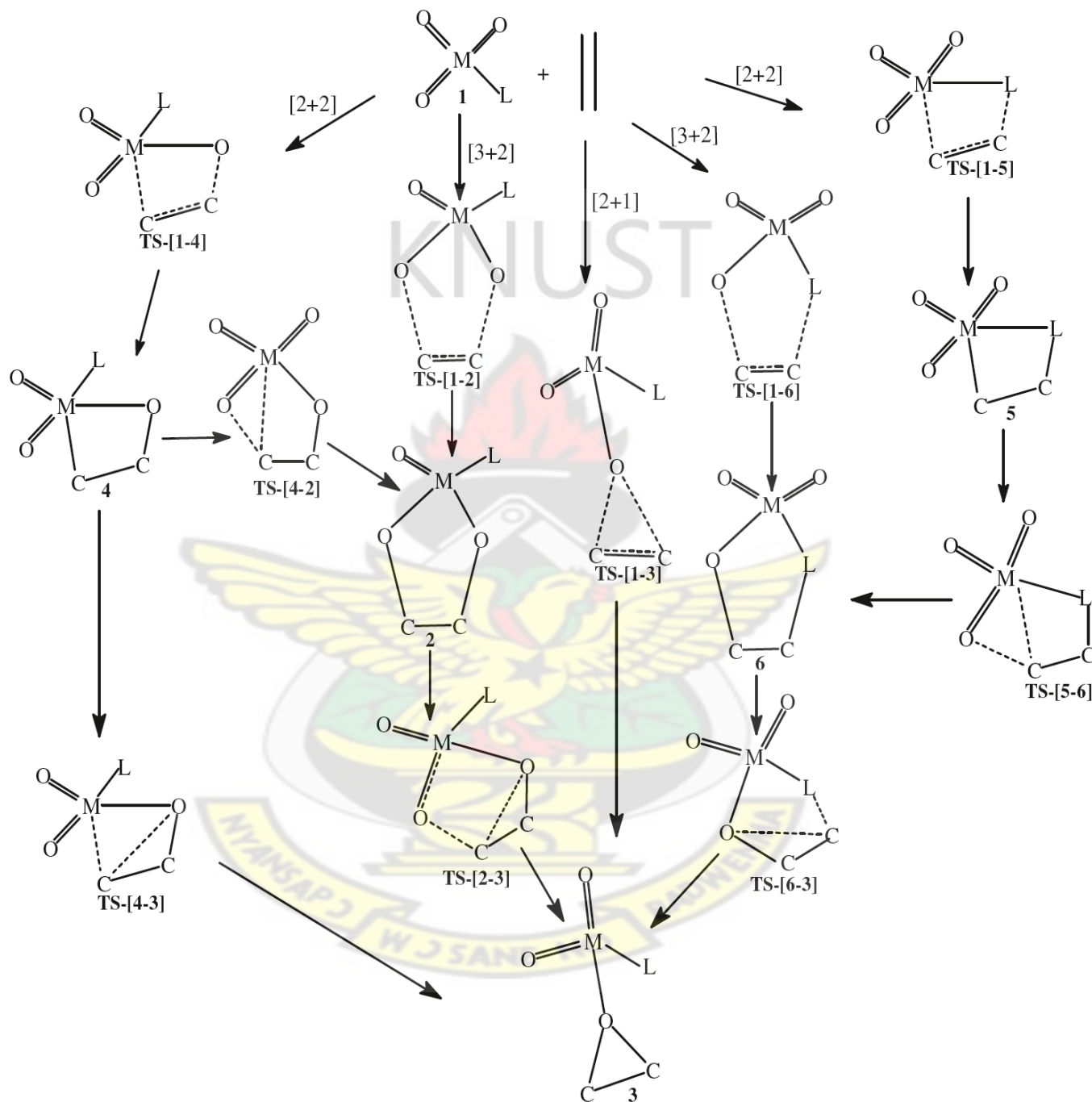
The aim of this work is to extend the work of Gisdakis and Rösch, (2001) by reporting the calculated potential energy surfaces for the [3 + 2] and [2 + 2] addition of LTcO_3 (L= O⁻, Cl, Cp,

CH₃, OCH₃, NPH₃) to ethylene in order to explore the mechanistic pathway for the formation of the epoxide precursor by employing hybrid density functional theory at the B3LYP/LACVP* level of theory. Other [3+2] and [2+2] addition pathways are explored in addition to those already studied. The singlet, doublet, triplet and quartet electronic states of each species are explored where possible.

KNUST



Scheme 3.1: Proposed pathway for the reaction of LMO₃ with ethylene



3.2 DETAILS OF CALCULATION

All calculation were carried out with Spartan '08 V1.1.0 Molecular Modeling programs (Wavefunction, 2008; 2010) at the DFT B3LYP/LACVP* level of theory. The LACVP* basis set is a relativistic effective core –potential that describes the atoms H-Ar with the 6-31G* basis while heavier atoms are modeled with the LANL2DZ basis set which uses the all-electron valence double zeta basis set (D95V), developed by Dunning, for first row elements(Dunning and Hay, 1976) and the Alamos ECP plus double zeta basis set developed by Wadt and Hay for the atoms Na-La, Hf-Bi (Hay and Wadt, 1985a; 1985b; Wadt and Hay, 1985).

The starting geometries of the molecular systems were constructed using Spartan's graphical model builder and minimized interactively using the sybyl force field (Clark's *et. al.*, 1989). All geometries were fully optimized without any symmetry constraints. A normal mode analysis was employed to verify the nature of the stationery point. Equilibrium geometries were characterized by the absence of imaginary frequencies.

The transition state structures will be located by a series of constrained geometry optimization in which the forming-and breaking–bonds are fixed at various lengths whiles the remaining internal coordinates were optimized. The approximate stationary points located from such a procedure were then fully optimized using the standard transition state optimization procedure in Spartan. All first–order saddle- point were shown to have a Hessian matrix with a single negative eigenvalue, characterized by an imaginary vibrational frequency along the reaction coordinate. All computations shall be performed on Dell precision T3400 Workstation computers.

3.3 Results and Discussion

3.3.1 Reaction of TcO_4^- with ethylene

The optimized geometries and relative energies of the main stationary points involved in the reaction between TcO_4^- and ethylene are shown in Fig.3.1 and Fig.3.2, respectively. The density functional theory (DFT) geometry optimization of TcO_4^- (**B1**) on a singlet potential energy surface [PES] has all the Tc-O bonds at 1.74 Å. A triplet pertechnetate reactant (**B1/t**) has been computed to be 65.16 kcal/mol less stable in relation to the singlet reactant. The singlet reactant **B1/s** is 117.37 kcal/mol more stable than the doublet reactant (**B1/d**). No quartet reactant could be located on the reaction surface.

On the singlet surface, the direct [3+2] addition of the C=C bond of ethylene across the O=Tc=O bonds of TcO_4^- through transition state **TS-[B1-B2]/s** to form the dioxylate **C2/s** has an activation barrier of 24.22 kcal/mol and reaction energy of 9.46 kcal/mol exothermic. The calculated transition state is highly symmetrical and synchronous with respect to the newly-forming C-O bonds (1.90 Å). Gisdakis and Rösch, (2001) had computed the barrier along this route to be +27.30 kcal/mol by the hybrid B3LYP approach, with effective core potentials and double-zeta basis sets, LanL2DZ, for the transition metals and 6-311G(d,p) basis sets for H, C, O, and F

No triplet transition state linking the reactant to the products could be located. However, a triplet dioxylate species product **B2/t** was located and found to be -58.14 kcal/mol exothermic. In the singlet product **B2/s**, the two Tc=O bonds to the 'spectator' oxygen atoms (the oxygen atom not part of the ring) are equal (1.73 Å) and those to the oxygen atom involved in the ring are also equal (1.98 Å). The triplet product **B2/t** has the two Tc=O double bonds to the 'spectator'

oxygen atoms equal (1.75 Å) and those to the oxygen atom involved in the ring are also equal (1.98 Å). The doublet **B2/d** and quartet **B2/q** dioxylate species have reaction energies of -70.26 and -18.94 kcal/mol respectively.

The formation of the singlet metallaoxetane **B3/s** through the transition state **TS-[B1-B3]/s** by [2+2] addition of C=C bond of ethylene across Tc=O bond of the pertechnetate complex **B1** has an activation barrier of 48.20 kcal/mol and reaction energy of 17.40 kcal/mol. A triplet metallaoxetane **B3/t** has reaction energy of -16.58 kcal/mol. No triplet transition state could be located on the surface. The Tc-C and C-O bonds in the singlet metallaoxetane **C3/s** are 2.18 and 1.40 Å respectively. The Tc-C bond is 0.02 Å shorter in the triplet rhenaoxetane **B3/t**. However, the C-O bond is 0.018 Å longer in the triplet metallaoxetane. The doublet species **B3/d** with a metallaoxetane-like structure but with an elongated M-C bond (3.539 Å) have reaction energy of -32.50 kcal/mol. No quartet metallaoxetane structure was located was found on the reaction surface.

The re-arrangement of the metallaoxetane to the dioxylate (**TS-[4-3]** in Scheme 1) as suggested by Sharpless *et. al.* (1977) in the chromyl chloride oxidation of olefins was also explored for the reaction of TcO_4^- with ethylene. The re-arrangement of the singlet metallaoxetane to the dioxylate through transition state **TS-[B3-B2]/s** has activation barrier of +56.53 kcal/mol. Thus, the barrier for the re-arrangement of the singlet metallaoxetane to the dioxylate is higher than the activation barrier for the direct [3+2] addition across the two oxygen atoms of TcO_4^- . This rule out the two-step process for the formation of dioxylate from the metallaoxetane and therefore the dioxylate intermediate would be formed from the direct [3+2] addition of ethylene across the O=Tc=O bond of singlet TcO_4^- .

The potential energy surface of the reaction of TcO_4^- with ethylene was further explored in an attempt to locate an epoxide precursor ($\text{O}_3\text{-Tc-OC}_2\text{H}_4$) (**3** in Scheme 3.1), but no such minimum was found on these reaction surfaces.

The reaction of TcO_4^- with ethylene is likely to occur on a singlet PES and the [3+2] addition of the O=Tc=O bonds of TcO_4^- across the C=C bond of ethylene is kinetically and thermodynamically favorable than the two-step process via the [2+2] addition of the Tc=O bond across C=C bond of ethylene to form the metallaoxetane intermediate and subsequent rearrangement.



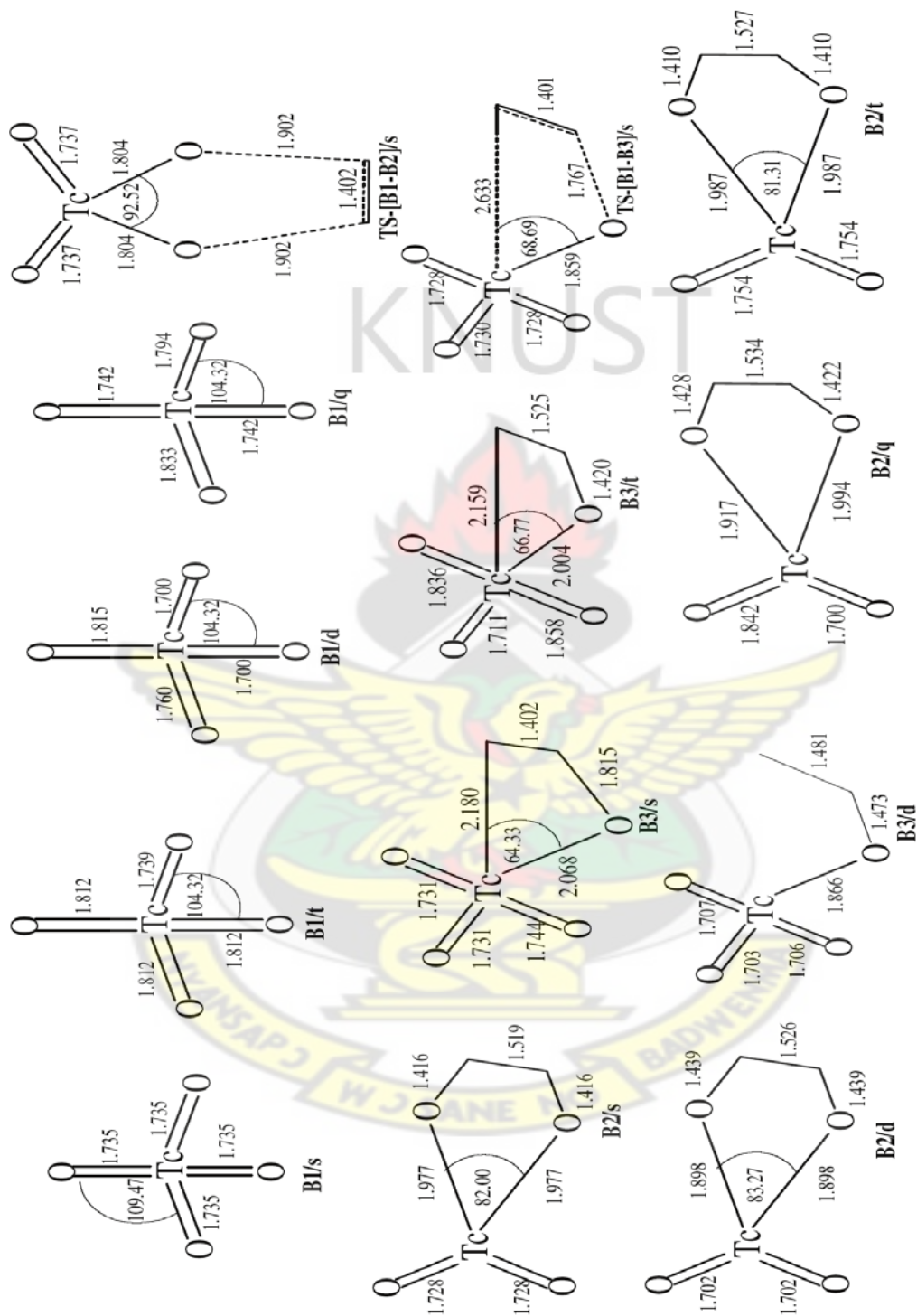


Figure 3.1: Optimized geometries parameters of the main stationary points involved in the reaction between TcO_4^- and ethylene. Bond distances in Å and angles in degrees

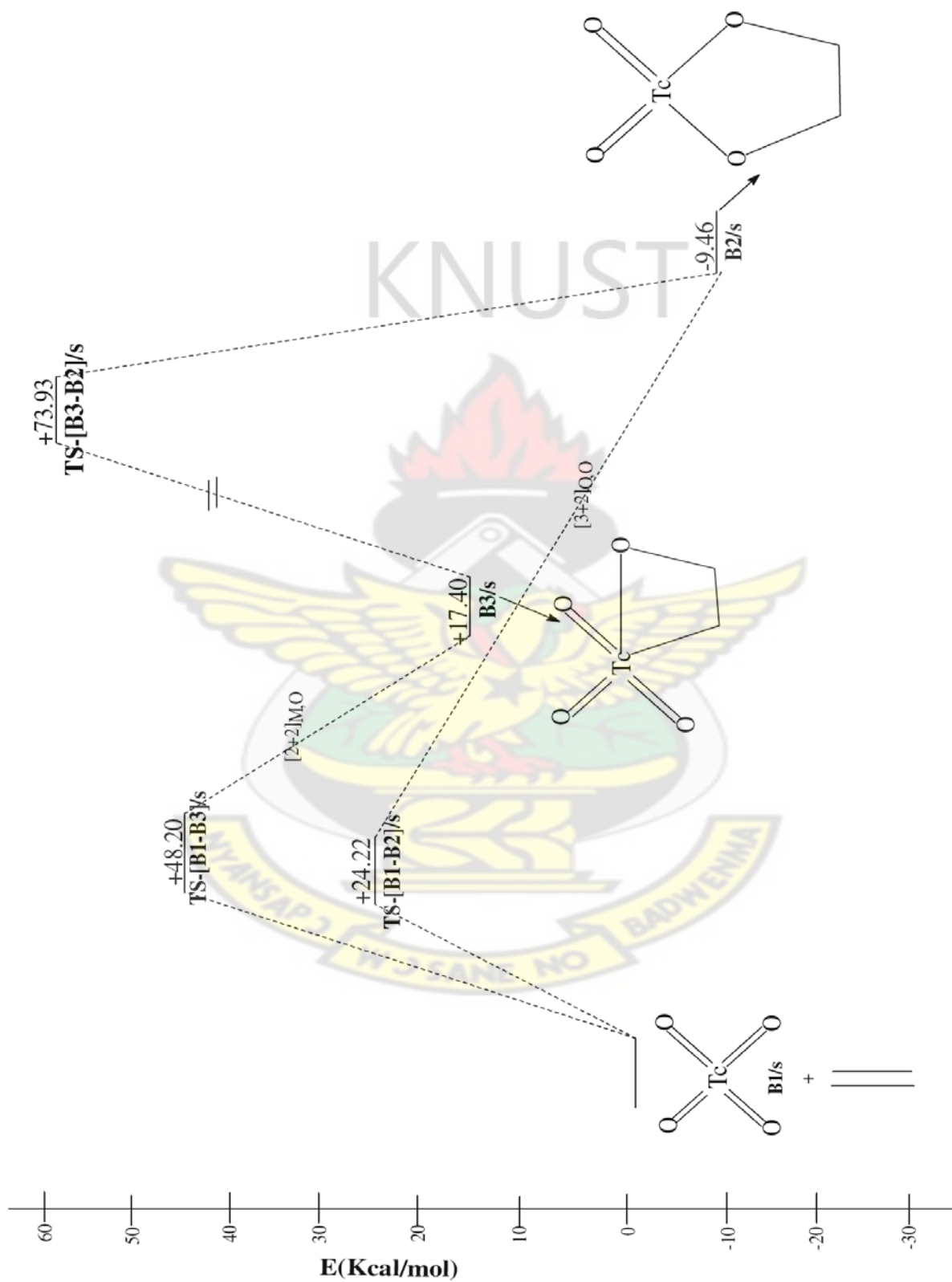


Figure 3.2: Energetics of the reaction of TcO_4^- and ethylene. Relative energies in kcal/mol (s=singlet, d=doublet)

3.3.2 Reaction of TcO₃Cl with ethylene

Figures 3.3 and 3.4 shows the optimized geometries and relative energies of the main stationary points involved in the reaction between TcO₃Cl and ethylene respectively. The DFT geometry optimization of TcO₃Cl on a singlet potential energy surface yielded a minimum **B4/s** in which the three Tc=O bonds is each 1.70 Å long and the Tc-Cl bond is 2.26 Å long.

In addition to the singlet reactant, a doublet and a triplet have also been optimized. A doublet reactant **B4/d** has been computed to be 62.89 kcal/mol more stable than the singlet reactant **B4/s** and 111.26 kcal/mol more stable in relation to the triplet reactant **B4/t**. In the doublet reactant **B4/d**, the Tc-Cl bond is 0.13 Å longer than that in the singlet structure **B4/s** and 0.12 Å longer than that in the triplet structure **B4/t**. A quartet reactant **B4/q** has also been computed and found to be 58.88 kcal/mol less stable than the doublet reactant. Thus of all the reactants structures optimized, the doublet is the most stable.

On the singlet surface, the [3+2] addition of the C=C bond of ethylene across the O=Tc=O bonds of singlet TcO₃Cl through transition state **TS-[B4-B5]/s** to form the dioxylate **B5/s** has an activation barrier of 7.57 kcal/mol and reaction energy of -28.13 kcal/mol in agreement with the activation and reaction energies reported by Gisdakis and Rösch (2001) at the hybrid B3LYP approach, with effective core potentials and double-zetabasis sets, LanL2DZ, for the transition metals and 6-311G(d,p) basis sets for H, C, O, and F.

On the doublet surface, the [3+2] addition of the C=C bond of ethylene across the O=Tc=O functionality of TcO₃Cl could follow either a stepwise or a concerted pathway. On the concerted pathway, the [3+2] addition of ethylene across the two oxygen atoms of doublet TcO₃Cl has an activation barrier has +20.18 kcal/mol and reaction energy of 17.22 kcal/mol exothermic through the doublet transition state **TS-[B4-B5]/d** to form the dioxylate **B5/d**. The Tc-Cl bond in the

doublet transition state is 0.01 Å short, in comparison to the Tc-Cl bond distance (2.393 Å) in the doublet reactant. On the stepwise pathway, one of the C=C π of ethylene attacks an oxo-ligand of TcO₃Cl to form the organometallic intermediate **X/d** through transition state **TS-[B4-X]/d**. The activation barrier for the first-step that leads to the formation of the intermediate **X/d** is +30.38 kcal/mol. The intermediate **X/d** has endothermicity of +24.67 kcal/mol. The intermediate **X/d** could re-arrange through transition state **TS-[X-B5]/d** to form the dioxylate intermediate **B5/d**. The activation barrier and reaction energy of the dioxylate intermediate **B5/d** are -4.45 and -41.89 kcal/mol.

No triplet transition state connecting the reactant to the product could be located. However, a triplet dioxylate **B5/t** was located and found to be 44.73 and 55.64 kcal/mol more stable than the singlet **B5/s** and doublet **B6/d** dioxylate products respectively. A quartet dioxylate **B5/q** product has been found to be 53.45 kcal/mol exothermic.

On the doublet surface, the [3+2] addition of the C=C bond of ethylene across the O=Tc-Cl functionality of doublet TcO₃Cl, a pathway not explored in the study of Gisdakis and Rösch (2001) leads to an organometallic intermediate **X/d**. The intermediate **X/d** re-arranges through transition state **TS-[X-B6]/d** to form the five membered metallacycle **B6/d**. The activation barrier and reaction energy along this route are 18.12 and -14.71 kcal/mol.

On the singlet pathway, the direct [3+2] addition of the C=C bond of ethylene across the O=Tc-Cl functionality of singlet TcO₃Cl has activation barrier and reaction energy of +14.68 and -1.69 kcal/mol respectively. A triplet dioxylate **B6/t** is 37.28 kcal/mol more stable than the doublet dioxylate **B6/d**. The quartet dioxylate species **B6/q** is computed to be 44.06 kcal/mol more

stable than the doublet product **B6/d**. No triplet and quartet transition state linking the reactants to the products were located on the reaction surfaces.

The formation of doublet metallaoxetane **B7/d** through the doublet transition state **TS-[B4-B7]/d** by [2+2] addition of the C=C bond of ethylene across Tc=O bond of the doublet TcO₃Cl complex has an activation barrier of 29.12 kcal/mol and exothermicity of 6.53 kcal/mol exothermic. Attempts at forming the metallaoxetane intermediate from the stepwise pathway, proved unsuccessful. This indicates that the metallaoxetane intermediate is formed from the concerted pathway and not the stepwise route.

The singlet transition state **TS-[B4-B7]/s** linking the reactants to the product **B7/s** has an activation barrier of 32.07 kcal/mol and reaction energy of 0.41 kcal/mol. A triplet metallaoxetane **B7/t** has been computed to be 33.71 kcal/mol more stable than the singlet metallaoxetane **B7/s**. A quartet metallaoxetane intermediate **B7/q** has reaction energy of 34.23 kcal/mol. No triplet and quartet [2+2] transition states connecting the reactants to the products could not be located on the reaction surface explored.

The re-arrangement of the singlet, doublet, triplet and quartet metallaoxetane to the five-membered dioxylate (**TS-[4-2]** in Scheme 3.1) was explored for the reaction of TcO₃Cl with ethylene. The transition state **TS-[B7-B5]/s** for the re-arrangement of the singlet metallaoxetane to the singlet dioxylate have activation barrier of +27.83 kcal/mol. On the doublet surface, the activation barrier is +42.49. No transition state was located for the re-arrangement of the metallaoxetane to the dioxylate on the triplet and quartet surfaces.

The overall activation barriers (+26.75 and +42.49 kcal/mol) for the re-arrangement of the singlet and doublet metallaoxetane to the dioxylate is higher than the activation barrier for the

direct [3+2] addition across the two oxygen atoms of singlet and doublet TcO_3Cl . This means the formation of the dioxylate on both the singlet and doublet surfaces should proceed from the direct [3+2] addition of ethylene across the $\text{O}=\text{Tc}=\text{O}$ bonds of singlet and doublet TcO_3Cl .

An epoxide precursor was explored from the reaction of TcO_3Cl with ethylene; this was unsuccessful in the case of TcO_4^- .

The transition state (**TS-[B6-E]/s** in Fig 3.4) for the re-arrangement of the singlet five-membered metallacycle (**TS-[1-6]** in Scheme 3.1) to the epoxide precursor has activation barrier of +22.66 kcal/mol and endothermicity of +5.73 kcal/mol.

The transition states (**TS-[4-3]** in Scheme 3.1) for the rearrangement of the singlet four-membered metallaioxetane to the epoxide precursor have activation barrier and reaction energy of +33.76 and +3.62 kcal/mol. Also, the activation barrier and reaction energy for the singlet direct one-step addition of the $\text{C}=\text{C}$ bond across one oxygen atom of TcO_3Cl are +28.96 and 4.03 kcal/mol. The formation of the epoxide precursor from **X/d** through transition state **TS-[X-E]/d** to the epoxide precursor **E/d** has activation barrier and exothermicity of +14.46 and -9.64 kcal/mol. The most plausible pathway for the formation of the epoxide precursor is from the intermediate **X/d** followed by re-arrangement.

The reaction of ethylene with TcO_3Cl is likely to occur on the doublet PES and even though the formation of the epoxide and chlorohydrins precursors could also be occur, the dioxylate will preferentially be formed.

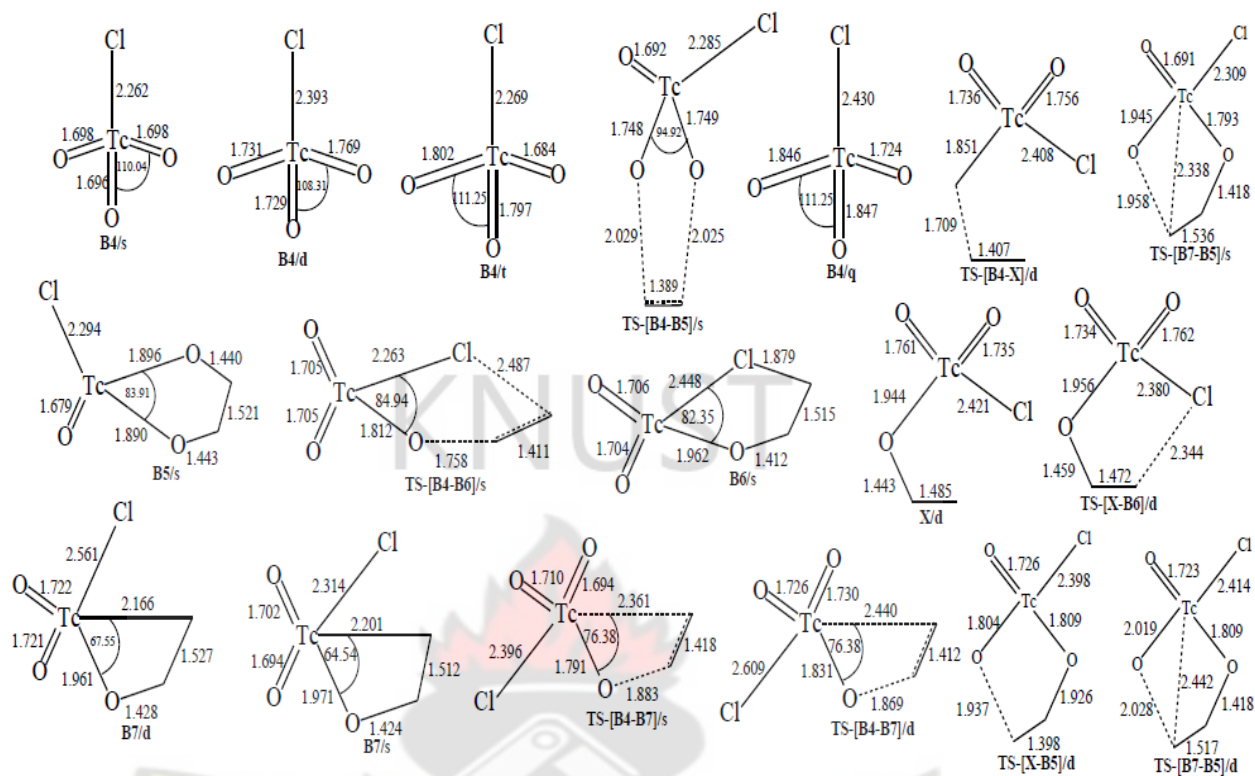


Figure 3.3: Optimized geometries parameters of the main stationary points involved in the reaction of TcO_2Cl with ethylene. Distance in Å

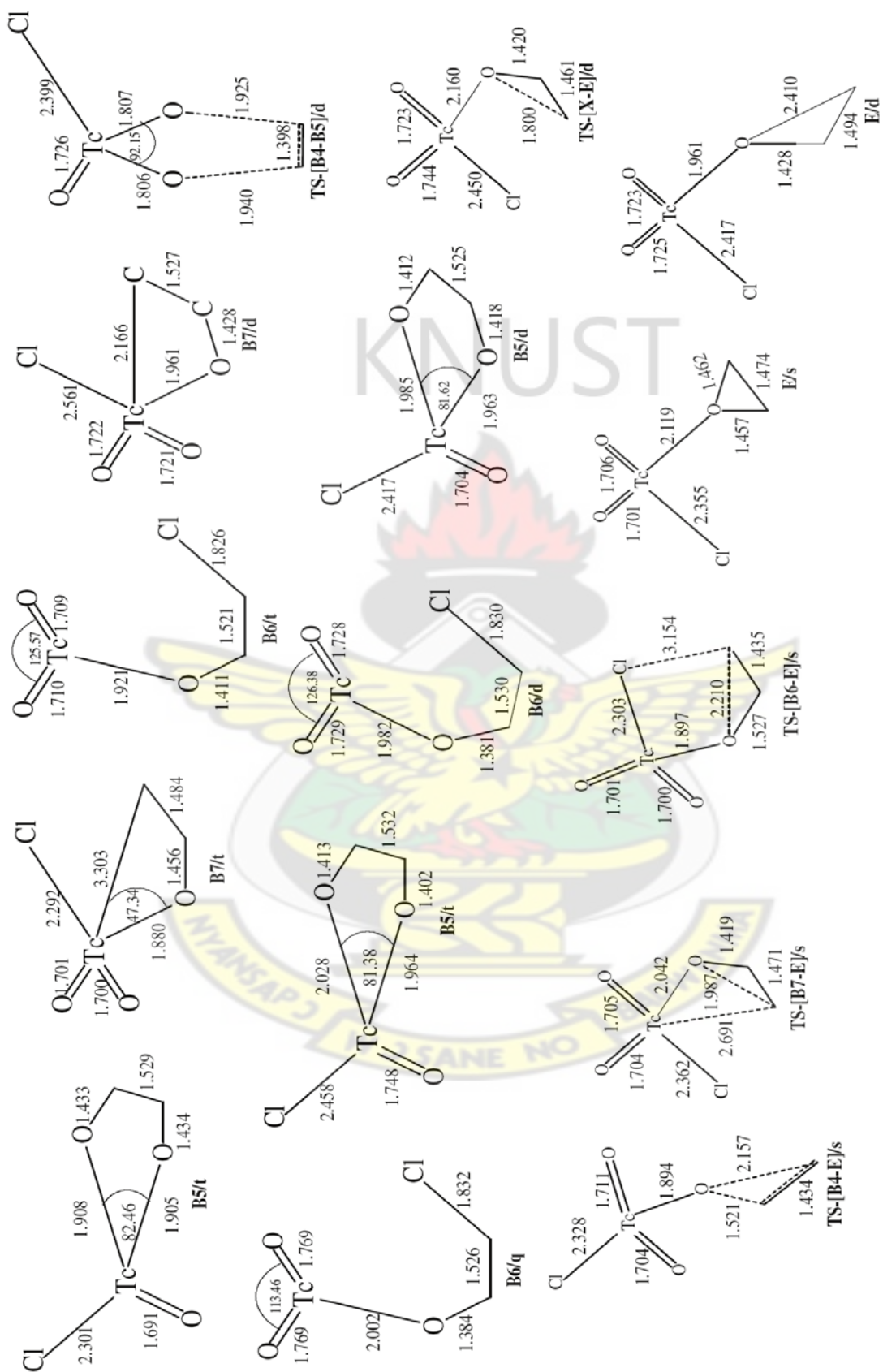


Figure 3.3 cont'd: Optimized geometries of the main stationary points involved in the reaction of TcO₃Cl with ethylene. Distance in Å

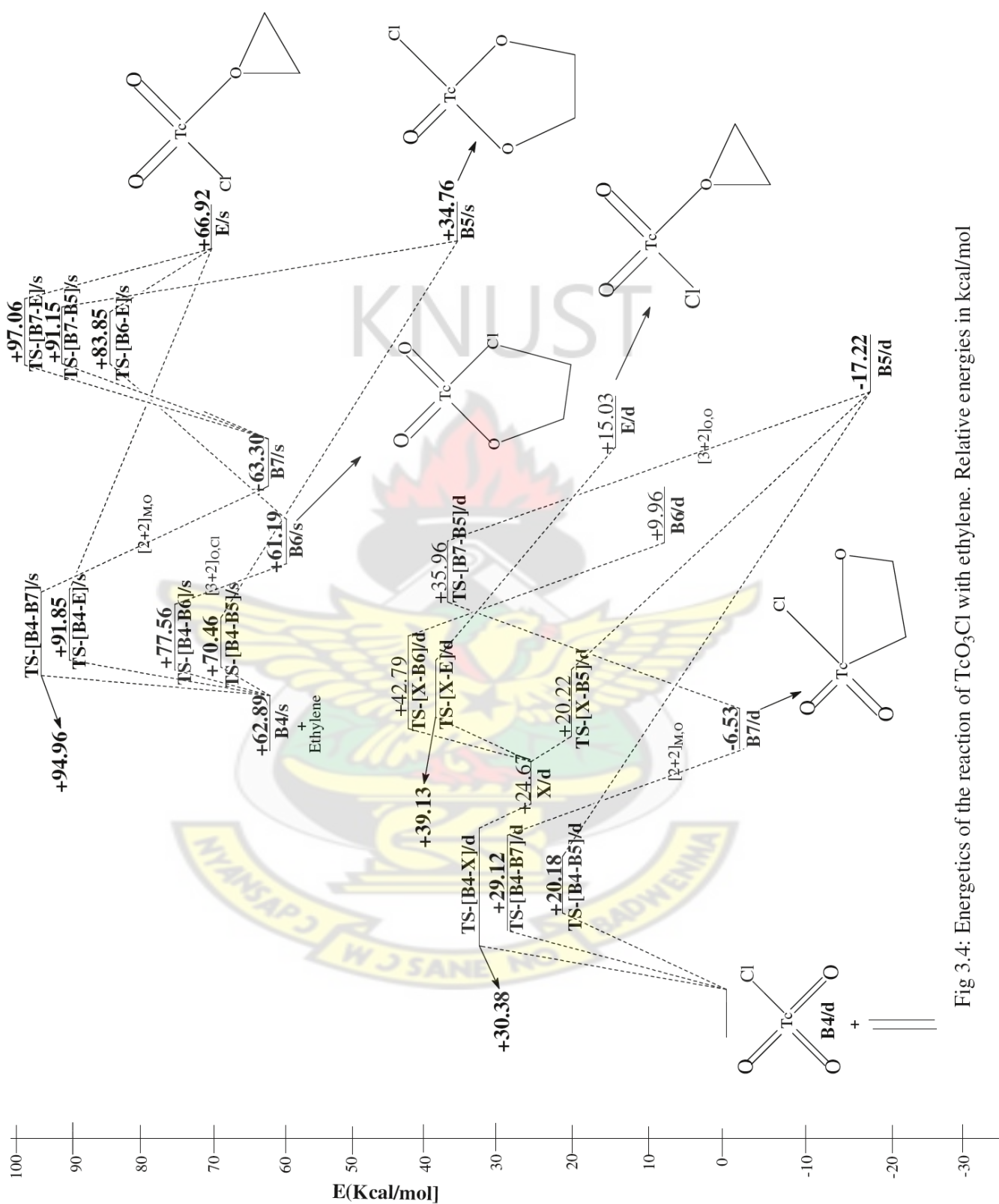


Fig 3.4: Energetics of the reaction of TcO₃Cl with ethylene. Relative energies in kcal/mol

3.3.3 Reaction of $\text{TcO}_3(\text{NPH}_3)$ with ethylene

Figures 3.5 and 3.6 respectively show the optimized geometries and relative energies of the main stationary points involved in the reaction between $\text{TcO}_3(\text{NPH}_3)$ and ethylene. The DFT geometry optimization of $\text{TcO}_3(\text{NPH}_3)$ on a singlet potential energy surface [PES] gives **B8/s** which has the Tc=N bond at 1.88 Å and Tc=O bonds at 1.71 Å. The N-P bond distance is 1.58 Å. A triplet $\text{TcO}_3(\text{NPH}_3)$ **B8/t** has been computed to be 47.79 kcal/mol less stable than the singlet reactant. The Tc=N and N-P bonds in the triplet are 1.89 and 1.60 Å respectively.

A doublet reactant **B8/d** of the complex has been computed to be 38.54 kcal/mol stable than the singlet reactant **B8/s** and 55.69 kcal/mol stable than the quartet structure **B8/q**. In the doublet reactant **B8/d**, the Tc=N bond at 1.78 Å, the N-P bond at 1.78 Å. Thus, the doublet reactant is the most stable of all the reactants computed.

A singlet and a doublet transition state have been located for the formation of the dioxylate intermediate through the [3+2] addition of the C=C bond of ethylene across the O=Tc=O bonds of singlet and doublet $\text{TcO}_3(\text{NPH}_3)$. As shown in Figure 3.6, If the reaction proceeds from a doublet reactant through the doublet transition state **TS-[B8-B9]/d** to a doublet product **B9/d**, the activation barrier is +34.37 kcal/mol and the reaction energy is 9.25 kcal/mol exothermic. If on the other hand, it proceeds from the singlet reactant through the singlet transition state **TS-[B8-B9]/s** to a singlet product **B9/s**, the activation barrier is +15.36 kcal/mol and the reaction energy is 20.22 kcal/mol exothermic.

A triplet species **B9/t** has been computed to have reaction energy of -55.39 kcal/mol. On the quartet PES, a seven-membered metallacyclic intermediate **B9/q** in which one of the oxo-ligands

part of the five-membered ring, forms a new bond with the phosphine moiety attached to nitrogen (O-P = 2.57 Å).

The [3+2] addition of the C=C bond of ethylene across the O=Tc=N bonds of singlet $\text{TcO}_3(\text{NPH}_3)$ through singlet transition state **TS-[B8-B10]/s** has an activation barrier of 16.64 kcal/mol and a reaction energy of 24.35 kcal/mol exothermic. On the doublet surface, no [3+2] transition state linking the reactant to the product was located. The doublet five membered metallacycle **B10/d** has reaction energy of 2.17 kcal/mol exothermic.

A triplet transition state **TS-[B8-B10]/t** linking the reactants to the product could not be located on the reaction surface. On the triplet and quartet PES, a seven-membered metallacyclic intermediate **B10/t** and where one of the oxo-ligands attached to the metal centre forms a new bond with the phosphine moiety attached to nitrogen (O-P = 1.88 Å). On the quartet PES, the (O-P = 1.790 Å). The triplet and quartet five membered metallacycle **B10/t** and **B10/q** have reaction energies of -56.72 and -44.67 kcal/mol.

The formation of the metallaoxetane **B11/s** through the singlet transition state **TS-[B8-B11]/s** by [2+2] addition of the C=C bond of ethylene across Tc=O bond of singlet $\text{TcO}_3(\text{NPH}_3)$ has an activation barrier of 28.17 kcal/mol and reaction energy of -2.04 kcal/mol.

On the doublet surface, the transition state **TS-[B8-B11]/d** linking the reactants to the product has an activation barrier of 25.89 kcal/mol and a reaction energy for the doublet metallaoxetane intermediate **B11/d** is 1.430 kcal/mol.

A triplet transition state **TS-[B8-B11]/t** linking the reactants to the product could not be located. The triplet metallaoxetane has been computed to be 11.28 kcal/mol more stable than the singlet product **B11/s**. A quartet rhenaoxetane **C11/q** has an exothermicity of -22.35 kcal/mol.

A search of the surface for the reaction for the re-arrangement of the metallaoxetane to the dioxylate (**TS-[4-2]** in Scheme 3.1) proved unsuccessful.

The formation of a four membered metallacycle **B9/s** by the [2+2] addition of the C=C bond of ethylene across the Tc=N bond of singlet TcO₃(NPH₃) has an activation barrier and reaction energy to be 41.34 and -12.73 kcal/mol through singlet transition state **TS-[B8-B9]/s**. The product, a six-membered metallacyclic intermediate **B9/s** where one of the oxo ligand on the metal centre bonds with phosphine (PH₃) attached to the nitrogen (O-P = 1.84 Å) is formed.

A doublet transition state **TS-[B8-B9]/d** linking the reactants to the product, has an activation barrier of +21.21 kcal/mol (Fig 3.6). The doublet product, a six-membered metallacyclic intermediate **B9/d** results from the interaction of one of the oxo-ligand attached to the metal center bonds with the phosphine (PH₃) attached to the nitrogen (O-P = 1.68 Å). The doublet product has a reaction energy to be -11.36 kcal/mol.

A triplet transition state **TS-[B8-B9]/t** connecting the reactants to the product could not be located on the reaction surface. The triplet product, a six-membered metallacyclic intermediate **B9/t** results from the interaction of one of the oxo-ligand present at the metal center with the phosphine (PH₃) attached to the nitrogen (O-P = 1.87 Å) is formed. The triplet species is 7.73 kcal/mol less stable than the singlet product **B9/s**.

A search on the reaction surface for the re-arrangement of the four-membered metallacycle to the five-membered metallacycle (**TS-[5-6]** in Scheme 3.1) did not yield any positive results.

The transition state **TS-[B10-K]/s** for the re-arrangement of the singlet five-membered metallacycle (**TS-[1-6]** in Scheme 3.1) to the epoxide precursor has activation barrier of +56.31 kcal/mol and endothermicity of +43.63 kcal/mol.

Also the re-arrangement of the singlet five-membered metallacycle (**TS-[2-3]** in Scheme 3.1) through transition state **TS-[B9-K]/s** to the epoxide precursor has an activation barrier of +70.04 kcal/mol and endothermicity of 39.50 kcal/mol. The transition state (**TS-[4-3]/s** in Scheme 3.1) for the rearrangement of the singlet four-membered metallaoxetane to the epoxide precursor through transition state **TS-[B11-K]/s** have activation barrier and reaction energy of +52.80 and 21.32 kcal/mol. Also, the singlet direct one-step addition of the C=C bond across one oxygen atom of $\text{TcO}_3(\text{NPH}_3)$ has activation barrier of +32.01 kcal/mol and endothermicity of +19.28 kcal/mol. The most plausible pathway for the formation of the epoxide precursor is by the direct [2+1] addition pathway.

From the energetics in Fig 3.6, the addition of $\text{TcO}_3(\text{NPH}_3)$ to ethylene is likely to occur on the doublet PES and the [2+2] addition of ethylene across the $\text{Tc}=\text{N}$ bond of doublet $\text{TcO}_3(\text{NPH}_3)$ is kinetically and thermodynamically most favorable.

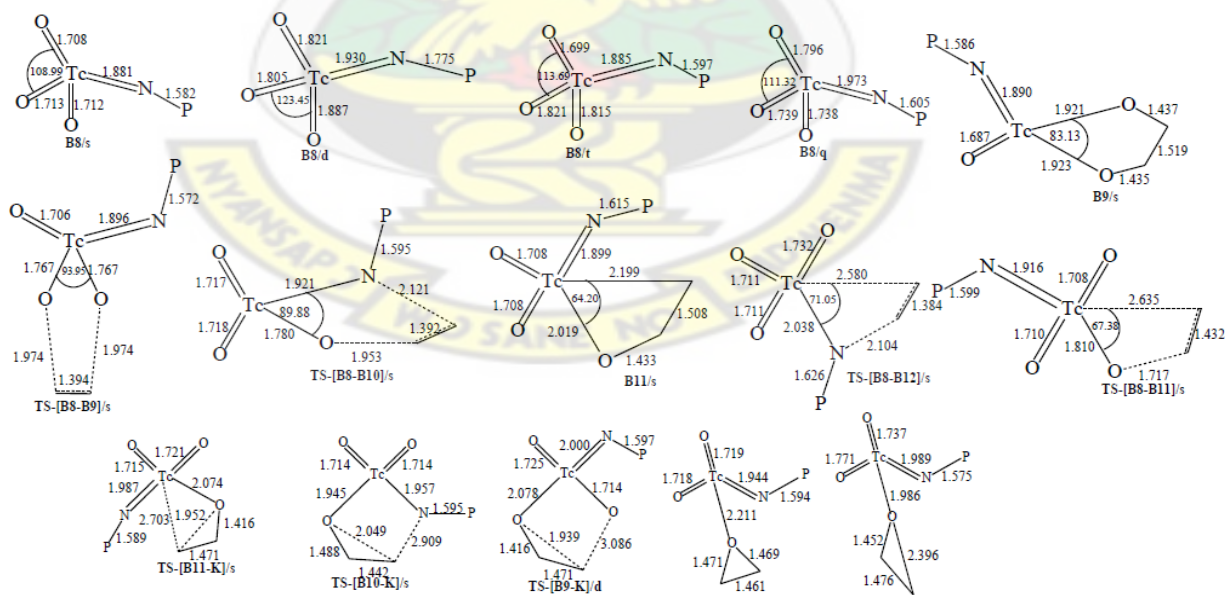


Figure 3.5: Optimized geometrical parameters of the main stationary points involved in the reaction of $\text{TcO}_3(\text{NPH}_3)$ with ethylene. Distance in Å and angles in degrees.
*Hydrogen's omitted from Phosphorus atoms

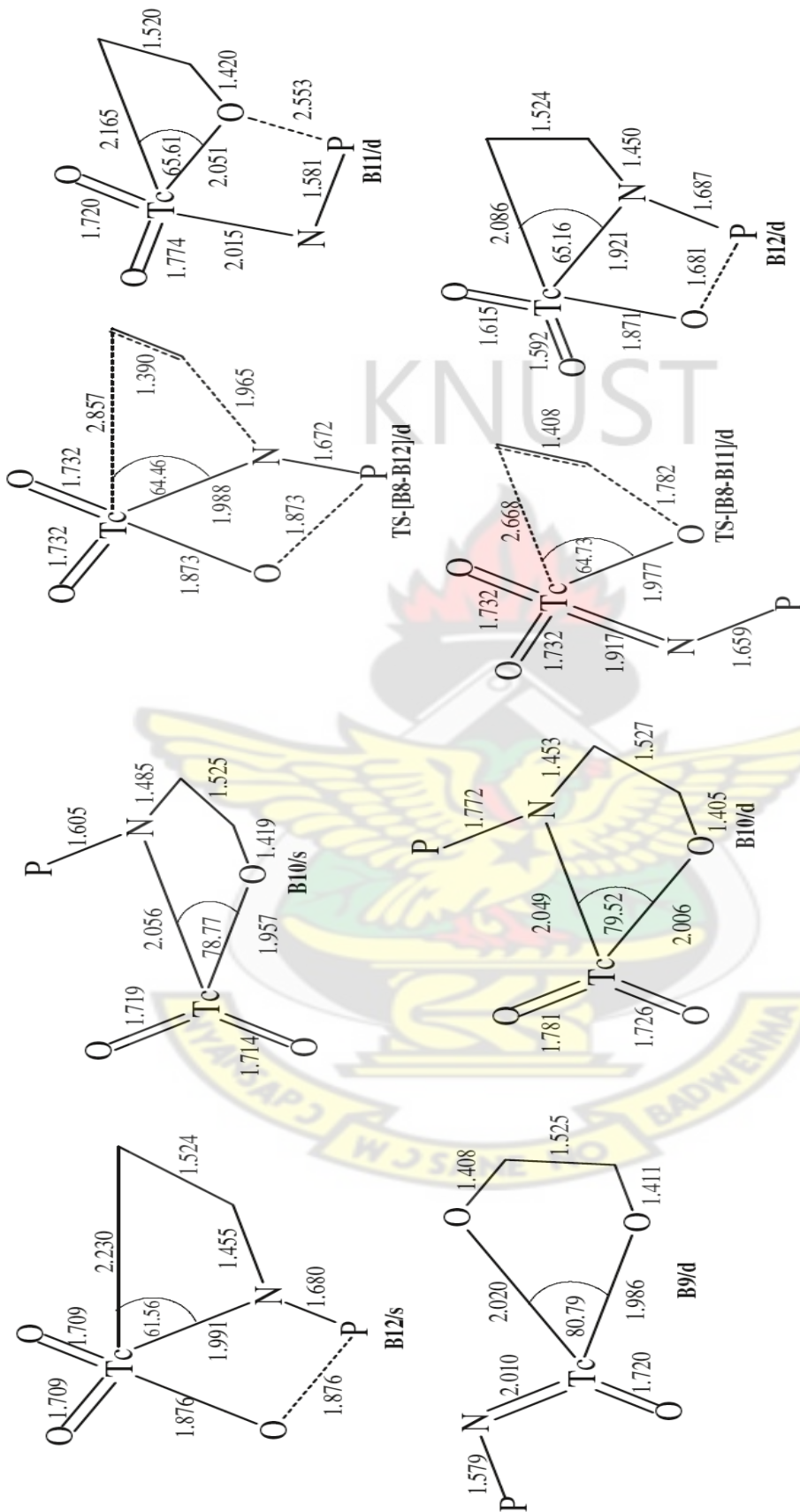


Figure 3.5 contd: Optimized geometrical parameters of the main stationary points involved in the reaction of $\text{TeO}_3(\text{NPH}_3)_3$ with ethylene. Distance in Å

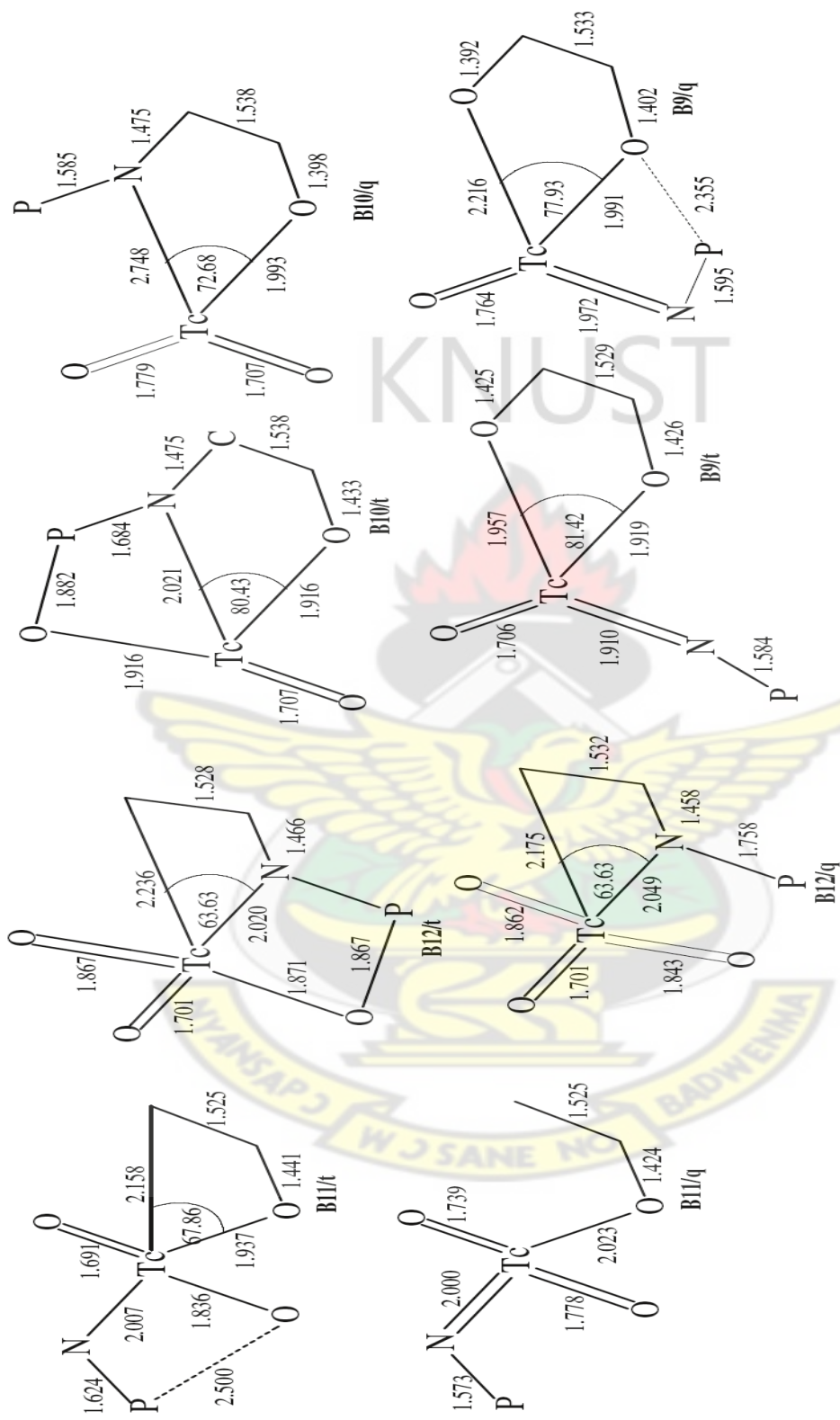


Figure 3.5 cont'd: Optimized geometrical parameters of the main stationary points involved in the reaction of $\text{TcO}_3(\text{NPH}_3)$ with ethylene. Distance in Å.
 *Hydrogen's omitted from Phosphorus and Carbon atoms

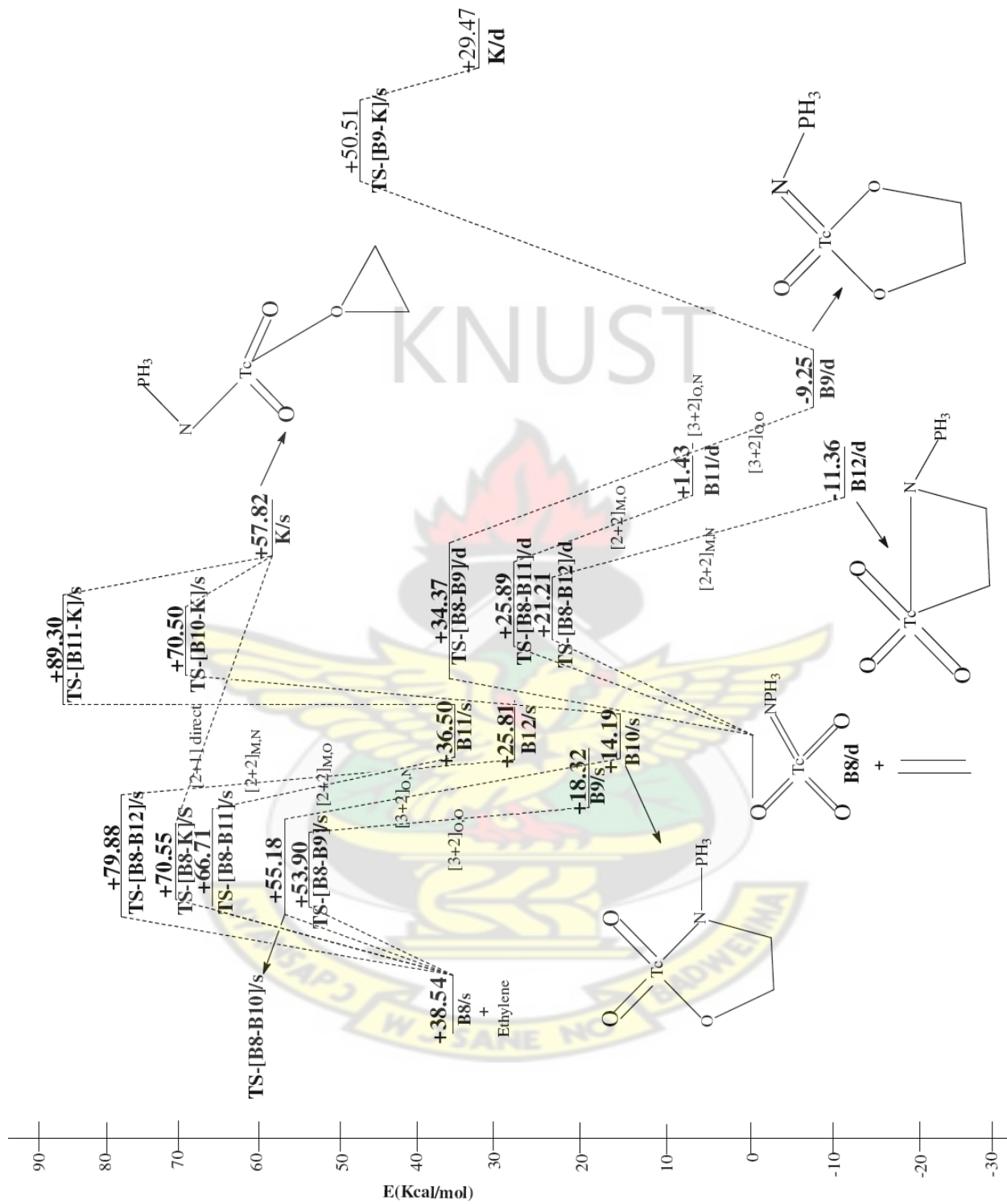


Fig 3.6: Energetics of the reaction of $TcO_3(NPH_3)_3$ with ethylene. Relative energies in kcal/mol

3.3.4 Reaction of $\text{TcO}_3(\text{CH}_3)$ with ethylene

Figure 3.7 and 3.8 shows the optimized geometries and relative energies of the main stationary points involved in the reaction between $\text{TcO}_3(\text{CH}_3)$ and ethylene respectively. The DFT geometry optimization of $\text{TcO}_3(\text{CH}_3)$ on a singlet potential energy surface yields **B13/s** which has the $\text{Tc}=\text{O}$ bonds at 1.70 Å and the $\text{Tc}-\text{C}$ bond is 2.09 Å long.

A doublet reactant **B13/d** has been computed and found to be 44.42 kcal/mol more stable than the singlet reactant **B13/s** and 94.17 kcal/mol more stable than the triplet reactant **B13/t**. In the doublet reactant **B13/d**, the $\text{Tc}-\text{C}$ bond is 0.03 Å longer in the doublet reactant **B13/d** than in the singlet reactant **B13/s** and 0.03 Å longer in the doublet reactant than in the triplet structure **B13/t**. A quartet reactant **B13/q** has been computed to be 72.54 kcal/mol less stable in relation to the doublet reactant **B13/d**.

The [3+2] addition of the $\text{C}=\text{C}$ bond of ethylene across the $\text{O}=\text{Tc}=\text{O}$ functionality of doublet $\text{TcO}_3(\text{CH}_3)$ through a doublet transition state **TS-[B13-B14]/d** to form the dioxylate **B14/d** has an activation barrier of 27.91 kcal/mol and reaction energy of -6.05 kcal/mol.

The observed transition state is symmetric with respect to the forming $\text{C}-\text{O}$ bonds (1.87 Å). The $\text{Tc}-\text{C}$ bond distance (2.13 Å) in the doublet transition state is the same as in the doublet reactant (2.12 Å). The triplet and quartet dioxylate species **B14/t** and **B14/q** has exothermicity of -63.44 and -63.86 kcal/mol. No triplet and quartet transition state linking the reactants to the products was located on the reaction surfaces.

The activation barrier and reaction energy for the [3+2] addition of the $\text{C}=\text{C}$ bond of ethylene across the $\text{O}=\text{Tc}=\text{O}$ functionality of singlet $\text{TcO}_3(\text{CH}_3)$ through a singlet transition state

TS-[B13-B14]/s has been computed to be 19.83 and -12.11 kcal/mol. Gisdakis and Rösch, (2001) calculated the barrier along this route to be +23.70 kcal/mol.

The formation of the doublet metallaoxetane **B15/d** through the transition state **TS-[B13-B15]/d** by [2+2] addition of the C=C bond of ethylene across Tc=O bond of doublet $\text{TcO}_3(\text{CH}_3)$ complex, has an activation barrier of 33.60 kcal/mol and reaction energy of 1.13 kcal/mol exothermic. A triplet metallaoxetane **B15/t** has been computed to be 30.67 kcal/mol more stable than the doublet metallaoxetane **B15/d**. No quartet species was located on the reaction surface and the triplet and quartet transition states were located on the reaction surface explored.

The formation of the singlet metallaoxetane **B15/s** through transition state **TS-[B13-B15]/s** by [2+2] addition of the C=C bond of ethylene across Tc=O bond of singlet $\text{TcO}_3(\text{CH}_3)$ complex, has an activation barrier of 33.05 kcal/mol and reaction energy of -1.84 kcal/mol.

The re-arrangement of the singlet metallaoxetane to the singlet dioxylate (**TS-[4-2]** in Scheme 3.1) through transition state **TS-[B15-B14]/d** has a barrier of +33.60 kcal/mol. No doublet, triplet and quartet transition state were located for re-arrangement of the metallaoxetane to dioxylate. Thus the activation barrier for the re-arrangement of the singlet metallaoxetane to the dioxylate is higher than the activation barrier for the direct [3+2] addition of C=C π of ethylene across O=Tc=O of singlet $\text{TcO}_3(\text{CH}_3)$. This rule out the two-step process for the formation of the dioxylate from the metallaoxetane. The dioxylate would be formed from the direct [3+2] addition of ethylene across the two oxygen atoms of $\text{TcO}_3(\text{CH}_3)$.

The reaction of $\text{TcO}_3(\text{CH}_3)$ with ethylene was explored for the formation of an epoxide precursor. A search for a transition state (**TS [2-3]** in Scheme 3.1) for the re-arrangement of the five-membered metallacycle to the epoxide precursor yielded no positive results, indicating that

such a re-arrangement may not be possible. The transition state **TS [B15-E]/s** for the rearrangement of the singlet four-membered metallaoxetane to the epoxide precursor have activation barrier of +44.77 kcal/mol and endothermicity of +16.66 kcal/mol. Also, the activation energy for the formation of the singlet epoxide precursor from direct attack of the C=C bond on the oxygen atom of $\text{TcO}_3(\text{CH}_3)$ has been computed to have activation barrier of +34.32 kcal/mol and endothermicity of +14.82 kcal/mol. On the doublet surface, the activation and reaction energies are +25.17 and 17.35 kcal/mol respectively. The triplet and quartet epoxide precursors have reaction energies of -31.77 and -43.02 kcal/mol. Therefore, the most plausible pathway for the formation of the epoxide precursor is by direct [2+1] addition on the doublet surface.

The reaction of $\text{TcO}_3(\text{CH}_3)$ with ethylene would take place on the doublet surface and the formation of the epoxide precursor is likely to be competitive with the dioxylate intermediate. The latter was found to be the most thermodynamically favorable product.

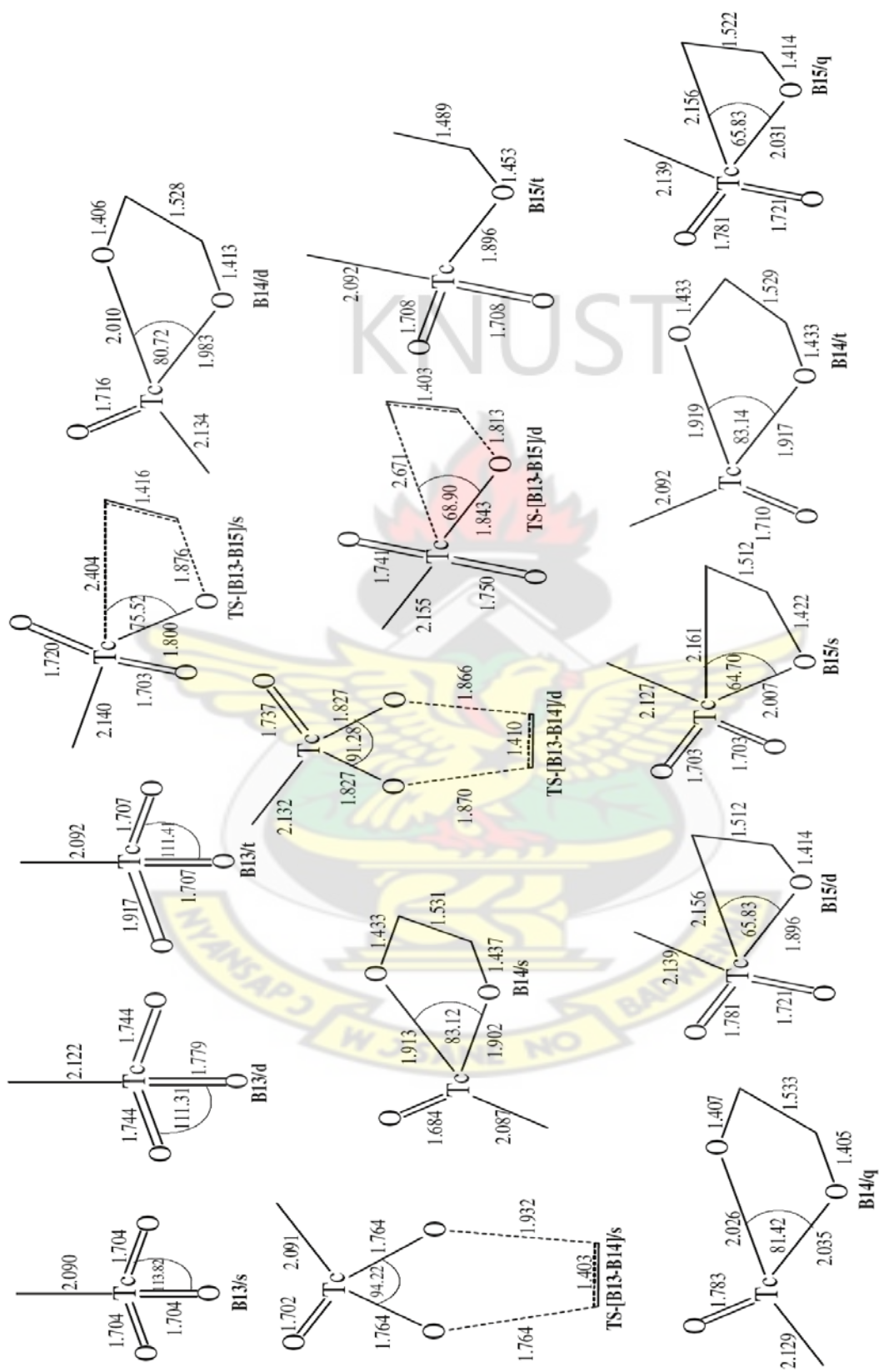


Fig 3.7: Optimized geometrical parameters of the main stationary points involved in the reaction of $\text{TeO}_3(\text{CH}_3)$ with ethylene. Distance in Å and angles in degrees.

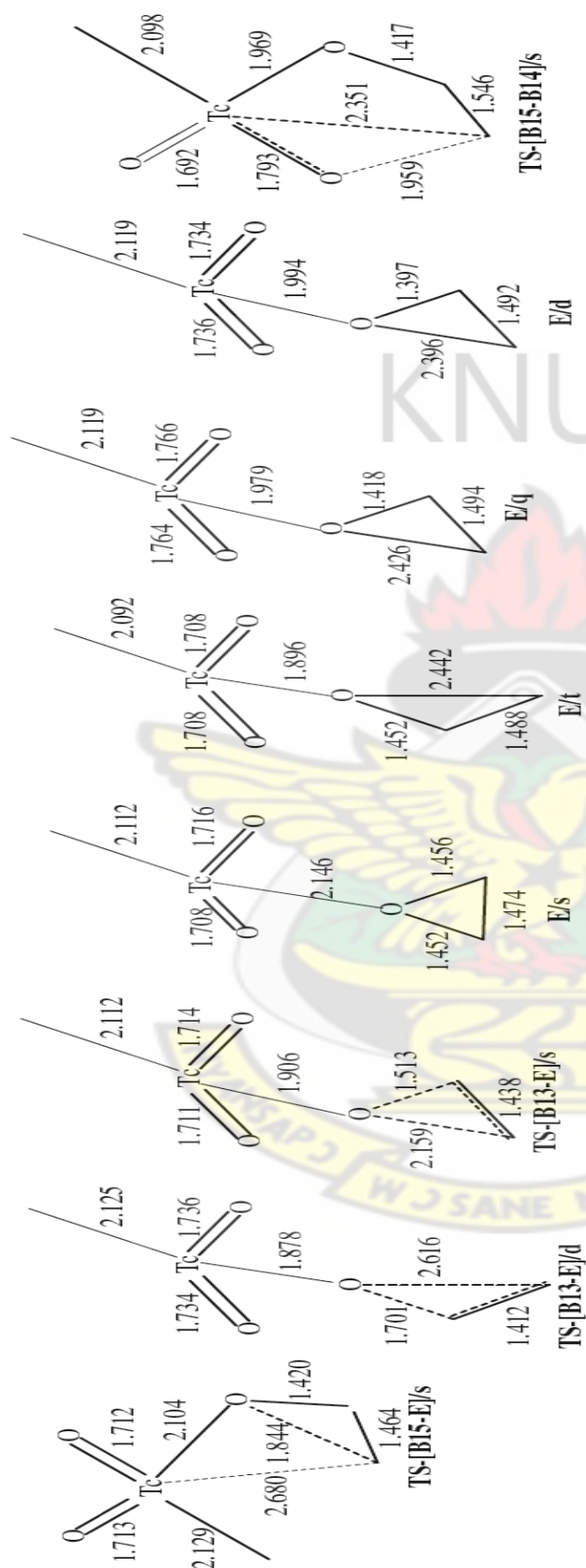


Fig 3.7 cont'd: Optimized geometrical parameters of the main stationary points involved in the reaction of $\text{TcO}_3(\text{CH}_3)_3$ with ethylene. Distance in Å

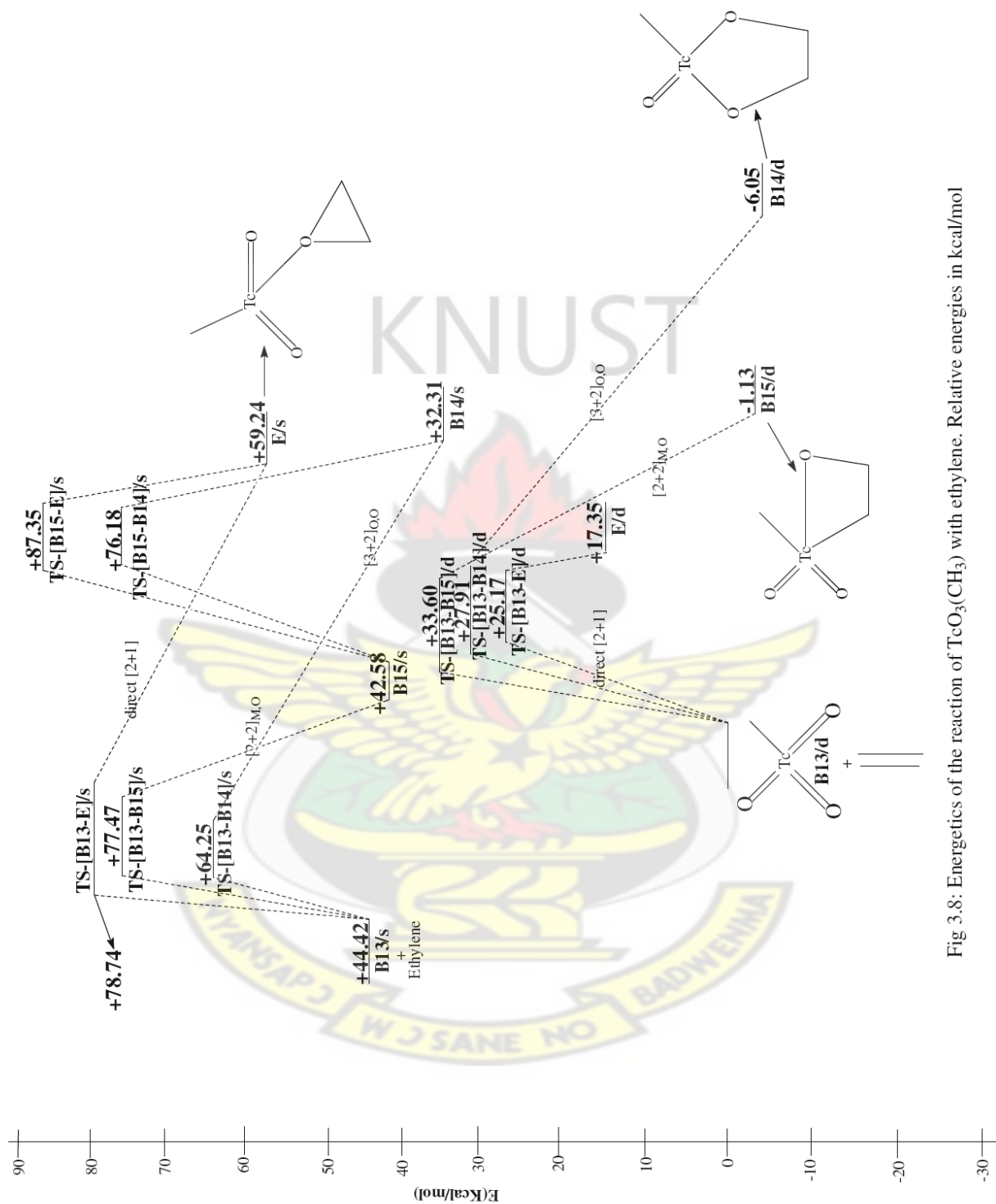


Fig 3.8: Energetics of the reaction of $\text{TcO}_3(\text{CH}_3)_3$ with ethylene. Relative energies in kcal/mol

3.3.5 Reaction of $\text{TcO}_3(\text{OCH}_3)$ with ethylene

Figure 3.9 shows the optimized geometries of the main stationary points involved in the reaction between $\text{TcO}_3(\text{OCH}_3)$ and ethylene. The corresponding energy profile is shown in fig 3.10. A singlet, doublet, triplet and quartet species has been optimized for the reactant $\text{TcO}_3(\text{OCH}_3)$. The singlet reactant **B16/s** has the Tc=O bonds at 1.71 Å. The Tc-O bond distance is 1.87 Å.

A doublet reactant **B16/d** has been computed to be 47.09 kcal/mol more stable than the singlet reactant **B16/s** and 98.91 kcal/mol more stable than the triplet reactant **B16/t**. The Tc-O bond is 0.08 Å longer, while the O-C bond is 0.03 Å shorter in doublet structure **B16/d**. A quartet reactant **B16/q** of C_1 symmetry is 46.43 kcal/mol less stable than the doublet **B16/d**. The quartet reactant is 0.66 kcal/mol less stable than singlet reactant **B16/s** and 52.48 kcal/mol more stable than the triplet ground state reactant.

The [3+2] addition of the C=C bond of ethylene across the O=Tc=O bond of doublet $\text{TcO}_3(\text{OCH}_3)$ through a doublet transition state **TS-[B16-B17]/d** to form the dioxylate **B17/d** has an activation barrier of 23.90 kcal/mol and reaction energy of 8.52 kcal/mol exothermic. The calculated transition state is highly asynchronous with respect to the newly forming C-O bonds. On the triplet PES, the reaction energy for the dioxylate intermediate is 60.04 kcal/mol more stable than the doublet product **B17/d**.

The [3+2] addition of the C=C bond of ethylene across the O=Tc=O bond of singlet $\text{TcO}_3(\text{OCH}_3)$ through a singlet transition state **TS-[B16-B17]/s** to form the dioxylate **B17/s** has an activation barrier of 13.11 kcal/mol and reaction energy of -21.97 kcal/mol. The calculated transition state is highly synchronous and symmetric with respect to the newly forming C-O

bonds. A quartet dioxylate has been computed to be 32.97 kcal/mol more stable than the doublet product **B17/d**.

The formation of the singlet metallaoxetane **B18/s** by [2+2] addition of the C=C bond of ethylene across the Tc=O bond of singlet TcO₃(OCH₃) through a singlet transition state has an activation barrier of 30.63 kcal/mol and reaction energy of -4.51 kcal/mol.

The formation of the doublet metallaoxetane **B18/d** through the transition state **TS-[B16-B18]/d** by [2+2] addition of the C=C bond of ethylene across the Tc=O bond of doublet TcO₃(OCH₃) has an activation barrier of 31.82 kcal/mol and exothermicity of 2.78 kcal/mol. A triplet metallaoxetane **B18/t** computed has been computed to have reaction energy of 12.26 kcal/mol more stable than the quartet species **B18/q**.

The re-arrangement of the metallaoxetane to the dioxylate (**TS-[4-2]** in Scheme 3.1) was explored for the reaction of TcO₃(OCH₃) with ethylene. NO singlet, doublet, triplet and quartet re-arrangement species were located on the reaction surface.

An epoxide precursor was optimized from the reaction of TcO₃(OCH₃) with ethylene. The transition state (**TS [2-3]** in Scheme 3.1) for the re-arrangement of the five-membered metallacycle to the epoxide precursor yielded no positive results, indicating that such a re-arrangement may not be possible. The transition state **TS [B18-E]/s** for the rearrangement of the singlet four-membered metallaoxetane to the epoxide precursor has an activation barrier of +45.49 kcal/mol and endothermicity of +13.64 kcal/mol. Also, the activation energy for the formation of the singlet epoxide precursor from direct attack of the C=C bond on the oxygen atom of TcO₃(CH₃) has been computed to have a barrier of +37.65 kcal/mol and endothermicity of 9.13 kcal/mol. The formation of the epoxide precursor is not a favorable reaction.

Therefore, the most plausible pathway for the formation of the epoxide, if it is to form at all, is by direct [2+1] addition on the singlet surface.

The reaction of ethylene with $\text{TcO}_3(\text{OCH}_3)$ would take place on the doublet PES and the [3+2] addition of ethylene across the two oxygen atoms of doublet $\text{TcO}_3(\text{OCH}_3)$ is kinetically and thermodynamically most favorable (Fig 3.10)

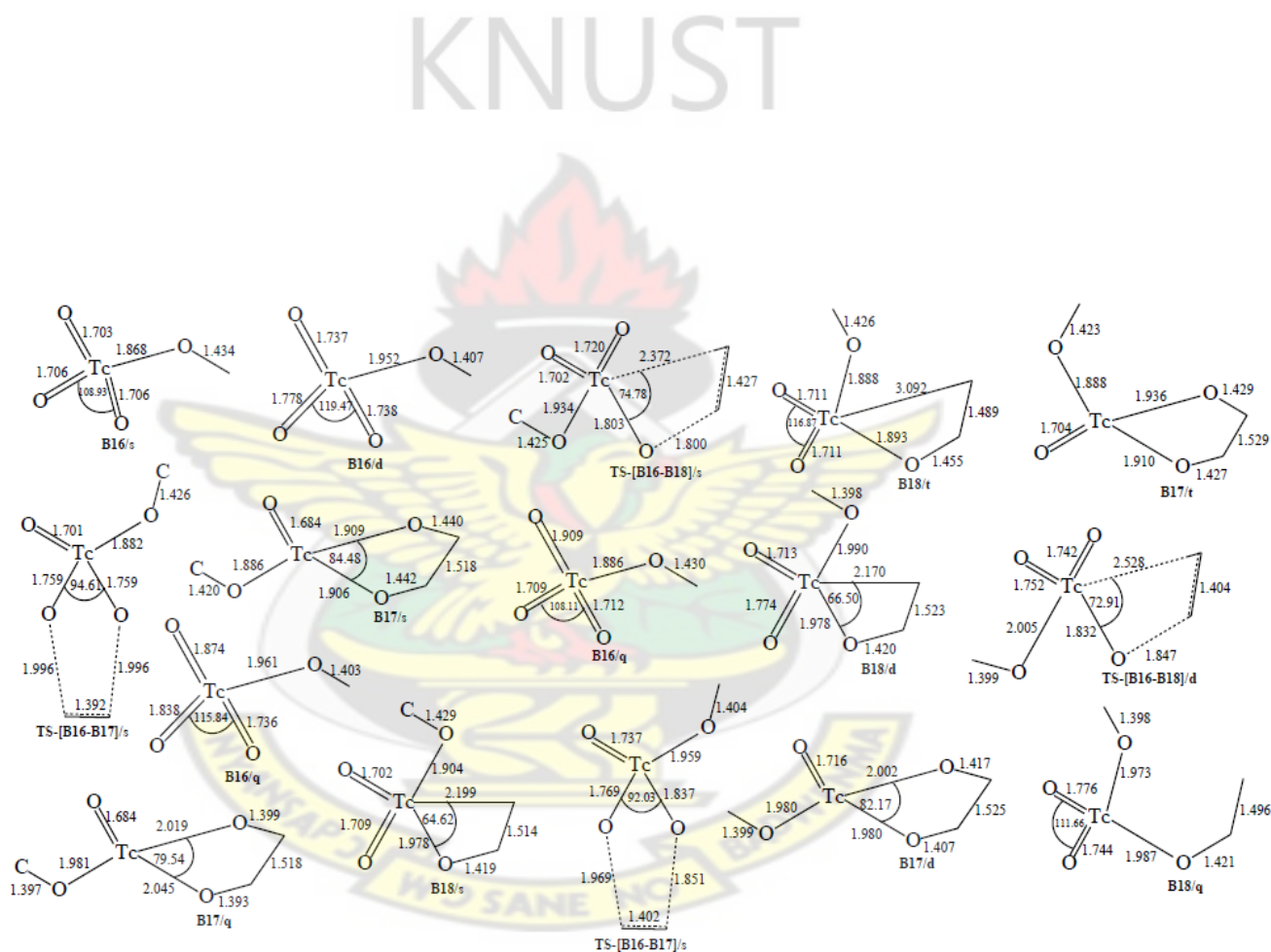


Fig 3.9: Optimized geometrical parameter of the main stationary points involved in the reaction of $\text{TcO}_3(\text{OCH}_3)$ with ethylene. Distance in Å and bond angles in degrees.

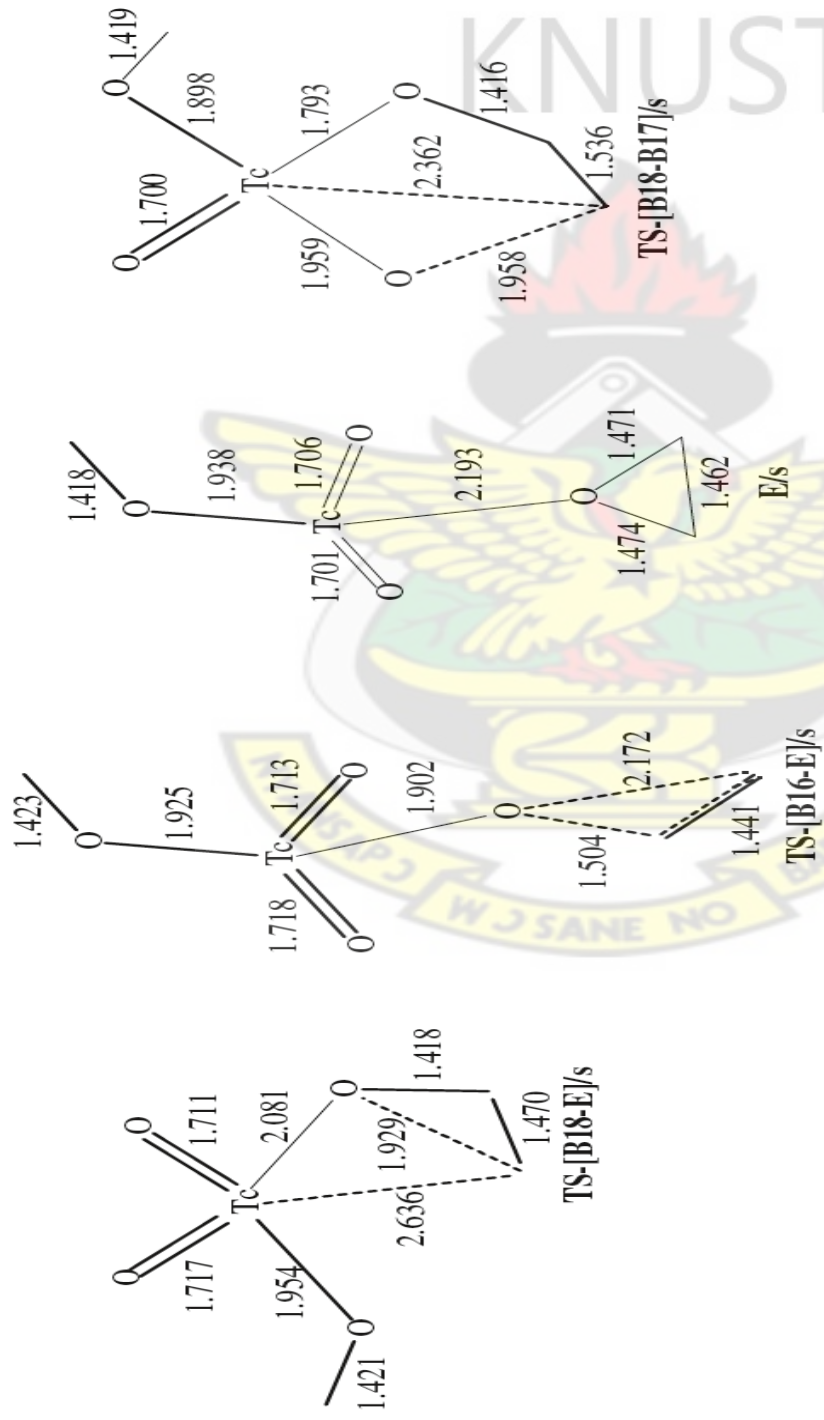


Figure 3.9 cont'd: Optimized geometrical parameter of the main stationary points involved in the reaction of $\text{TcO}_3(\text{OCH}_3)_3$ with ethylene. Distance in Å and bond angles in de

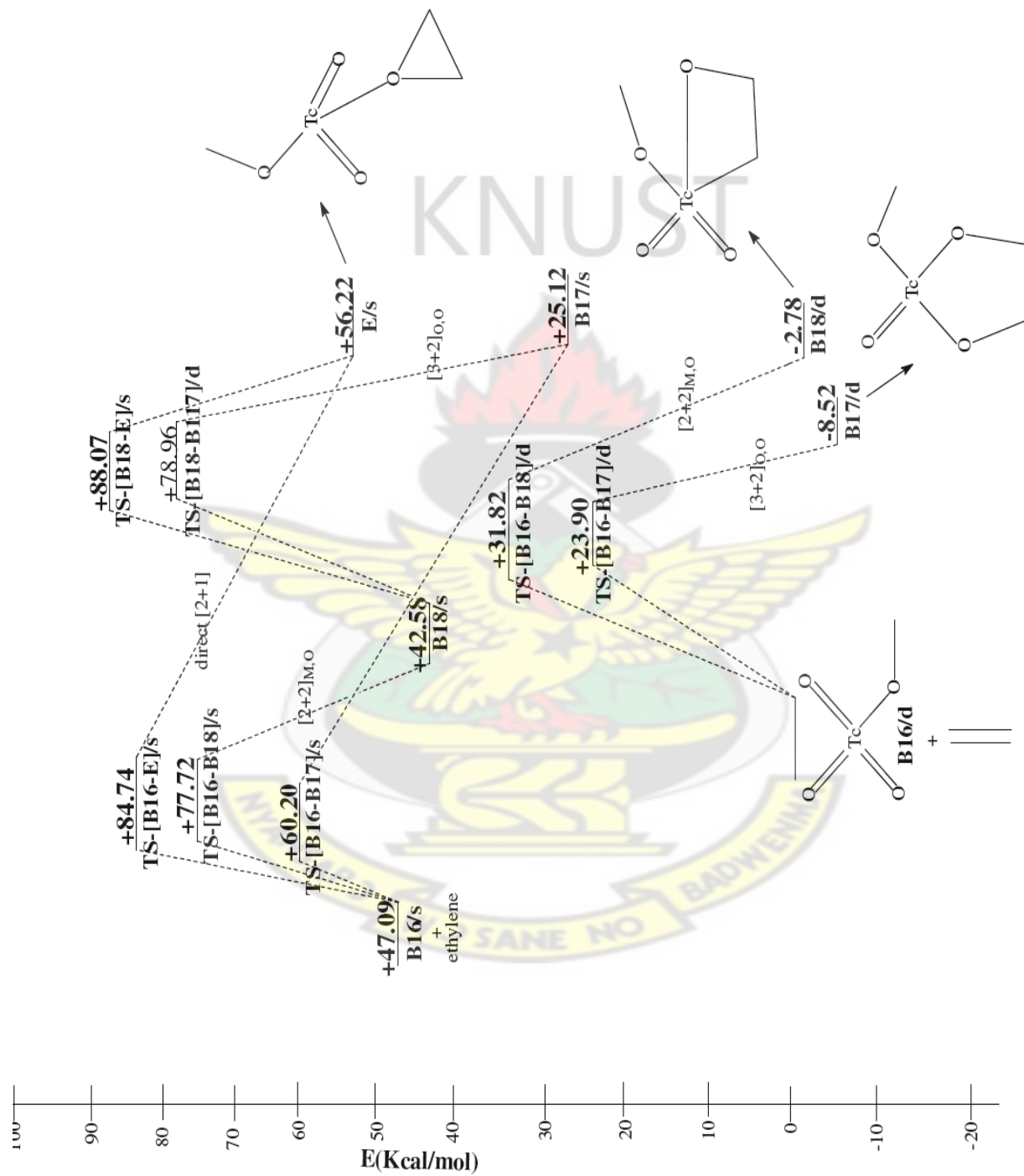


Fig 3.10: Energetics of the reaction of $\text{TcO}_3(\text{OCH}_3)_3$ with ethylene. Relative energies in kcal/mol

3.3.6 Reaction of TcO₃Cp with ethylene

Figure 3.11 shows the optimized geometries and of the main stationary points involved in the reaction between TcO₃Cp and ethylene and fig 3.12 shows the corresponding energy profile. The DFT geometry optimization of TcO₃Cp on a singlet potential energy surface gives **B19/s** which has the Tc=O bonds at 1.72 Å. The cyclopentadienyl ligand (Cp) is bonded to the metal center in a η^5 fashion i.e. Tc-C (Cp) = 2.486, 2.492, 2.492, 2.483 and 2.503Å. For MnO₃Cp, Gisdakis and Rösch (2001) employing the hybrid B3LYP approach, with effective core potentials and double-zetabasis sets, LanL2DZ, for the transition metals and 6-311G(d,p) basis sets for H, C, O, and F found the Cp ligand to be bound to the metal center in η^1 fashion. No doublet, triplet and quartet reactants could be located on the doublet, triplet and quartet PES.

The [3+2] addition of C=C bond of ethylene across the O=Tc=O bonds of singlet TcO₃Cp through a singlet transition state **TS-[B19-B20]/s** to form the metalladioxolane intermediate **B20/s** has an activation barrier of 2.66 kcal/mol and reaction energy of - 46.50 kcal/mol in agreement with the reported activation and reaction energies by Gisdakis and Rösch (2001) at the hybrid B3LYP approach, with effective core potentials and double-zetabasis sets, LanL2DZ, for the transition metals and 6-311G(d,p) basis sets for H, C, O, and F. The calculated transition state is highly synchronous with respect to the newly forming C-O bonds. The Cp ligand in the singlet [3+2] transition state structure shows η^5 -bonding to the metal centre i.e.(Tc-C (Cp) =2.358, 2.455, 2.463, 2.628, 2.635Å). The Cp ligand in the singlet TcO₃Cp- dioxylate **B20/s** also shows a η^5 -bonding fashion to the Tc centre (Tc-C (Cp) =2.348, 2.359, 2.422, 2.502, 2.545Å).

The reaction energy of the doublet product **B20/d** is -67.63 kcal/mol making it +55.52 kcal/mol more stable than the singlet product **B20/s**. In the doublet dioxylate, the Cp ligand in TcO₃Cp dioxylate **B20/d** shows η^5 -bonding fashion to the Tc centre (Tc-C (Cp) =2.323, 2.571

and 2.617, 2.437, 2.298 Å). A triplet dioxylate **B20/t** has been computed to have reaction energy of -24.70 kcal/mol. The Cp ligand in the triplet TcO₃Cp-dioxylate **B20/t** also shows η⁵-bonding fashion to the Tc centre (Tc-C (Cp) = 2.318, 2.412, 2.466, 2.536 and 2.581 Å). The quartet metalladioxolane intermediate **B20/q** has reaction energy of -56.50 kcal/mol, making it 31.80 kcal/mol more stable than the triplet dioxylate **B20/t**. The Cp ligand in the quartet TcO₃Cp-dioxylate **B20/q** shows η⁵-bonding fashion to the Tc centre (Tc-C (Cp) = 2.424, 2.733, 2.998, 2.865, 2.518 Å).

The formation of the manganooxetane **B21/s** through the transition state **TS-[B19-B21]/s** on the singlet PES by [2+2] addition of C=C bond of ethylene across Tc=O bond of the TcO₃Cp complex has activation barrier of 28.56 kcal/mol and reaction energy of 10.30 kcal/mol exothermic. The Cp ligand in the singlet [2+2] transition state structure shows η³-bonding to the metal centre i.e. (Tc-C (Cp) = 2.191, 2.843, 2.883, 3.556 and 3.577 Å). The Cp ligand in the singlet TcO₃Cp-oxetane **B21/s** shows a η³-bonding mode to the Tc centre, (Tc-C (Cp) = 2.907, 2.190, 2.999, 3.798, 3.750 Å) in contrary to the η⁵-bonding mode in the singlet reactant **B19/s**.

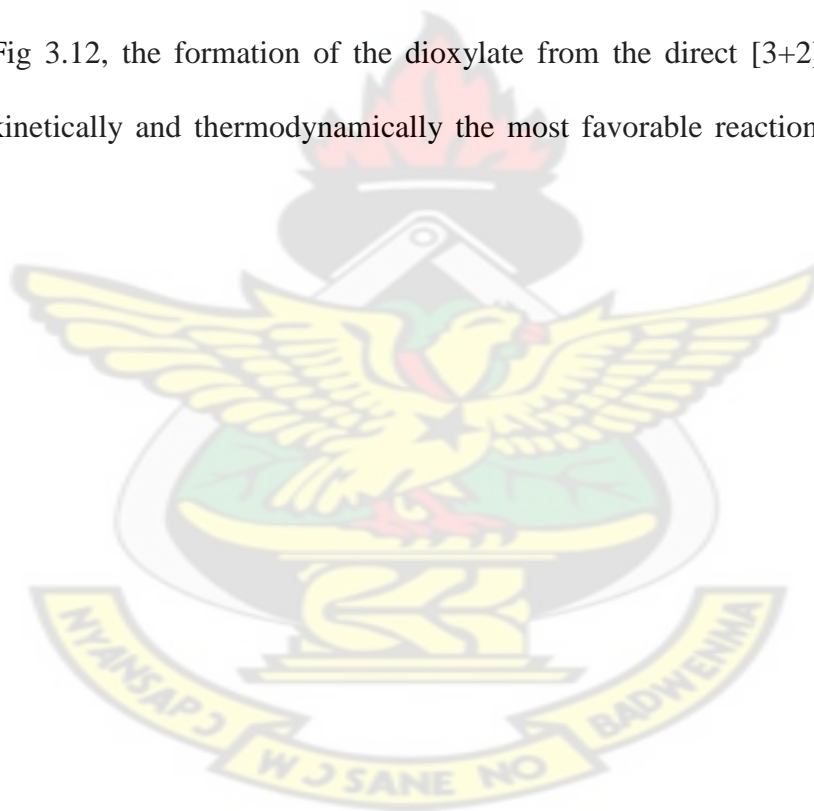
A triplet species with a metallaoxetane-like structure but having an elongated metal-oxygen bond has been found to have a reaction energy of 25.62 kcal/mol. The Cp ligand in the triplet TcO₃Cp-oxetane shows a η⁵-bonding mode to the Tc centre, (Tc-C (Cp) = 2.327, 2.520, 2.727, 2.696 and 2.482 Å). No metallaoxetane intermediate could be located on the reaction surface.

The re-arrangement of the singlet metallaoxetane to the singlet dioxylate (**TS-[4-2]** in Scheme 3.1) through transition state **TS-[B21-B20]/s** has an activation barrier of +12.89 kcal/mol. No doublet, triplet and quartet transition state was located for re-arrangement of the metallaoxetane to dioxylate. Thus the activation barrier for the re-arrangement of the singlet metallaoxetane to

the dioxylate is higher than the activation barrier for the initial [3+2] addition of $C=C\pi$ of ethylene across $O=Tc=O$ of singlet and doublet TcO_3Cp . Thus, the dioxylate intermediate would be formed from the direct addition of ethylene across the two oxygen atoms of singlet TcO_3Cp . It would not be formed from the re-arrangement of the metallaoxetane.

The potential energy surface of the reaction of TcO_3Cp with ethylene was further explored in an attempt to locate an epoxide precursor ($O_2(Cp)-Tc-OC_2H_4$) (**3** in Scheme 3.1), but no such minimum was found on these reaction surfaces.

Thus from Fig 3.12, the formation of the dioxylate from the direct [3+2] addition on the singlet PES is kinetically and thermodynamically the most favorable reaction for the TcO_3Cp system.



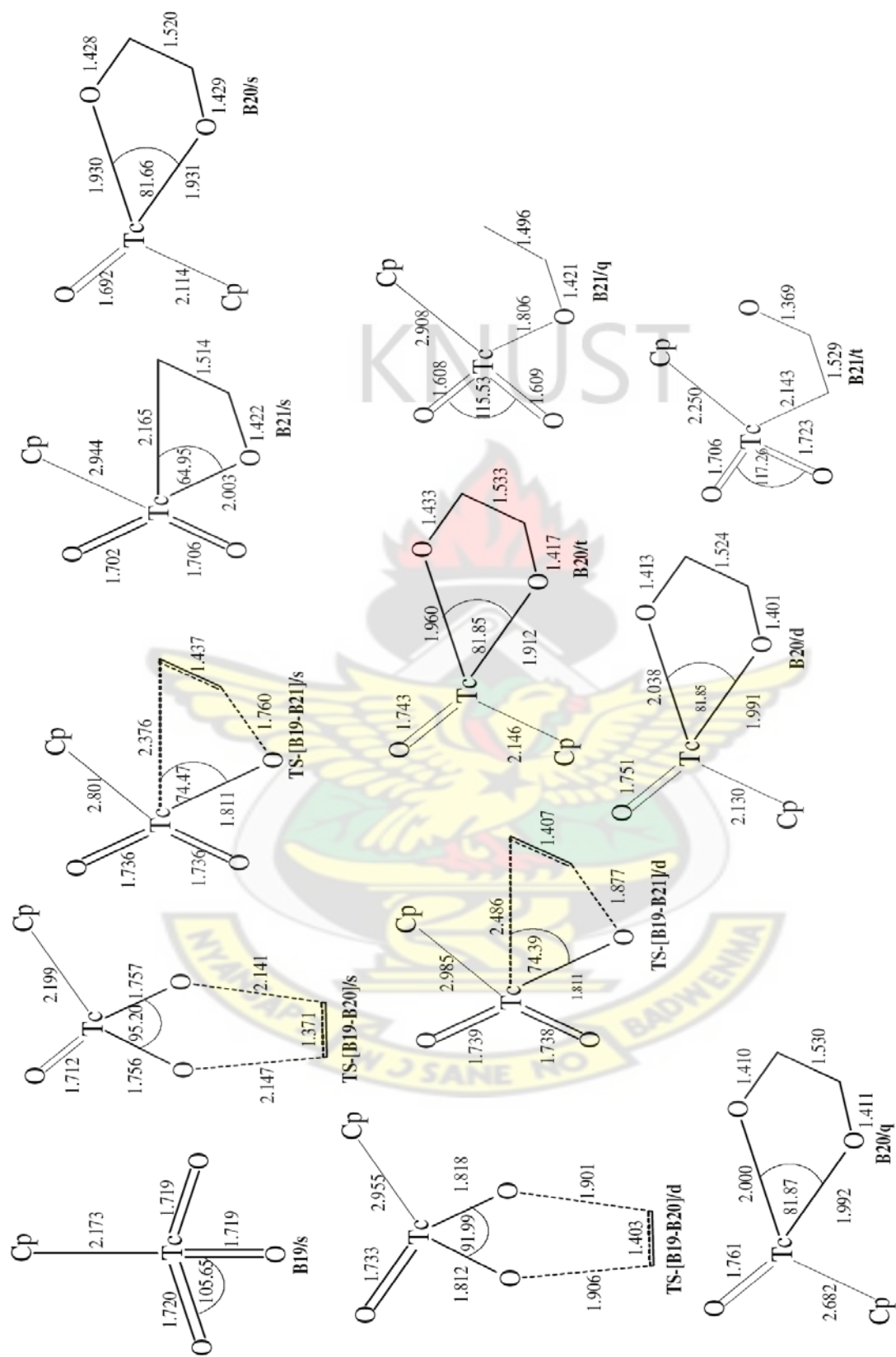


Fig 3.11: Optimized geometries of the main stationary points involved in the reaction of TeO_3Cp with ethylene. Distance in Å and bond angles in degrees.

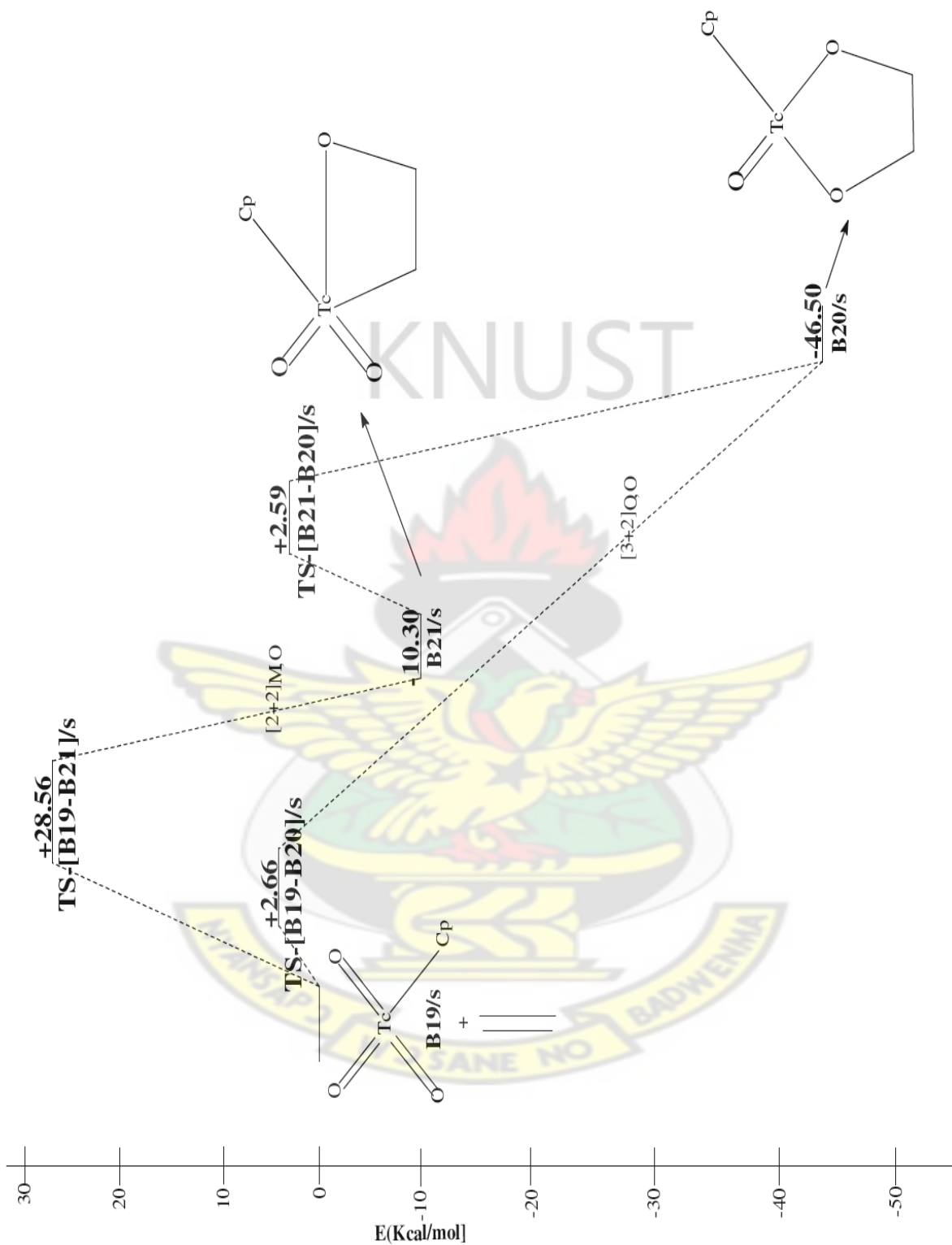


Fig 3.12: Energetics of the reaction of TcO_3Cp with ethylene. Relative energies in kcal/mol

3.4 Conclusion

1. In the reaction between ethylene and the pertechnetate (TcO_4^-), the direct [3+2] addition of the C=C bond of ethylene across O=Tc=O bond of TcO_4^- to form the dioxylate intermediate has a lower activation barrier than the two-step process via the [2+2] addition of to form the metallaoxetane intermediate and subsequent re-arrangement of the metallaoxetane to the dioxylate. The dioxylate intermediate is more stable than the metallaoxetane intermediate. The reaction between pertechnetate and ethylene would not result in the formation of the epoxide precursor.
2. In the oxidation of ethylene by TcO_3Cl , the direct [3+2] addition of the C=C bond of ethylene across the O=Tc=O bonds of doublet TcO_3Cl to form the dioxylate intermediate has a lower activation barrier than the two-step reaction via the [2+2] addition of the C=C bond of ethylene across Tc=O bond of TcO_3Cl to form the metallaoxetane intermediate and subsequent rearrangement of the metallaoxetane intermediate to the dioxylate. The most plausible pathway that leads to the epoxide precursor is from the organometallic intermediate **X/d** followed by re-arrangement. Thus in the reaction of TcO_3Cl with ethylene, the formation of the dioxylate intermediate is thermodynamically and kinetically favorable than the formation of the epoxide precursor and metallaoxetane formation by the [2+2] addition pathway.
3. In the oxidation of ethylene by $\text{TcO}_3(\text{CH}_3)$, the formation of the epoxide precursor by the direct attack of ethylene on an oxo ligand of $\text{TcO}_3(\text{CH}_3)$ has a lower activation barrier than the direct [3+2] addition of the C=C bond of ethylene across the O=Tc=O bond of singlet and doublet $\text{TcO}_3(\text{CH}_3)$ to form the dioxylate intermediate and the metallaoxetane formation and subsequent re-arrangement from the [2+2] addition pathway. However, the

dioxylate formation on the doublet surface is thermodynamically favorable than the epoxide precursor formation. Thus the formation of the epoxide precursor is kinetically favorable while the formation of the dioxylate is thermodynamically favorable for ethylene addition to $\text{TcO}_3(\text{CH}_3)$.

4. In the reaction of ethylene with TcO_3Cp , the direct [3+2] addition of the C=C bond of ethylene across the O=Tc=O of singlet TcO_3Cp to form the dioxylate intermediate has a lower activation barrier than the two-step process via the [2+2] addition pathway to form the metallaoxetane intermediate and subsequent re-arrangement to form the dioxylate. Thus in the reaction of TcO_3Cp with ethylene, the [3+2] addition pathway is more feasible kinetically and thermodynamically than the [2+2] addition pathway leading to the formation of the metallaoxetane intermediate. The reaction of TcO_3Cp with ethylene does not result in the formation of an epoxide precursor, in agreement with the related works of Burrell *et al.*, (1995), Herrmann *et al.* (1984); Klahn-olive *et al.*, 1984 and Kühn *et al.*, (1994) who reported ReO_3Cp reacts with ethylene to predominately form dioxylates.
5. In the oxidation of ethylene by $\text{TcO}_3(\text{OCH}_3)$, the direct [3+2] addition of the C=C bond of ethylene across the O=Tc=O bond of doublet $\text{TcO}_3(\text{OCH}_3)$ to form the dioxylate intermediate has a lower activation barrier than the [2+2] addition of ethylene across the Tc=O bond of singlet and doublet $\text{TcO}_3(\text{OCH}_3)$ to form the metallaoxetane intermediate and subsequent re-arrangement to the dioxylate. The most plausible pathway to the formation of the epoxide precursor is by direct attack of the ethylene on one of the oxo ligand of singlet $\text{TcO}_3(\text{OCH}_3)$. Thus in the reaction of $\text{TcO}_3(\text{OCH}_3)$ with ethylene, the direct [3+2] addition across the two oxygen atoms of doublet $\text{TcO}_3(\text{OCH}_3)$ is

kinetically and thermodynamically favorable than the [2+2] addition pathway to form the metallaoxetane intermediate and subsequent re-arrangement to the dioxylate.

6. In the reaction between $\text{TcO}_3(\text{NPH}_3)$ and ethylene, the direct[2+2] addition of the C=C bond of ethylene across the Tc=N bond of doublet $\text{TcO}_3(\text{NPH}_3)$ to form the four membered metallacycle has a lower activation barrier than the direct [3+2] addition of ethylene across the O=Tc=O and N=Tc=O bonds of singlet and doublet $\text{TcO}_3(\text{NPH}_3)$ leading to the formation of the five membered metallacycle. The two-step process via the [2+2] addition of ethylene across the Tc=O bond of $\text{TcO}_3(\text{NPH}_3)$ to form the metallaoxetane intermediate and the subsequent re-arrangement of the metallaoxetane to the dioxylate has a higher activation barrier. Thus the most plausible pathway to the formation of the epoxide precursor is by initial [3+2] addition across the two oxygen atoms of doublet $\text{TcO}_3(\text{NPH}_3)$ followed by re-arrangement. The formation of the four membered metallacycle by the direct [2+2] addition of the C=C bond of ethylene across the Tc=N bond of doublet $\text{TcO}_3(\text{NPH}_3)$ is kinetically and thermodynamically more favorable.
7. Generally, in the reaction of ethylene with LTcO_3 , the [3+2] addition pathway is favored kinetically and thermodynamically when $\text{L} = \text{O}^-$, Cp, OCH_3 and Cl while the [2+2] addition pathway is kinetically and thermodynamically favorable when $\text{L} = \text{NPH}_3$. The [2+1] addition pathway leading to the formation of the epoxide precursor is kinetically and thermodynamically favorable when $\text{L} = \text{CH}_3$.

REFERENCES

- Al-Ajlouni, A. M.; Espenson, J. H. (1995) Epoxidation of Styrenes by Hydrogen Peroxide As Catalyzed by Methyl rhenium Trioxide. *J. Am. Chem. Soc.* 117: 9243.
- Al-Ajlouni, A. M.; Espenson, J. H. (1996) Kinetics and Mechanism of the Epoxidation of Alkyl-Substituted Alkenes by Hydrogen Peroxide, Catalyzed by Methyl rhenium Trioxide. *J. Org. Chem.* 61: 3969.
- Burrell, A. K.; Cotton, F. A.; Daniels, L. M.; Petricek, V. (1995) Structure of Crystalline (C₅Me₅)ReO₃ and Implied Nonexistence of "(C₅Me₅)Tc₂O₃" *Inorg. Chem.* 34: 4253.
- Clark, M.; Cramer, R. D.; Opdenbosch, N. V. (1989) Validation of the general purpose tripos5.2 force field. *J. Comp. Chem.* 10: 982-1012.
- Criegee, R. (1936) Osmiumsauer-ester als Zwischenprodukte bei Oxydationen. *Justus Liebigs Ann. Chem.* 522:75-96.
- Criegee, R.; Marchand, B.; Wannowius, H. (1942) Zur Kenntnis der organischen Osmium-Verbindungen. II. Mitteilung. *Justus Liebigs Ann. Chem.* 550:99-133.
- Dickson, R. M.; Ziegler, T. (1996) A density functional study of the electronic spectrum of permanganate. *Int. J. Quantum Chem.* 58: 681-687.
- Döbler, C.; Mehlretter, G. M.; Sundermeier, U.; Beller, M. (2000) Osmium-Catalyzed Dihydroxylation of Olefins Using Dioxygen or Air as the Terminal Oxidant. *J. Am. Chem. Soc.* 122:10289.

Dunning, T. H. Jnr.; Hay, P. J. (1976) In: Modern Theoretical Chemistry, H. F. Schaefer, III, Vol.3; Plenum, New York.

Enemark, J. H.; Young, C. G. (1993) Bioinorganic Chemistry of Pterin-Containing Molybdenum and Tungsten Enzymes.*Adv.Inorg.Chem.* 40: 1.

Gisdakis, P.; Rösch, N. (2001) [2+3] Cycloaddition of Ethylene to Transition Metal Oxo Compounds. Analysis of Density Functional Results by Marcus Theory.*J. Am. Chem. Soc.* 123:697 - 701.

Herrmann, W. A.; Alberto, R.; Kiprof, P.; Baumgartner, F. (1990) Alkyl technetium Oxides: First Examples and Reactions.*Angew. Chem., Int. Ed. Engl.* 29: 189.

Herrmann, W. A.; Fischer, R. W.; Scherer, W.; Rauch, M. U. (1993) Methyltrioxorhenium (VII) as Catalyst for Epoxidation: Structure of the Active Species and Mechanism of Catalysis.*Angew. Chem., Int. Ed. Engl.* 32: 1157.

Herrmann, W. A.; Kühn, F. E. (1997) Organorhenium Oxides. *Acc. Chem. Res.* 30: 169.

Herrmann, W. A.; Serrano, R.; Bock, H. (1984) Multiple Bonds between Main-Group Elements and Transition Metals. 130 (Cyclopentadienyl) trioxorhenium (VII): Synthesis, Derivatives, and Properties. *Angew. Chem., Int. Ed. Engl.* 23: 383.

Jonsson, S. Y.; Färnegårdh, K.; Bäckvall, J.-E. (2001) Osmium-Catalyzed Asymmetric Dihydroxylation of Olefins by H₂O₂ Using a Biomimetic Flavin-Based Coupled Catalytic System. *J. Am. Chem. Soc.* 123:1365-1371.

Jorgensen, K. A. (1989) Transition-metal-catalyzed epoxidation.*Chem. Rev.* 89:431- 458.

Klahn-Oliva, A. H.; Sutton, D. (1984) (Pentamethylcyclopentadienyl) trioxorhenium, ($\eta^5\text{-C}_5\text{Me}_5$) ReO_3 . *Organometallics* 3: 1313 - 1314.

Kühn, F. E.; Herrmann, W. A.; Hahn, R.; Elison, M.; blümel, J.; Herdtweck, E. (1994) Multiple Bonds between Main-Group Elements and Transition Metals. 130. (Cyclopentadienyl)trioxorhenium(VII): Synthesis, Derivatives, and Properties. *Organometallics*. 13:1601-1606.

March, J. (1985) *Advanced Organic Chemistry*, 3rd ed.; Wiley: New York, 732.

Mijs, W.; Jonge, C. R. (1986) (Eds.) *Organic Synthesis by oxidation with Metal Compound*. Plenum, New York, 1986.

Romão, C. C.; Kühn, F. E.; Herrmann, W. A. (1997) Rhenium (VII) Oxo and Imido Complexes: Synthesis, Structures, and Applications. *Chem. Rev.* 97: 3197-3246.

San Filippo, J.; Chern, C. (1977) chemisorbed chromyl chloride as a selective oxidant *J. Org. Chem.* 42: 2182.

Schröder, M. (1980) Osmium tetroxide cis-hydroxylation of unsaturated substrates. *Chem. Rev.* 80: 187 - 213.

Sharpless, K. B.; Akashi, K. (1975) Oxidation of alcohols to Aldehydes by reagents derived from chromyl chloride. *J. Am. Chem. Soc.* 97: 5927.

Spartan, Waefunction, Inc.; 18401 Von Karman Ave., # 370, Irvine, CA, 92715, USA.

Wadt, W. R.; Hay, P. J. (1985) Ab initio effective core potentials for molecular calculations. Potentials for main group elements Na to Bi. *J. Chem. Phys.* 82: 284.

Wadt, W. R.; Hay, P. J. (1985) Ab initio effective core potentials for molecular calculations. Potentials for K to Au including the outermost core orbitals. *J. Chem. Phys.* 82: 299.

Haunschuld, R.; Frenking, G. (2008) Quantum chemical study of ethylene addition to group-7 oxo complexes $\text{MO}_2(\text{CH}_3)(\text{CH}_2)$ ($\text{M} = \text{Mn}, \text{Tc}, \text{Re}$). *J. Organomet. Chem.* 24: 362.

KNUST



CHAPTER FOUR

A COMPUTATIONAL STUDY OF THE MECHANISMS OF OXIDATION OF ETHYLENE BY RHENIUM OXO COMPLEXES

4.1 INTRODUCTION

The role of transition metal oxo compounds in the dihydroxylation of olefins is an important class of oxygen transfer reactions (Kolb *et.al.*, 1994; Johnson and Sharpless, 1993; Schröder, 1980). Many experimental and theoretical investigations have focused on mechanistic aspects of this type of reaction. Olefin dihydroxylation catalyzed by transition metal oxo species of the type LMO_3 has been the subject of extensive theoretical studies (Dapprich *et. al.*, 1996; Pidun *et. al.*, 1996; Torrent *et. al.*, 1997; Del Monte *et. al.*, 1997; Nelson *et. al.*, 1997; Corey *et. al.*, 1996; Haller *et. al.*, 1997; Houk *et.al.*, 1999; Torrent *et. al.*, 1998).

In the initial step of the dihydroxylation reaction catalyzed by transition metal oxo compounds such as MnO_4^- , the olefin reacts directly with a $O=Mn=O$ functionality of MnO_4^- in a [2+3] manner to form a metalladioxolane, a five-membered metallacycle (structure **2** in Scheme 4.1)(Criegee *et. al.*, 1936; 1942).

The intermediacy of a metallaoxetane (structure **4**) arising from the [2+2] addition pathway as suggested by Sharpless (Sharpless *et. al.*, 1977) for chromyl chloride oxidation of olefins was ruled out, at least for MnO_4^- , by density functional theory (DFT) calculations (Houk *et. al.*, 1999) and corroborated by experimental kinetic isotope effects studies (Del Monte *et. al.*, 1997; Rouhi *et. al.*, 1997).

However, for ethylene addition to $Cl_2(O)ReCH_2$, the activation barrier for the [2+2] addition pathway across the Re-C bond of the complex was found to be lower than the barrier for the

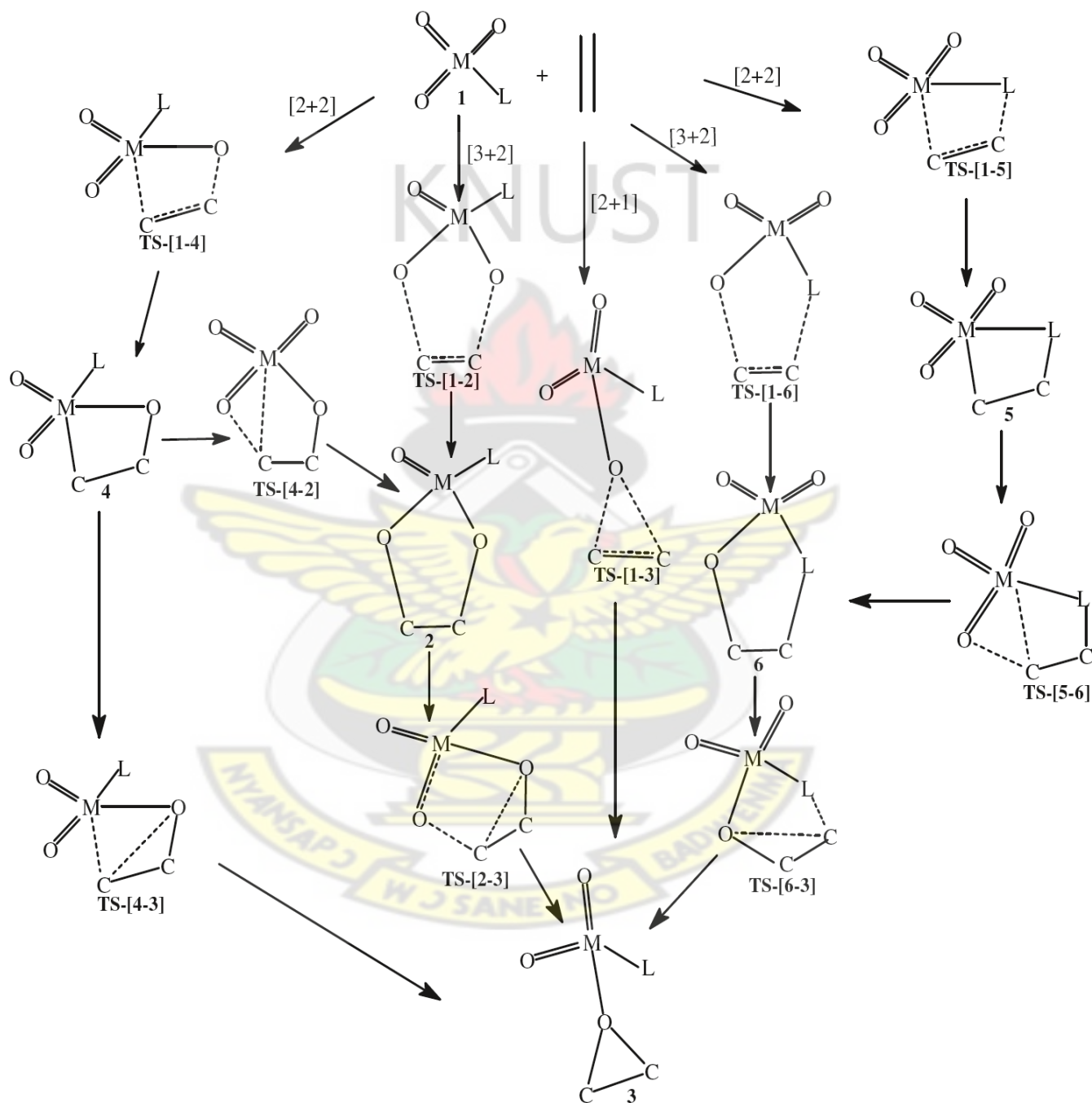
[3+2] addition across the O-Re-C and O-Re-Cl bonds of $\text{Cl}_2(\text{O})\text{ReCH}_2$ (Tia and Adei, 2011). Deubel *et al.* (2001) found that the activation barrier for the [2+2] addition pathway becomes lower than the [3+2] addition pathways for ketene addition to LReO_3 ($\text{L} = \text{NPH}_3, \text{O}^-$).

Theoretical calculations focusing on the [3+2] and [2+2] addition pathways were explored for the transition metal-oxo complexes of the type LReO_3 (Pietsch. *et al.*, 1998; Deubel and Frenking, 1999) with ethylene. Pietsch *et al.* (1998) employed a hybrid density functional theory B3LYP in conjunction with the Hay-Wadt relativistic effective core potential (ECP) for Re (LANL2). This basis was combined with the 6-31G* basis set for other ligands, to compare the [2+2] and [2+3] addition pathways by focusing only on the reaction energies for the addition of LReO_3 ($\text{L} = \text{Cp}^*, \text{Cp}, \text{Cl}, \text{CH}_3, \text{OH}, \text{OCH}_3, \text{O}^-$) to ethylene, yielding either the metalladioxolane via the [3+2] addition pathway or the metallaoxetane via the [2+2] addition pathway. By employing qualitative molecular orbital diagrams they asserted that the π donor strength of the ligands L is responsible for the reactivity differences of this type of complexes. To corroborate these claims, Deubel and Frenking, (1999) reported the calculated potential energy surfaces for the [3+2] and [2+2] addition of LReO_3 ($\text{L} = \text{O}^-, \text{Cl}, \text{Cp}$) to ethylene and for the interconversion of the metallaoxetane to the dioxylate, at the B3LYP level (Becke *et al.*, 1993) in conjunction with relativistic small-core ECPs with a valence basis set splitting (441/2111/21) were used for Re, and 6-31G (d) all-electron basis sets were employed for all other atoms. Their results indicated that for all complexes of the type LReO_3 ($\text{L} = \text{O}^-, \text{Cl}, \text{Cp}$), the [2+2] pathway has a higher activation barrier than the corresponding [3+2] pathway. The activation barriers of the rearrangement of the metallaoxetane intermediate to the dioxylate were calculated to be higher (>50 kcal/mol). Deubel and Frenking, (1999) rationalized the reactivity differences using a charge-transfer model and a frontier orbital argument.

Gisdakis and Rösch (2001) further extended the works of Pietsch *et. al.* (1998) and Deubel and Frenking (1999) by assigning charges ($q = -1, 0, 1$) to the complex $LReO_3^q$, such that the systems are isoelectronic to OsO_4 . They explored the mechanism of the [2+3] cycloaddition of $LReO_3$ ($L = O^-, CH_3, Cl, Cp$) to ethylene using the hybrid B3LYP approach, with effective core potentials and double-zetabasis sets, LanL2DZ, for the transition metals and 6-311G(d,p) basis sets for H, C, O, and F. Taking a cue from the work of Frenking and Deubel (1999) that the [2+2] pathway has a higher barrier, Gisdakis and Rösch (2001) did not study the formation of the diol from the metallaoxetane along the [2+2] addition pathway.

The aim of this work is to extend the works of Pietsch *et. al.*(1998), Deubel and Frenking, (1999) and Gisdakis and Rösch (2001) by reporting the calculated potential energy surfaces for the [3+2] and [2+2] addition of $LReO_3$ ($L = O^-, Cl, Cp, CH_3, OCH_3, NPH_3$) to ethylene, explore the mechanistic pathway to the formation of the epoxide precursor by employing a hybrid density functional theory at the B3LYP/LACVP* level of theory. Other [3+2] and [2+2] addition pathways have been explored in addition to those already studied. The singlet, doublet, triplet and quartet electronic states of each species are explored where possible.

Scheme 4.1: Proposed pathway for the reaction of LMO₃ (M=Re) with ethylene



4.2 DETAILS OF CALCULATION

All calculation were carried out with Spartan '08 V1.2.0 and Spartan'10.1.10 Molecular Modeling programs (Wavefunction, 2008; 2010) at the DFT B3LYP/LACVP* level of theory. The B3LYP functional is a Hartree-Fock density functional. The LACVP* basis set is a relativistic effective core –potential that describes the atoms H-Ar with the 6-31G* basis while heavier atoms are modeled with the LANL2DZ basis set which uses the all-electron valence double zeta basis set (D95V), developed by Dunning, for first row elements (Dunning and Hay, 1976) and the Alamos ECP plus double zeta basis set developed by Wadt and Hay for the atoms Na-La, Hf-Bi (Hay and Wadt, 1985a; 1985b; Wadt and Hay, 1985).

The starting geometries of the molecular systems were constructed using Spartan's graphical model builder and minimized interactively using the sybyl force field (Clark's *et. al.*, 1989). All geometries were fully optimized without any symmetry constraints. A normal mode analysis was performed to verify the nature of the stationery points. Equilibrium geometries were characterized by the absence of imaginary frequencies.

The transition state structures were located by a series of constrained geometry optimization in which the forming-and breaking–bonds are fixed at various lengths whiles the remaining internal coordinates were optimized. The approximate stationary points located from such a procedure were then fully optimized using the standard transition state optimization procedure in Spartan. All first–order saddle- point were shown to have a Hessian matrix with a single negative eigenvalue, characterized by an imaginary vibrational frequency along the reaction coordinate. All computations were performed on Dell precision T3400 Workstation computers.

4.3 RESULTS AND DISCUSSION

4.3.1 Reaction of ReO_4^- with Ethylene

The optimized geometries and relative energies of the main stationary points involved in the reaction between ReO_4^- and ethylene are shown in Fig.4.1 and Fig.4.2, respectively. The density functional theory (DFT) geometry optimization of $\text{ReO}_4\text{C1/s}$ on a singlet potential energy surface (PES) has all the Re-O bonds at 1.738 Å. A doublet C1/d and quartet C1/d reactant has been computed to be 121.97 and 194.12 kcal/mol less stable than the singlet reactant C1/s .

The [3+2] addition of the C=C bond of ethylene across the O=Re=O bonds of ReO_4^- through the singlet transition state TS-[C1-C2]/s to form dioxorhena-2, 5-dioxolane C2/s has an activation barrier of 36.30 kcal/mol and endothermicity of 16.53 kcal/mol in agreement with the reported activation and reaction energies of +37.7 and 19.40 kcal/mol by Deubel and Frenking, (1999) and Gisdakis and Rösch, (2001). The calculated transition state structure is symmetrical and synchronous with respect to the newly forming C-O bonds (1.80 Å).

On the triplet surface, the transition state linking the reactant to the product could not be located. However, a triplet dioxyate species C2/t was located and found to be 24.99 kcal/mol less stable than the singlet product. In the singlet product C2/s , the two Re=O bonds to the 'spectator' oxygen atoms (the oxygen atom not part of the ring) are equal (1.73 Å) and those to the oxygen atom involved in the ring are also equal (1.98 Å), in agreement with the reported values by Deubel and Frenking,(1999).In the triplet product C2/t , has the two Re=O bonds to the 'spectator' oxygen atoms unequal (1.74 and 1.78 Å) and those to the oxygen atom involved in the ring are also unequal (1.97 and 2.01Å). The quartet dioxyate intermediate could however be located on the reaction surface.

The formation of the rhenaoxetane **C3/s** through transition state **TS-[C1-C3]** on a singlet PES by [2+2] addition of C=C bond of ethylene across Re=O bond of the perrhenate complex **C1** has an activation barrier of 46.68 kcal/mol and an endothermicity of 20.26 kcal/mol. This agrees with the work of Deubel and Frenking (1999) who calculated a barrier and endothermicity of 47.2 and 21.60 kcal/mol respectively along the [2+2] addition route. A triplet rhenaoxetane **C3/t** has an endothermicity of 68.91 kcal/mol making it 48.65 kcal/mol less stable than the singlet rhenaoxetane **C3/s**. The Re-C and C-O bonds in the singlet rhenaoxetane **C3/s** are 2.18 and 1.41 Å respectively, which are comparable to the lengths of 2.19 and 1.41 Å computed by Deubel and Frenking (1999). The Re-C bond is 0.02 Å shorter in the triplet rhenaoxetane **C3/t** than in the singlet rhenaoxetane **C3/s**. while, the C-O bond is 0.018 Å longer in the triplet rhenaoxetane than in the singlet rhenaoxetane. The quartet metallaoxetane intermediate **C3/q** has reaction energy of -25.75 kcal/mol.

The reaction surface was explored for the re-arrangement of the metallaoxetane to the dioxylate (**TS-[4-2]** in Scheme 4.1) as suggested by Sharpless *et. al.* (1977) for the chromyl chloride oxidation of olefins. The re-arrangement of the singlet rhenaoxetane to the dioxylate through transition state **TS-[C3-C2]/s** is +36.40 kcal/mol. No transition state was located for the re-arrangement of the doublet, triplet and quartet rhenaoxetane to the dioxylate. The overall activation barrier for the re-arrangement of the singlet rhenaoxetane to the dioxylate is +16.14 kcal/mol, which is lower than the activation barrier for the direct [3+2] addition of ethylene across the two oxygen atoms of singlet ReO_4^- . However, since the first-step features a higher activation barrier (+46.68 kcal/mol in Figure 4.1), the re-arrangement is unfeasible and the dioxylate is formed from the direct addition pathway.

The potential energy surface of the reaction of rhenium tetraoxide with ethylene was further explored in an attempt to locate an epoxide precursor ($O_3\text{-Re-OC}_2\text{H}_4$) (**3** in Scheme 4.1), but no such minimum was found on the reaction surface. From the work of Ziegler *et al.* (1999) and Tia and Adei (2009) on the chromyl chloride, the epoxide precursor could arise from three pathways:

- d) A two-step process involving the formation of a metallaoxetane, followed by re-arrangement.
- e) A two-step process involving the formation of the five membered metallacycle, followed by re-arrangement.
- f) A direct one-step addition of the C=C bond across one oxygen atom of ReO_4^- .

Attempt to locate transition states TS [4-3], TS [2-3] and TS [1-3] (Scheme 4. 1) which could account for the metallaoxetane, dioxylate or the direct addition to the epoxide precursor proved futile. All these are indication that the reaction of rhenium tetraoxide with ethylene does not lead to the formation of an epoxide. Thus in the reaction of ReO_4^- with ethylene, the [3+2] addition pathway leading to the formation of the dioxylate intermediate is kinetically and thermodynamically favorable than the [2+2] addition pathway to form the metallaoxetane intermediate.

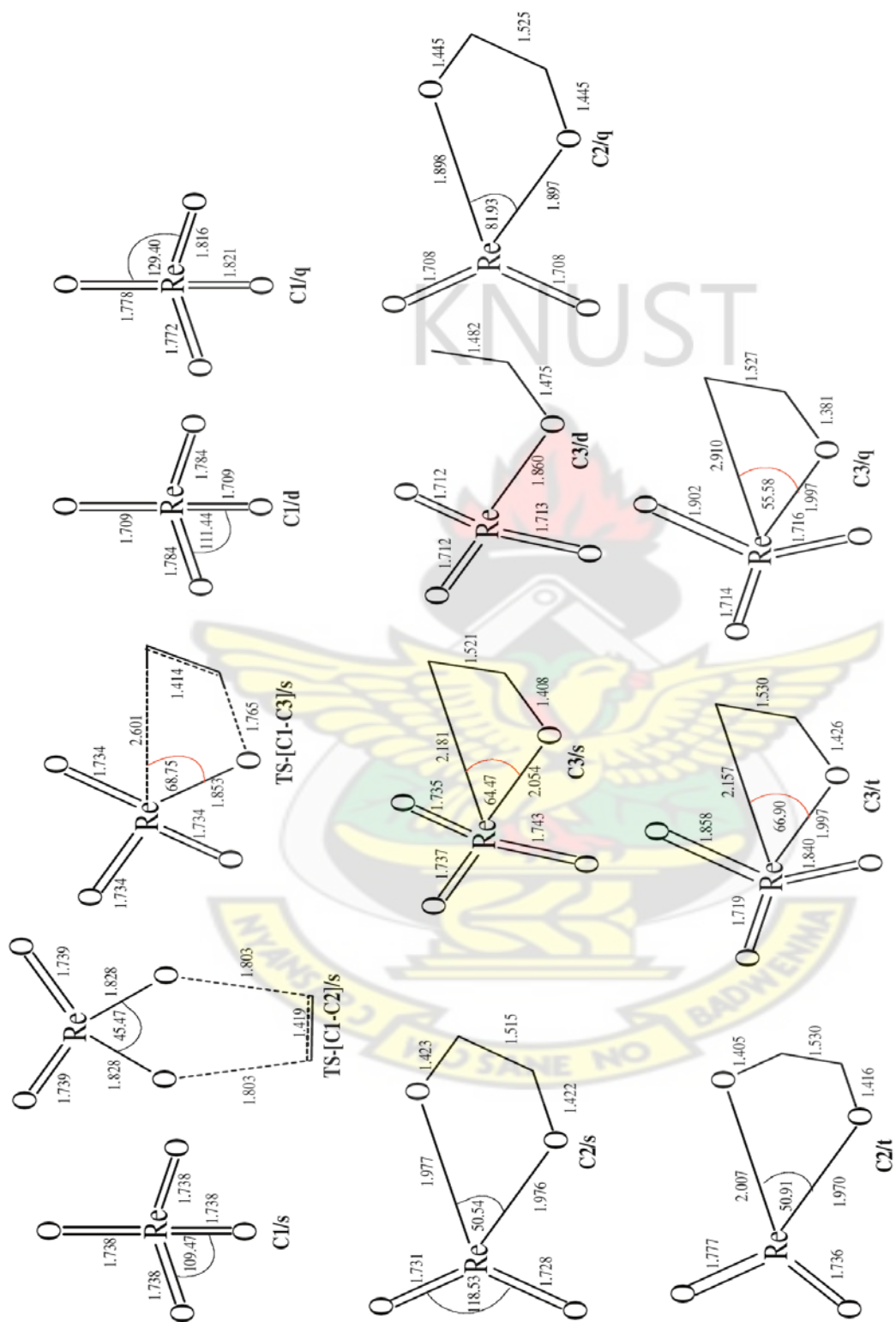


Figure 4.1: Optimized geometrical parameters of the main stationary points involved in the reaction between ReO_4^- and ethylene. Bond distances in Å

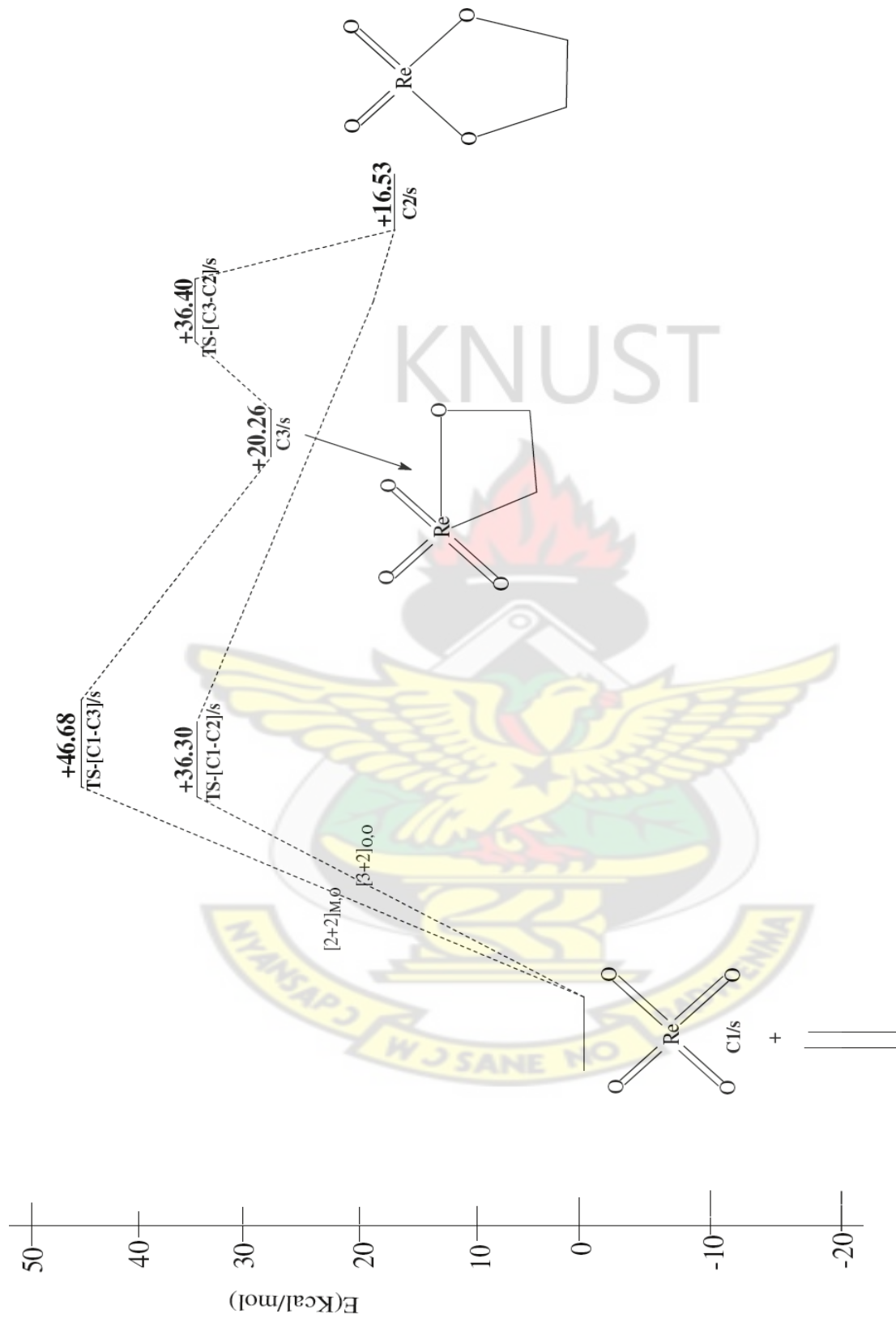


Figure 4. 2: Energetics of the reaction of ReO_4^- and ethylene. Relative energies in kcal/mol

4.3.2 Reaction of ReO_3Cl with ethylene

Figures 4.3 and 4.4 respectively shows the optimized geometries and relative energies of the main stationary points involved in the reaction between ReO_3Cl and ethylene. The DFT geometry optimization of ReO_3Cl on a singlet potential energy surface yielded a minimum **C4/s** of C_{3v} symmetry in which each of the three $\text{Re}=\text{O}$ bonds is 1.70 Å long and the $\text{Re}-\text{Cl}$ bond is 2.27 Å long.

A doublet reactant **C4/d** has been computed to be 49.85 kcal/mol more stable than the singlet reactant **C4/s** and 112.54 kcal/mol more stable in relation to a triplet reactant **C4/t** that has been located. The $\text{Re}-\text{Cl}$ bond in the doublet reactant **C4/d** is 0.24 Å longer than in the singlet structure **C4/s** and 0.19 Å longer than in the triplet structure **C4/t**.

A quartet reactant **C4/q** has also been computed and found to be 58.88 kcal/mol less stable than the doublet reactant. Thus of all the reactant structures optimized, the doublet is most stable: 49.85, 11.25 and 58.88 kcal/mol more stable than the singlet, triplet and quartet reactants respectively.

On the singlet surface, the direct [3+2] addition of $\text{C}=\text{C}$ bond of ethylene across the $\text{O}=\text{Re}=\text{O}$ bonds of singlet ReO_3Cl through a singlet transition state **TS-[C4-C5]/s** to form the dioxylate **C5/s** has an activation barrier of 20.99 kcal/mol and an endothermicity of 0.52 kcal/mol in agreement with the works of Deubel and Frenking, (1999) and Gisdakis and Rösch, (2001)

On the doublet surface, the [3+2] addition of the $\text{C}=\text{C}\pi$ bond of ethylene across the $\text{O}=\text{Re}=\text{O}$ bonds of doublet ReO_3Cl could either follow the concerted or stepwise addition mechanism. For ethylene addition to ReO_3Cl through the concerted addition pathway, the activation barrier is +33.17 kcal/mol.

On the stepwise addition pathway, the C=C π bond attaches itself to an oxo-ligand of the doublet reactant ReO₃Cl **C4/d** through the transition state **TS-[C4-X]/d** to form the intermediate **X/d**. The activation barrier for the first-step is +29.32 kcal/mol. The intermediate **X/d** could then re-arrange through transition state **TS-[X-C5]/d** to form the dioxylate species **C5/d** which has activation barrier and exothermicity of +43.13 and 17.96 kcal/mol respectively. Thus, the barrier along stepwise addition pathway is higher than the concerted route.

The triplet counterpart of the transition state **TS-[C4-C5]/s** linking the reactant to the product could not be located. However, a triplet dioxylate product **C5/t** was located and found to be 56.33 and 47.85 kcal/mol more stable than the singlet **C5/s** and doublet **C6/d** dioxylate products respectively. A quartet dioxylate **C5/q** product has been computed to be 31.17 kcal/mol more stable than the doublet product **C5/d**.

The stepwise [3+2] addition of the C=C bond of ethylene across the O=Re-Cl bonds of doublet ReO₃Cl through transition state **TS-[C4-X]/d** leads to the intermediate **X/d**, a pathway that was not reported in earlier studies of Deubel and Frenking (1999) and Boehme *et. al.*, (1999). The formation of the intermediate requires an activation barrier of +29.32 kcal/mol. The transition state **TS-[X-C6]/d** for the re-arrangement of the intermediate **X/d** to the five-membered metallacycle **C6/d** has activation barrier of +15.07 kcal/mol. The resulting five membered metallacycle **C6/d** is 14.04 kcal/mol less stable than the separated reactants.

On the singlet surface, the concerted [3+2] addition of the C=C π bond of ethylene across the O=Re-Cl functionality of singlet ReO₃Cl through a singlet transition state **TS-[C4-C6]/s** has an activation barrier of 26.26 kcal/mol and the resulting five-membered species **C6/s** is 20.18

kcal/mol endothermic. No stepwise pathway was found [3+2] addition of the C=C π bond of ethylene across the O=Re-Cl functionality of singlet ReO₃Cl.

No transition states were located connecting the reactants to the products on the triplet and quartet surfaces. A triplet species **C6/t** is 9.87 kcal/mol more stable than the doublet dioxylate **C6/d**. The quartet product **C6/q** is computed to be 25.54 kcal/mol more stable than the doublet product **C6/d**.

A singlet and a doublet transition state has been located for the concerted [2+2] addition of the C=C π bond of ethylene across the Re=O bond of singlet and doublet ReO₃Cl. The formation of doublet rhenaoxetane **C7/d** through the doublet transition state **TS-[C4-C7]/d** has an activation barrier of 27.28 kcal/mol and exothermicity of 7.13 kcal/mol.

The concerted [2+2] addition through the singlet transition state **TS-[C4-C7]/s** linking the reactants to the product **C7/s** has an activation barrier of 29.62 kcal/mol and endothermicity of 2.88 kcal/mol. Also, attempts were made to form the doublet metallaoxetane **C7/d** from intermediate **X/d** through transition state **TS-[X-C7]/d** in the step-wise addition pathway. Animating the motion of the atoms along the reaction co-ordinate in the transition state **TS-[X-C7]/d**, points to the reaction being concerted, indicating that the formation of the metallaoxetane intermediate follows a concerted mechanism rather than a stepwise mechanism.

No triplet transition state could be located. A triplet rhenaoxetane **C7/t** has been computed to be 30.06 kcal/mol more stable than the singlet rhenaoxetane **C7/s**. A quartet rhenaoxetane intermediate **C7/q** has also been computed to be 4.22 kcal/mol more stable than the singlet rhenaoxetane **C7/s**.

The re-arrangement of the singlet, doublet, triplet and quartet metallaoxetane to the five-membered dioxylate through the transition state (TS-[4-2] in Scheme 4.1) was explored for the reaction of ReO_3Cl with ethylene. The transition state **TS-[C7-C5]/s** for the re-arrangement of the singlet metallaoxetane to the dioxylate is +99.21 kcal/mol. On the doublet PES, the re-arrangement of the metallaoxetane to the dioxylate through transition state **TS-[C7-C5]/d** is +50.27 kcal/mol. No triplet and quartet transition state was located for the re-arrangement of the metallaoxetane to the dioxylate.

The overall activation barrier(+46.48 kcal/mol) for the re-arrangement of the singlet metallaoxetane to the dioxylate is higher than the activation barrier for the direct [3+2] addition across the two oxygen atoms of singlet ReO_3Cl (+20.99 kcal/mol). Also, the activation barrier for the re-arrangement of the doublet metallaoxetane to the dioxylate (+57.40 kcal/mol) is higher than the activation barrier for the direct [3+2] addition of ethylene across the two oxygen atoms of doublet ReO_3Cl (+33.17 kcal/mol). Consequently the re-arrangement of the metallaoxetane to the dioxylate is not likely to be a competitive pathway in the formation of the dioxylate in the light of the available data.

The reaction of ReO_3Cl with ethylene was explored for the possibility of the formation of the epoxide precursor

The transition state **TS-[C6-D]/s** (ie **TS-[6-3]** in Scheme 4.1) for the re-arrangement of the singlet five-membered metallacycle to the epoxide precursor has an activation barrier of +18.86 kcal/mol above the reactants and endothermicity of 11.2 kcal/mol.

On the doublet surface, the epoxide precursor could arise from intermediate **X/d** through transition state **TS-[X-D]/d**. The activation barrier and reaction energy along that route are +29.44 and -2.96 kcal/mol.

The transition state **TS-[C7-D]/s** (**TS-[4-3]** in Scheme 4.1) for the rearrangement of the four-membered metallaioxetane to the epoxide precursor has an activation barrier and reaction energy of +56.81 and 28.50 kcal/mol. Also, the activation barrier and reaction energy for the direct one-step addition of the C=C bond across one oxygen atom of ReO_3Cl (**TS-[1-3]** in Scheme 1) are +31.24 and 24.73 kcal/mol on the doublet surface.

The most plausible pathway for the formation of the epoxide precursor, if it is to form at all, is by the re-arrangement of the intermediate **X/d** to the epoxide precursor.

The reaction of ReO_3Cl with ethylene is likely to preferentially take place on the doublet PES and the [2+2] addition of ethylene across the $\text{Re}=\text{O}$ bond of doublet ReO_3Cl is kinetically and thermodynamically favorable than the formation of the five membered metallacycles.

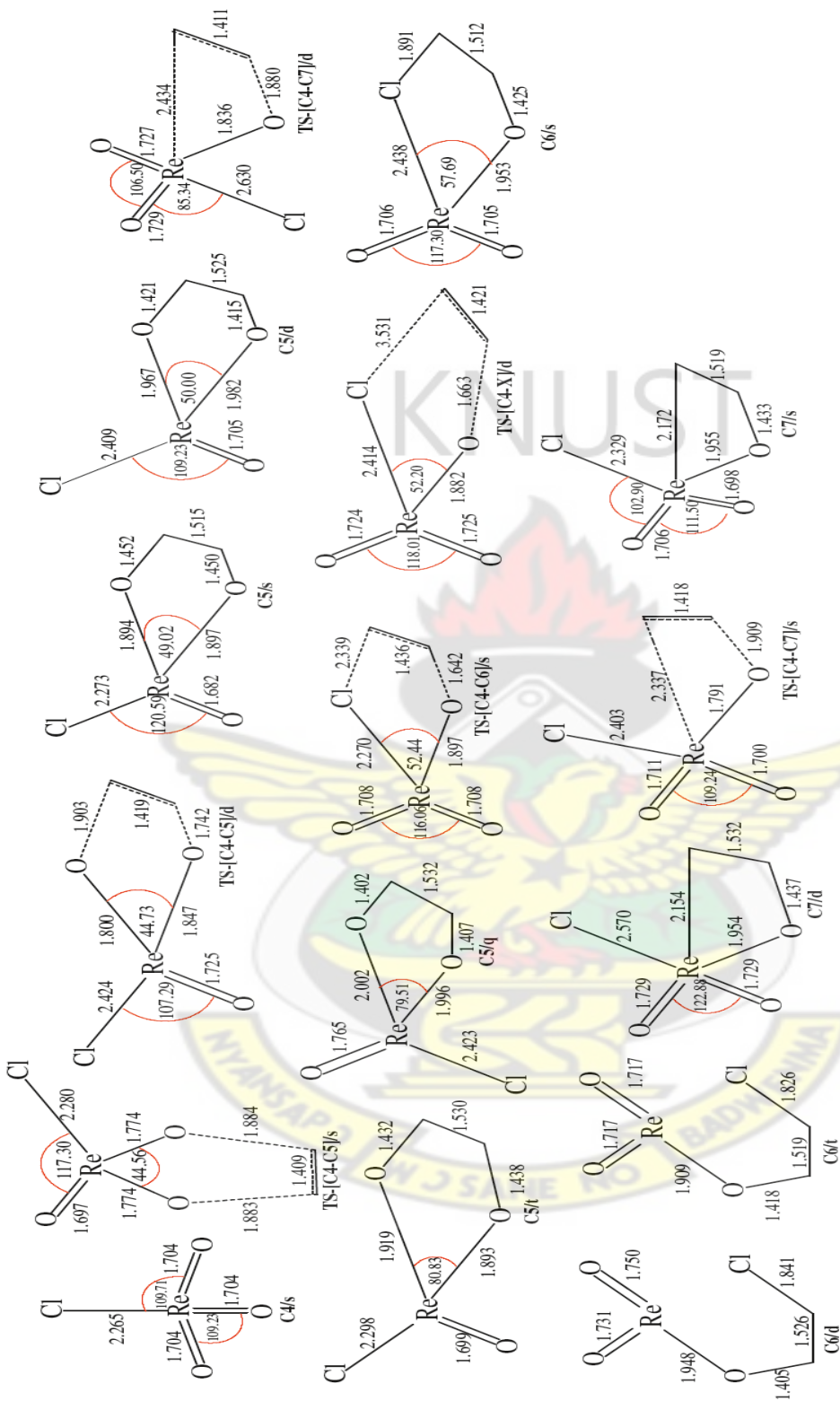


Figure 4.3: Optimized geometrical parameters of the main stationary points involved in the reaction of ReO_2Cl with ethylene. Distance in Å and bond angles in degrees.

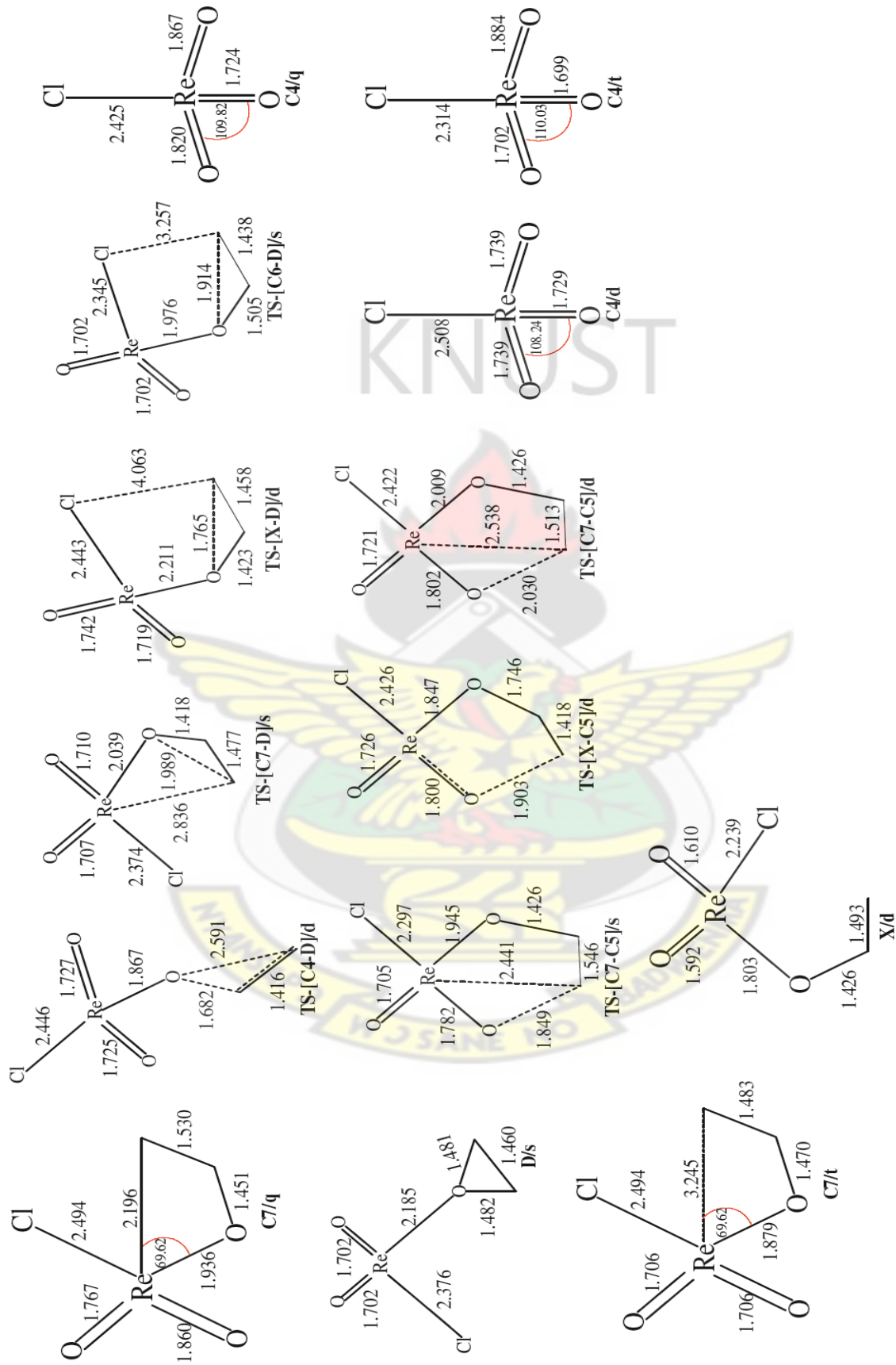
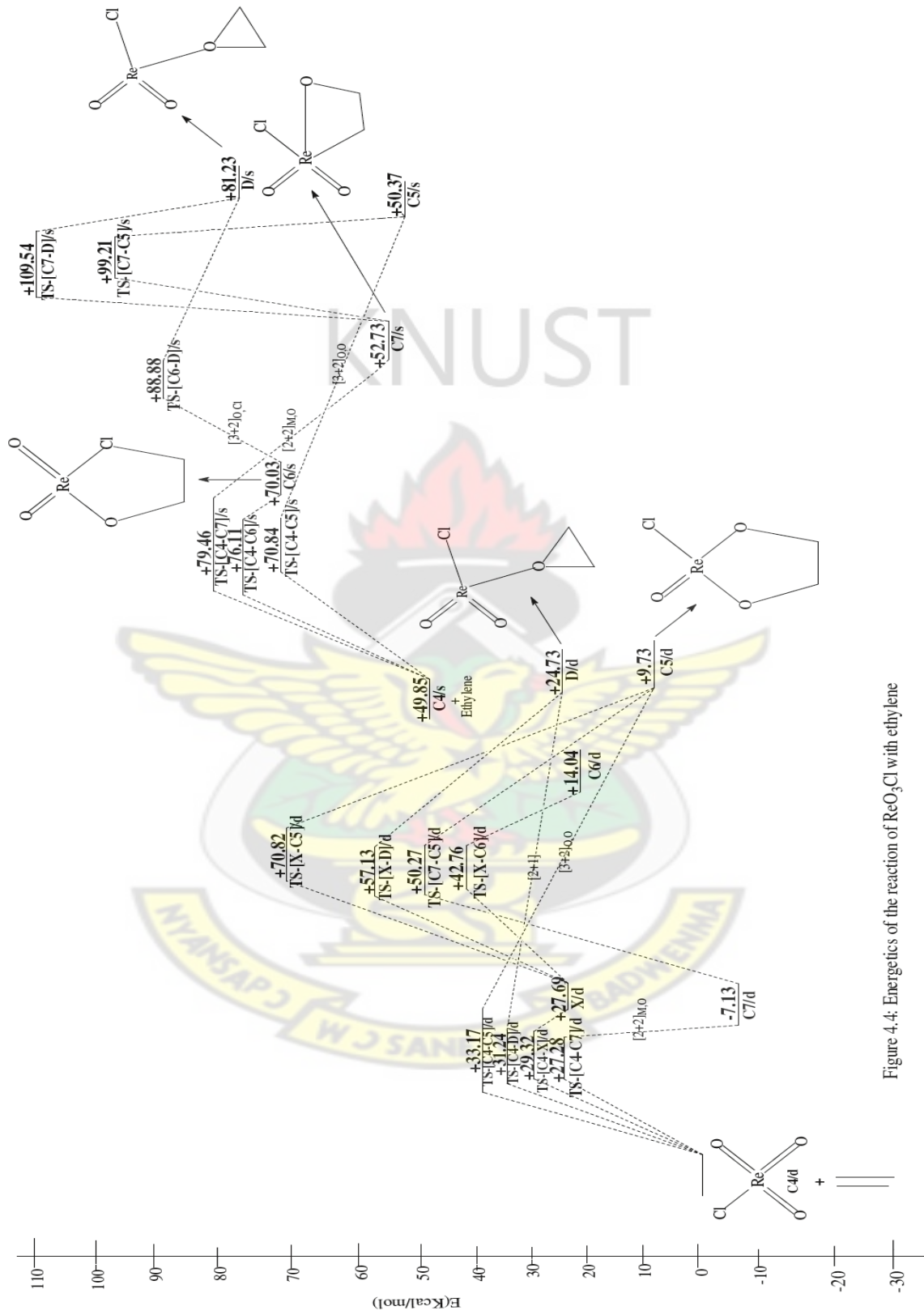


Figure 4.3 cont'd: Optimized geometrical parameters of the main stationary points involved in the reaction of ReO_3Cl with ethylene. Distance in Å and bond angles in degrees.



4.3.3 Reaction of $\text{ReO}_3(\text{NPH}_3)$ with ethylene

Figures 4.5 and 4.6 respectively show the optimized geometries and relative energies of the main stationary points involved in the reaction between $\text{ReO}_3(\text{NPH}_3)$ and ethylene. The DFT geometry optimization of $\text{ReO}_3(\text{NPH}_3)$ on a singlet potential energy surface gives **C8/s** which has the Re=N bond at 1.87 Å and the Re=O bonds at 1.72 Å. The N-P bond distance is 1.57 Å. A triplet $\text{ReO}_3(\text{NPH}_3)$ **C8/t** has been computed to be 68.70 kcal/mol less stable than the singlet reactant. The Re=N and N-P bonds in the triplet are 1.91 and 2.07 Å respectively.

A doublet reactant **C8/d** of the complex has been computed to be 20.85 and 55.69 kcal/mol more stable than the singlet **C8/s** and quartet reactant **C8/q**. Thus, the doublet reactant is the most stable of all the reactants computed. In the doublet reactant **C8/d**, the Re=O bond is 1.74 Å, Re=N bond is 1.81 Å and the N-P bond is 1.74 Å.

A singlet and a doublet concerted transition state have been located for the formation of the dioxylate intermediate species **C12/s** and **C12/d** by the [3+2] addition of the $\text{C}=\text{C}\pi$ bond of ethylene across the $\text{O}=\text{Re}=\text{O}$ bonds of singlet and doublet $\text{ReO}_3(\text{NPH}_3)$. If the reaction proceeds from the doublet reactant through the doublet transition state **TS-[C8-C12]/d** to the doublet product **C12/d**, the activation barrier is +34.37 kcal/mol and the reaction energy is 7.69 kcal/mol. The activation barriers for the formation of singlet dioxylate are +27.19 and 48.04 relative to the singlet and doublet reactant respectively, while the endothermicity are +7.17 and 28.00 kcal/mol respectively. Consequently on the global energy profile for the dioxylate formation, the pathway on the doublet PES which requires 34.37 kcal/mol might be preferable.

On the triplet surface, one of the $\text{C}=\text{C}\pi$ of ethylene attacks an oxo-ligand of triplet $\text{ReO}_3(\text{NPH}_3)$ to form the intermediate **B/t** through transition state **TS-[C8-B]/t**. The activation

barrier and reaction energy of the intermediate **B/t** are +21.40 and +4.57 kcal/mol. The intermediate then re-arranges to the triplet dioxylate species **C12/t** through transition state **TS-[B-C12]/t**. The activation barrier and reaction energy along this route is 9.60 and -20.29 kcal/mol. A triplet product **C12/t** has been computed to be 45.56 kcal/mol more stable than the singlet product **C12/s** and 46.08 kcal/mol more stable than the doublet dioxylate product **C12/d**.

On the quartet PES, a seven-membered metallacyclic intermediate **C12/q** in which one of the oxo-ligands part of the five-membered ring forms a new bond with the phosphine moiety attached to nitrogen (O- P = 2.57 Å). This species is 32.98 kcal/mol more stable than the doublet product **C12/d**.

The [3+2] addition of the C=C bond of ethylene across the O=Re=N bonds of singlet $\text{ReO}_3(\text{NPH}_3)$ through a singlet transition state **TS-[C8-C10]/s**, a pathway which was not explored in the studies of Deubel *et. al.*, (2001) has an activation barrier of 25.87 kcal/mol and reaction energy of -3.40 kcal/mol.

Alternatively, the [3+2] addition of the C=C bond of ethylene across the O=Re=N bonds of doublet $\text{ReO}_3(\text{NPH}_3)$ through a doublet transition state **TS-[C8-C10]/d** has an activation barrier of 27.84 kcal/mol and reaction energy of 4.84 kcal/mol which is 8.2 kcal/mol less stable than the singlet product **C10/s**.

On the triplet surface, a stepwise addition of one of the C=C π of ethylene to an oxo- ligand of $\text{ReO}_3(\text{NPH}_3)$ leads to an organometallic intermediate **B/t**. The activation barrier along this route is +21.40 kcal/mol. The intermediate then re-arrange to the triplet five membered metallacycle **C10/t** through transition state **TS-[B-C10]/t**. The activation barrier and exothermicity along this route are 15.97 and -26.63 kcal/mol.

On the triplet and quartet PES, a seven-membered metallacyclic intermediate **C10/t** and **C10/q** in which one of the oxo-ligands attached to the metal centre forms a new bond with the phosphine moiety attached to nitrogen (O-P = 1.94 Å). This O-P bond is much shorter (1.790 Å) on the quartet PES. The reaction energy of the quartet product is 31.88 kcal/mol exothermic; 36.72 kcal/mol more stable than the doublet product **C10/d**.

A singlet, doublet and triplet transition states have been located for the formation of the rhenaoxetane by [2+2] addition of the C=C π bond of ethylene across Re=O bonds of $\text{ReO}_3(\text{NPH}_3)$. The formation of the rhenaoxetane **C11/s** through the transition state **TS-[C8-C11]/s** have activation barrier and reaction energy of 41.65 and +2.95 kcal/mol respectively.

A doublet transition state **TS-[C8-C11]/d** linking the reactants to the product leads to an activation barrier of 25.84 kcal/mol and a reaction energy for the doublet rhenaoxetane intermediate **C11/d** to be +3.13 kcal/mol.

On the triplet surface, the addition of ethylene across the Re=O bonds of triplet $\text{ReO}_3(\text{NPH}_3)$ could proceed either as concerted or stepwise addition. The stepwise addition of one of the C=C π bond of ethylene to an oxo-ligand of $\text{ReO}_3(\text{NPH}_3)$ leads to the formation of the intermediate **B/t** through transition state **TS-[C8-B]/t**. The activation barrier and reaction energy for the stepwise formation of the intermediate **B/t** is +21.40 and +4.57 kcal/mol. The intermediate **B/t** can re-arrange through transition state **TS-[B-C11]/t** to give the metallaoxetane intermediate **C11/t**. The activation barrier and reaction energy for the formation of **C11/t** are +10.31 and 8.16 kcal/mol. A quartet rhenaoxetane species **C11/q** has exothermicity 5.74 kcal/mol.

The re-arrangement of the singlet, doublet, and triplet and quartet metallaoxetane to the five-membered metallacycle (**TS-[4-2]** in Scheme 4.1) was explored.

The re-arrangement of the singlet metallaooxetane to the singlet dioxylate through transition state **TS-[C11-C12]/s** has an activation barrier of +75.90 kcal/mol. No transition state was located for the re-arrangement of the doublet, triplet and quartet metallaooxetane to the quartet dioxylate. Thus the overall barrier for the re-arrangement of the singlet metallaooxetane (+52.10 kcal/mol) to the dioxylate is higher than the activation barrier for the direct [3+2] addition of ethylene to the two oxygen atoms of singlet $\text{ReO}_3(\text{NPH}_3)$. This rules out the re-arrangement of the metallaooxetane to the dioxylate since the first step and re-arrangement activation barrier are all higher than the direct [3+2] addition pathway leading to the dioxylate.

The formation of the four membered metallacycle by the [2+2] addition of the C=C bond of ethylene across the Re=N bond of singlet $\text{ReO}_3(\text{NPH}_3)$ (**TS-[1-5]** in Scheme 4.1) which was not explored in the work of Deubel *et. al.* 2003; Deubel and Frenking, (2003) has an activation barrier and reaction energy to be 30.52 and -7.14 kcal/mol respectively through a singlet transition state **TS-[C8-C9]/s**. This leads to a six-membered metallacyclic intermediate **C9/s** where one of the oxo ligands on the metal centre bonds with the phosphine (PH_3) attached to the nitrogen ($\text{O-P} = 1.90 \text{ \AA}$).

A doublet transition state **TS-[C8-C9]/d** linking the reactants to the product has an activation barrier of 19.48 kcal/mol. The doublet product, a six-membered metallacyclic intermediate **C9/d** resulting from the interaction of one of the oxo-ligands attached to the metal center bonds with the phosphine (PH_3) attached to the nitrogen ($\text{O-P} = 1.73 \text{ \AA}$). The doublet product has reaction energy to be -7.58 kcal/mol.

A triplet transition state **TS-[C8-C9]/t** connecting the reactants to the product has an activation barrier of 47.44 kcal/mol. The triplet product, a six-membered metallacyclic

intermediate **C9/t** resulting from the interaction of one of the oxo-ligands present at the metal center with the phosphine (PH_3) attached to the nitrogen ($\text{O-P} = 1.90 \text{ \AA}$). The triplet species has a reaction energy of 19.44 kcal/mol.

A search on the reaction surface for the re-arrangement of the singlet, doublet, and triplet and quartet four-membered metallacycle to the five-membered metallacycle (TS-[5-6] in Scheme 4.1) proved unsuccessful.

For a related reaction between $(\text{O}=\text{Os}(\text{=NH}))_2$ and ethylene, Deubel and Muniz, (2004) calculated the activation barrier for the [2+2] addition of the $\text{Os}=\text{N}$ bond across the $\text{C}=\text{C}$ bond of ethylene to form a four-membered metallacycle to be 36.4 and 34.2 kcal/mol higher than the [3+2] addition across $\text{O}=\text{Os}=\text{NH}$ and $\text{O}=\text{Os}=\text{O}$ moiety to form a five-membered metallacycle.

In this work, the activation barrier for the [2+2] addition of the $\text{Re}=\text{N}$ bond of doublet $\text{ReO}_3(\text{NPH}_3)$ across the $\text{C}=\text{C}$ bond of ethylene to form a four-membered metallacycle is 8.36 and 14.89 kcal/mol lower than the [3+2] addition across $\text{O}=\text{Re}=\text{N}$ and $\text{O}=\text{Re}=\text{O}$ functionality of $\text{ReO}_3(\text{NPH}_3)$ to form a five-membered metallacycle. On the singlet surface, the activation barrier for the [2+2] addition of the $\text{Re}=\text{N}$ bond of $\text{ReO}_3(\text{NPH}_3)$ across the $\text{C}=\text{C}$ bond of ethylene is 3.33 and 4.65 kcal/mol higher than the [3+2] addition across $\text{O}=\text{Os}=\text{O}$ and $\text{O}=\text{Os}=\text{NH}$ moiety to form a five-membered metallacycle.

The reaction of $\text{ReO}_3(\text{NPH}_3)$ with ethylene was explored for the formation of an epoxide precursor. The re-arrangement of the singlet five-membered metallacycle (**TS-[6-3]** in Scheme 4.1) to the epoxide precursor through transition state **TS-[C10-K]/s** has an activation barrier of +56.17 kcal/mol above the reactants and exothermicity of 3.4 kcal/mol. On the triplet surface, the epoxide precursor could arise from the re-arrangement of the intermediate **B/t** through transition

state **TS-[B-K]/t**. The activation barrier and reaction energy along this route are +27.27 and -0.19 kcal/mol respectively.

The re-arrangement of the singlet five-membered metallacycle (**TS-[2-3]** in Scheme 4.1) to the epoxide precursor through transition state **TS-[C12-K]/s** has an activation barrier of +70.38 kcal/mol and endothermicity of +33.97 kcal/mol.

The transition state **TS [C11-K]/s** for the rearrangement of the four-membered metallaoxetane to the epoxide precursor (**TS-[4-3]** in Scheme 4.1) has activation barrier of +74.84 kcal/mol and endothermicity of +38.19 kcal/mol. The activation barrier and reaction energy for the formation of the epoxide precursor from direct attack of the C=C bond on the oxygen atom of $\text{ReO}_3(\text{NPH}_3)$ has been computed to be +52.88 and 41.14 kcal/mol respectively.

The most plausible pathway for the formation of the epoxide precursor, if it is to form at all, is through the intermediate **B/t** followed by re-arrangement to the epoxide precursor.

In their study of the reaction of $\text{ReO}_3(\text{NPH}_3)$ with ethylene, Deubel *et. al.*(2001) found the [3+2] addition of the C=C bond of ethylene across the O=Re=O bond of singlet $\text{ReO}_3(\text{NPH}_3)$ to the dioxylate to be the most favorable reaction. However, in this work even on the singlet PES (which is not the preferred reaction surface) the addition across the N-Re=O of the complex $\text{ReO}_3(\text{NPH}_3)$ was found to be the most favored pathway. The most preferred PES for the reaction for the reaction $\text{ReO}_3(\text{NPH}_3)$ with ethylene is the doublet PES and the [2+2] addition of ethylene across the Re=N bonds of doublet $\text{ReO}_3(\text{NPH}_3)$ to form the four membered metallacycle is kinetically and thermodynamically most favorable.

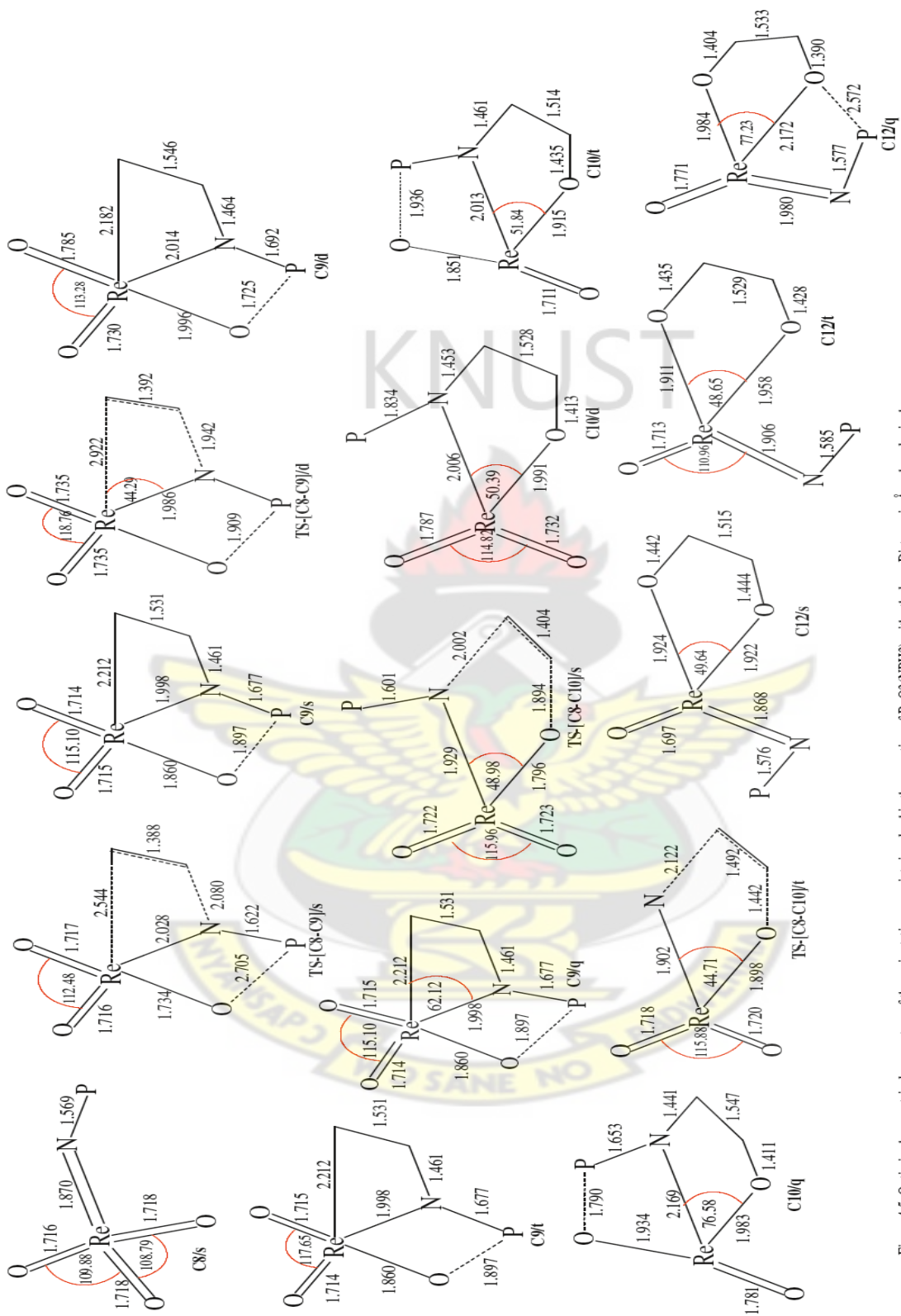


Figure 4.5: Optimized geometrical parameters of the main stationary points involved in the reaction of $\text{ReO}_3(\text{NPH}_3)$ with ethylene. Distance in Å and angles in degrees. *Hydrogen atoms have been omitted phosphorus atoms.

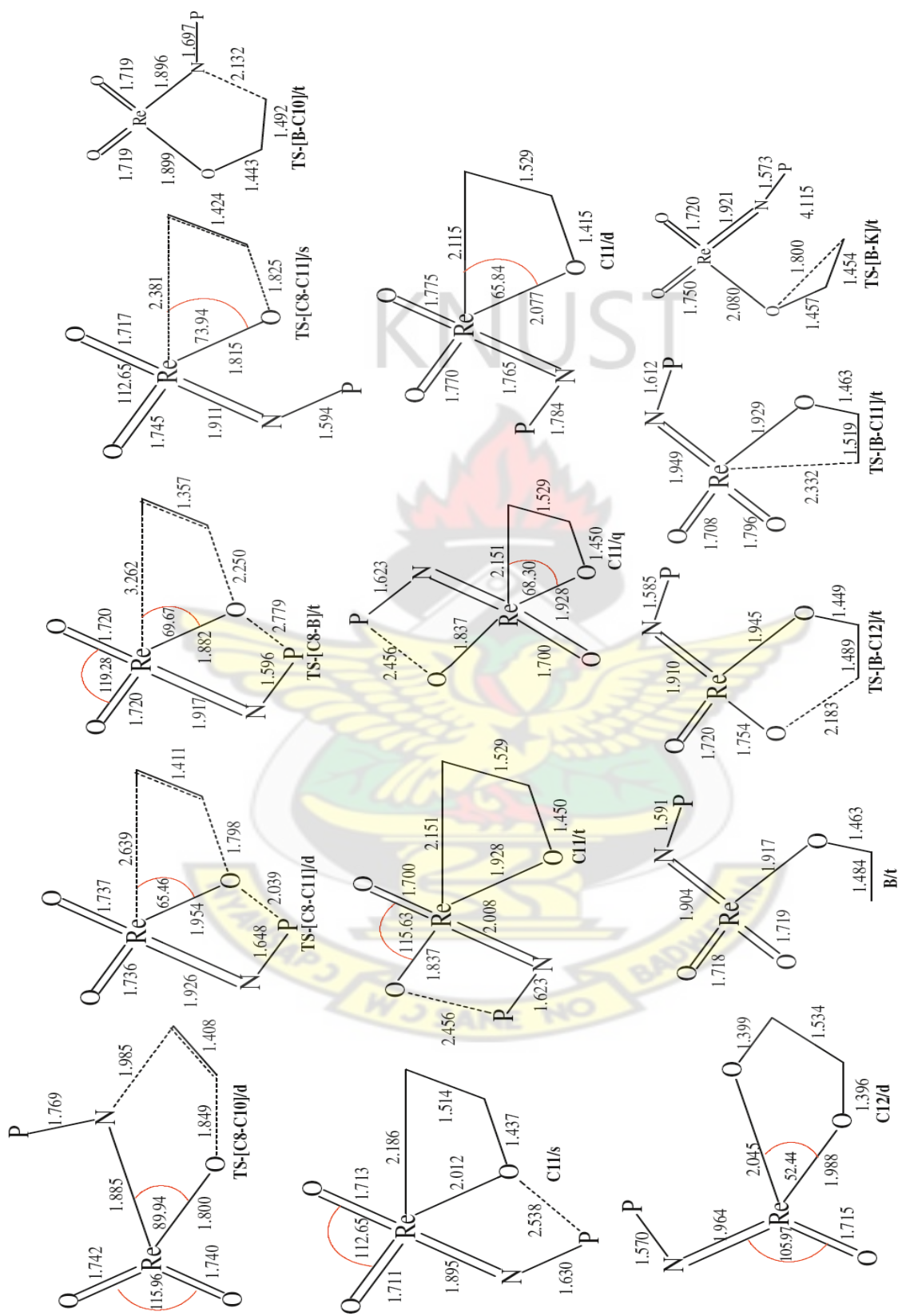


Figure 4.5 cont'd: Optimized geometrical parameters of the main stationary points involved in the reaction of $\text{ReO}_3(\text{NPH}_3)_3$ with ethylene. Distance in Å and angles in degrees. *Hydrogen atoms have been omitted Carbon and phosphorus atoms.

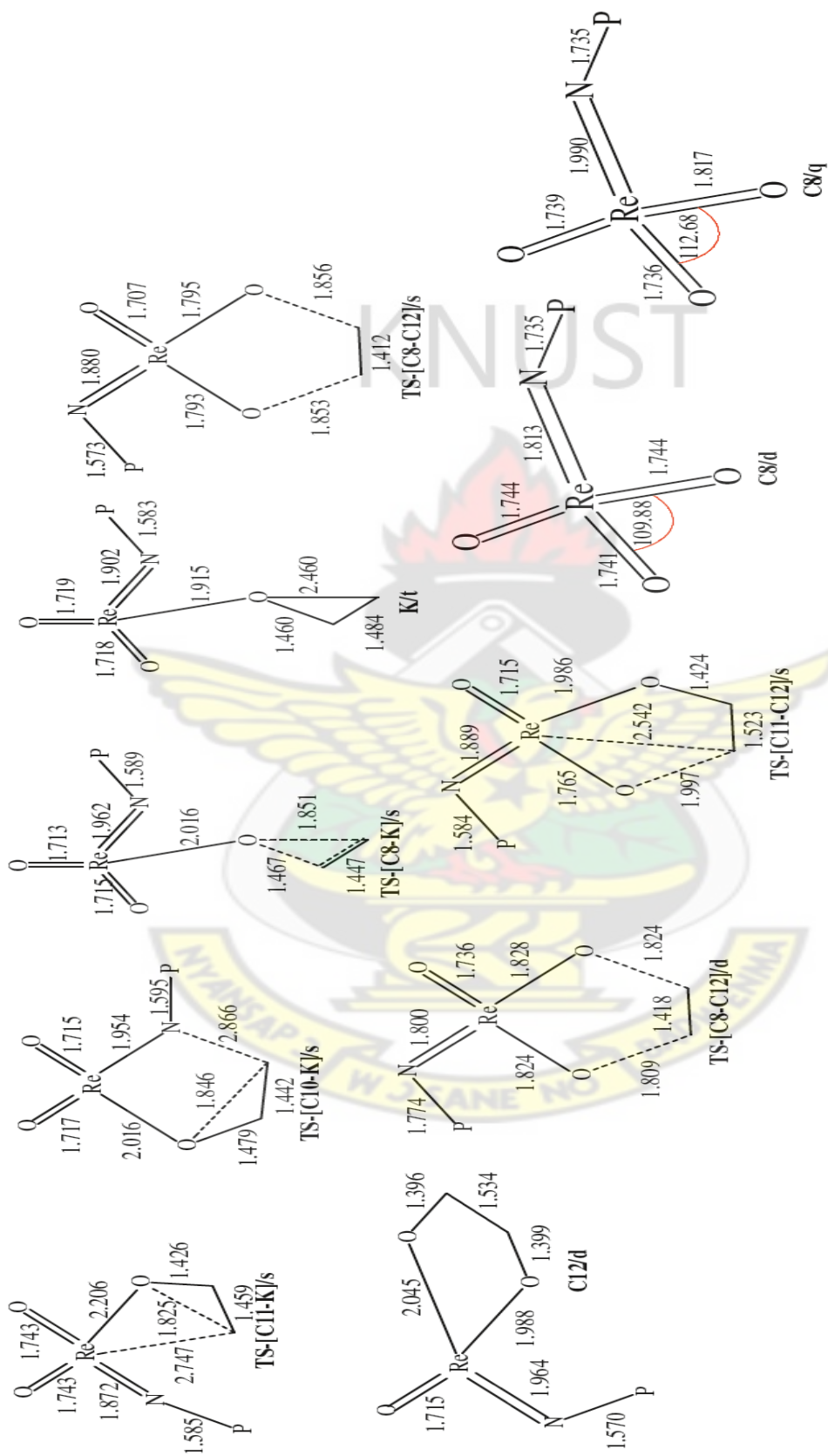


Fig 4.5 cont'd: Optimized geometrical parameters of the main stationary points involved in the reaction of $\text{ReO}_3(\text{NPH}_3)_3$ with ethylene. Distance in Å and angles in degrees.

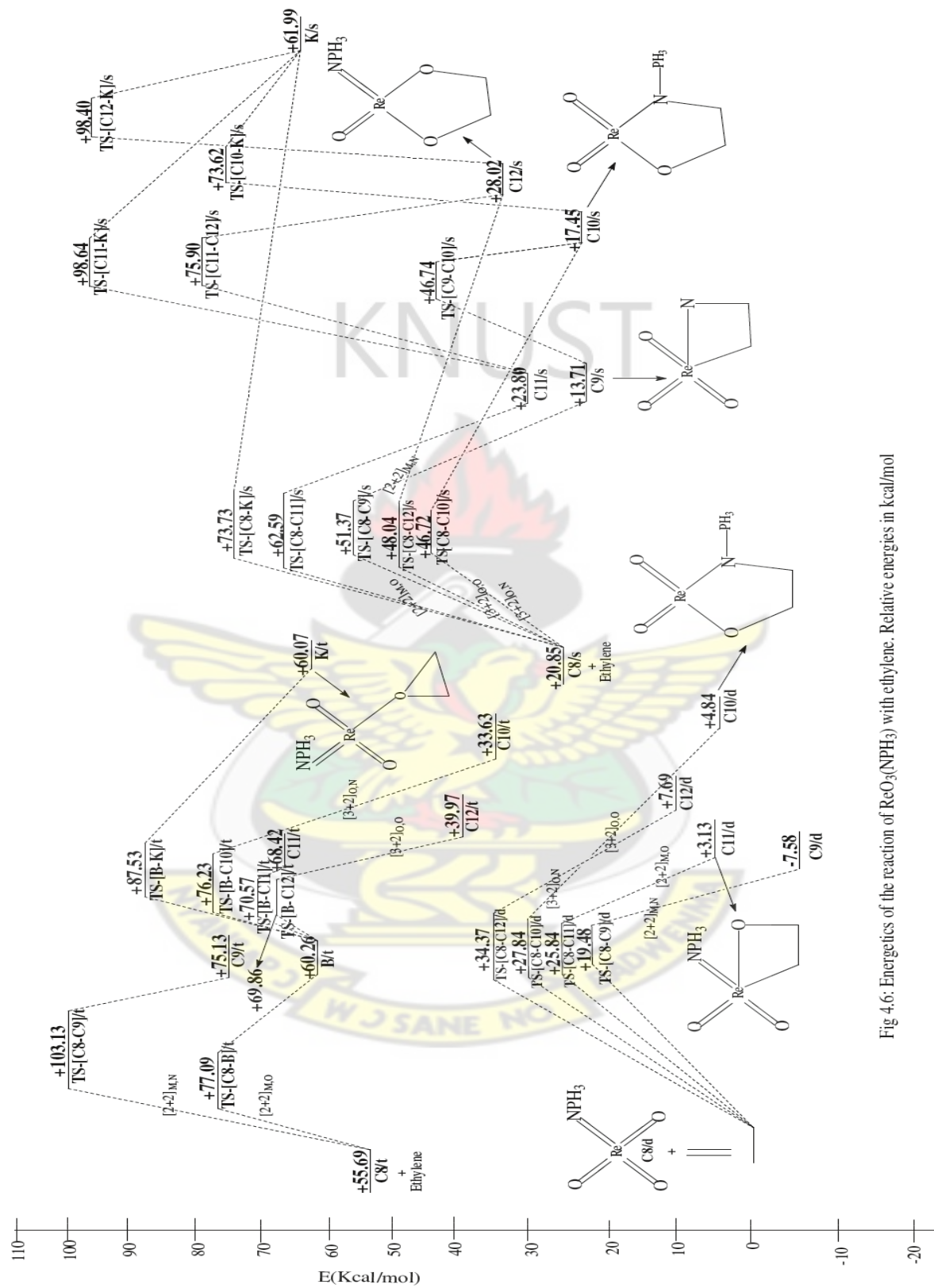


Fig 4.6: Energetics of the reaction of $\text{ReO}_3(\text{NPH}_3)$ with ethylene. Relative energies in kcal/mol

4.3.4 Reaction of $\text{ReO}_3(\text{CH}_3)$ with ethylene

Figures 4.7 and 4.8 respectively show the optimized geometries and relative energies of the main stationary points involved in the reaction between $\text{ReO}_3(\text{CH}_3)$ and ethylene. The DFT geometry optimization of $\text{ReO}_3(\text{CH}_3)$ on a singlet potential energy surface yields **C13/s** which has the Re=O bonds at 1.71 Å and the Re-C bond is 2.08 Å long.

A doublet reactant **C13/d** has been computed and found to be 28.83 kcal/mol more stable than the singlet reactant **C13/s**. A triplet structure **C13/t** has also been computed and found to be 96.79 kcal/mol less stable than the doublet **C13/d**. The Re-C is 0.05 Å longer in the doublet reactant **C13/d** than the singlet reactant **C13/s** and 0.04 Å longer in the doublet reactant than in the triplet structure **C13/t**.

A quartet reactant **C13/q** has been computed to be 72.54 kcal/mol less stable in relation to the doublet reactant **C13/d**. Thus the doublet reactant is the most stable of all the reactants species computed.

On the doublet surface, the [3+2] addition of the C=C π bond of ethylene across the O=Re=O functionality of $\text{ReO}_3(\text{CH}_3)$ through the transition state **TS-[C13-C14]/d** to form the doublet dioxylate **C14/d** has an activation barrier of 38.08 kcal/mol and reaction energy of 12.50 kcal/mol. The Re-C bond distance (2.13 Å) in the doublet transition state is the same as in the doublet reactant (2.13 Å). The transition state is asymmetric with respect to the forming C-O bonds (1.69 and 1.88 Å).

Also, the activation barrier and reaction energy for the [3+2] addition of the C=C bond of ethylene across the O=Re=O bond of singlet $\text{ReO}_3(\text{CH}_3)$ through the singlet transition state **TS-**

[**C13-C14**]/s has been computed to be 33.82 and 17.30 kcal/mol respectively in agreement with the reported activation and reaction energies reported by Gisdakis and Rösch, (2001).

A quartet and triplet dioxylate products **C14/q** and **C14/t** have reaction energies of -35.74 and -51.34 kcal/mol respectively. No triplet and quartet transition states were located on the reaction surface.

The formation of the doublet rhenaoxetane **C15/d** through the transition state **TS-[C13-C15]/d** by [2+2] addition of the C=C bond of ethylene across the Re=O bond of doublet $\text{ReO}_3(\text{CH}_3)$ complex, has an activation barrier of 25.87 kcal/mol and reaction energy of 1.18 kcal/mol (Fig 4.8). A triplet metallaioxetane **C15/t** has been computed to have reaction energy of -34.42 kcal/mol. A singlet **C15/s** and quartet metallaioxetane **C15/q** intermediates has been computed to have reaction energies of 4.76 and -29.71 kcal/mol.

The formation of the singlet rhenaoxetane **C15/s** through the transition state **TS-[C13-C15]/s** by [2+2] addition of the C=C bond of ethylene across Re=O bond of singlet $\text{ReO}_3(\text{CH}_3)$ complex, has an activation barrier of 47.63 kcal/mol. No transition state connecting the reactants to the products was located on the triplet and quartet PES.

Pietsch *et al.*, (1998) in a thermodynamic study of the reaction $\text{ReO}_3(\text{CH}_3)$ with ethylene, found the dioxylate and oxetane to be endothermic by 31 and 10 kcal/mol respectively.

In this work, the dioxylate and metallaioxetane computed on the singlet and doublet PES are endothermic, whiles dioxylate and metallaioxetane computed on the triplet and quartet reaction surfaces are exothermic.

The re-arrangement of the singlet metallaoxetane to the singlet dioxylate (**TS-[4-2]** in Scheme 4.1) through transition state **TS-[C15-C14]/s** has an activation barrier of +48.83 kcal/mol. On the triplet reaction surface, the activation barrier is +53.66 kcal/mol. No transition state was located for the re-arrangement of the doublet and quartet metallaoxetane to the dioxylate. Thus the overall activation barrier for the re-arrangement of the singlet metallaoxetane to the dioxylate (+48.83 kcal/mol) is higher than the activation barrier for the direct [3+2] addition of $C=C\pi$ of ethylene across $O=Re=O$ bond of singlet $ReO_3(CH_3)$. Thus the formation of the singlet dioxylate will proceed from the direct [3+2] addition of ethylene across the two oxygens of singlet $ReO_3(CH_3)$.

The PES for the reaction of $ReO_3(CH_3)$ with ethylene was explored in an attempt to locate an epoxide precursor. The search for transition state (**TS [2-3]** in Scheme 4.1) for the re-arrangement of the five-membered metallacycle to the epoxide precursor was not fruitful, indicating that such a transformation may not exist.

The rearrangement of the singlet four-membered metallaoxetane through transition state **TS [C15-B]/s** to the epoxide precursor has an activation barrier of +65.51 kcal/mol and endothermicity of +38.38 kcal/mol. Also, the activation barrier and reaction energy for the formation of the singlet epoxide precursor from direct attack of the $C=C$ bond on the oxygen atom of $ReO_3(CH_3)$ has been computed to be +56.49 and +43.14 kcal/mol. On the doublet surface, the activation barrier is +29.51 kcal/mol and endothermicity of +24.73 kcal/mol. Therefore if reactions considered here are irreversible, then the most plausible pathway for the formation of the epoxide precursor may direct [2+1] addition on the doublet surface.

The reaction of ethylene with $\text{ReO}_3(\text{CH}_3)$ is likely to occur on the doublet PES and the [2+2] addition of ethylene across the $\text{Re}=\text{O}$ bond of $\text{ReO}_3(\text{CH}_3)$ to form the metallaioxetane intermediate is kinetically and thermodynamically most favorable. The most competitive reaction on the doublet surface is the formation of the epoxide precursor.

KNUST



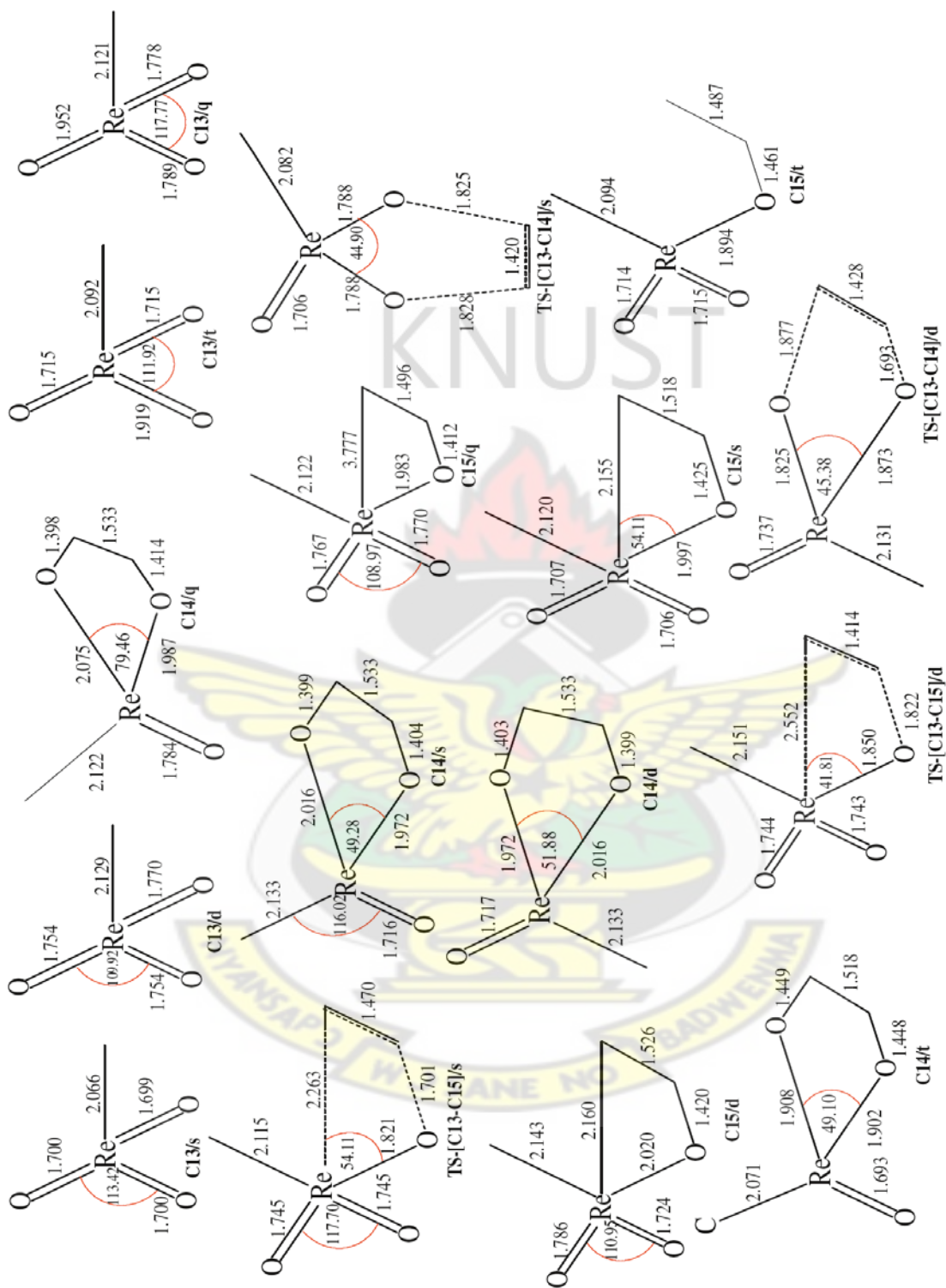


Fig 7: Optimized geometrical parameters of the main stationary points involved in the reaction of $\text{ReO}_3(\text{CH}_3)_3$ with ethylene. Distance in Å and angles in degrees.

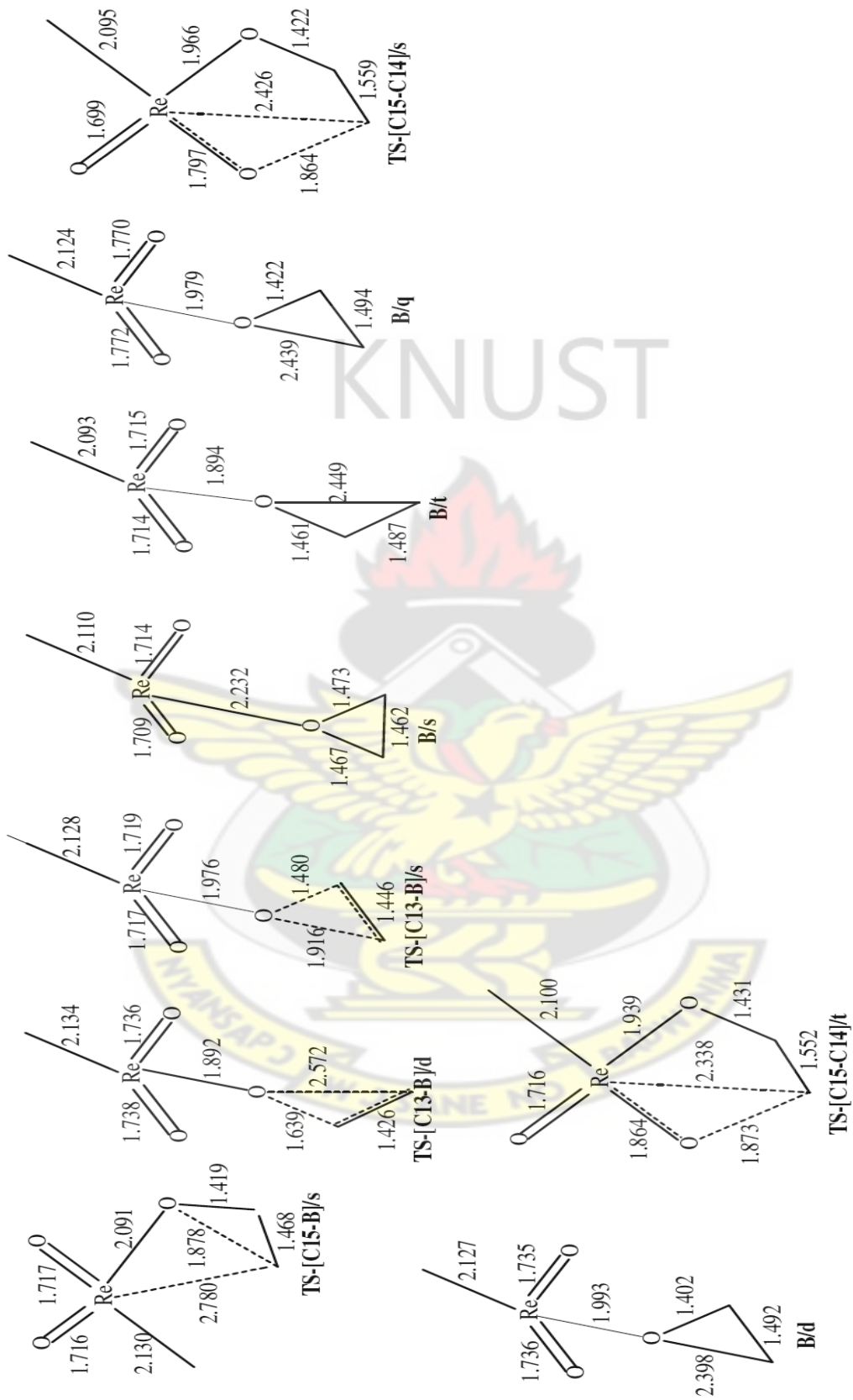


Fig 4.7 cont'd: Optimized geometrical parameters of the main stationary points involved in the reaction of $\text{ReO}_3(\text{CH}_3)_3$ with ethylene. Distance in Å and angles in degrees.

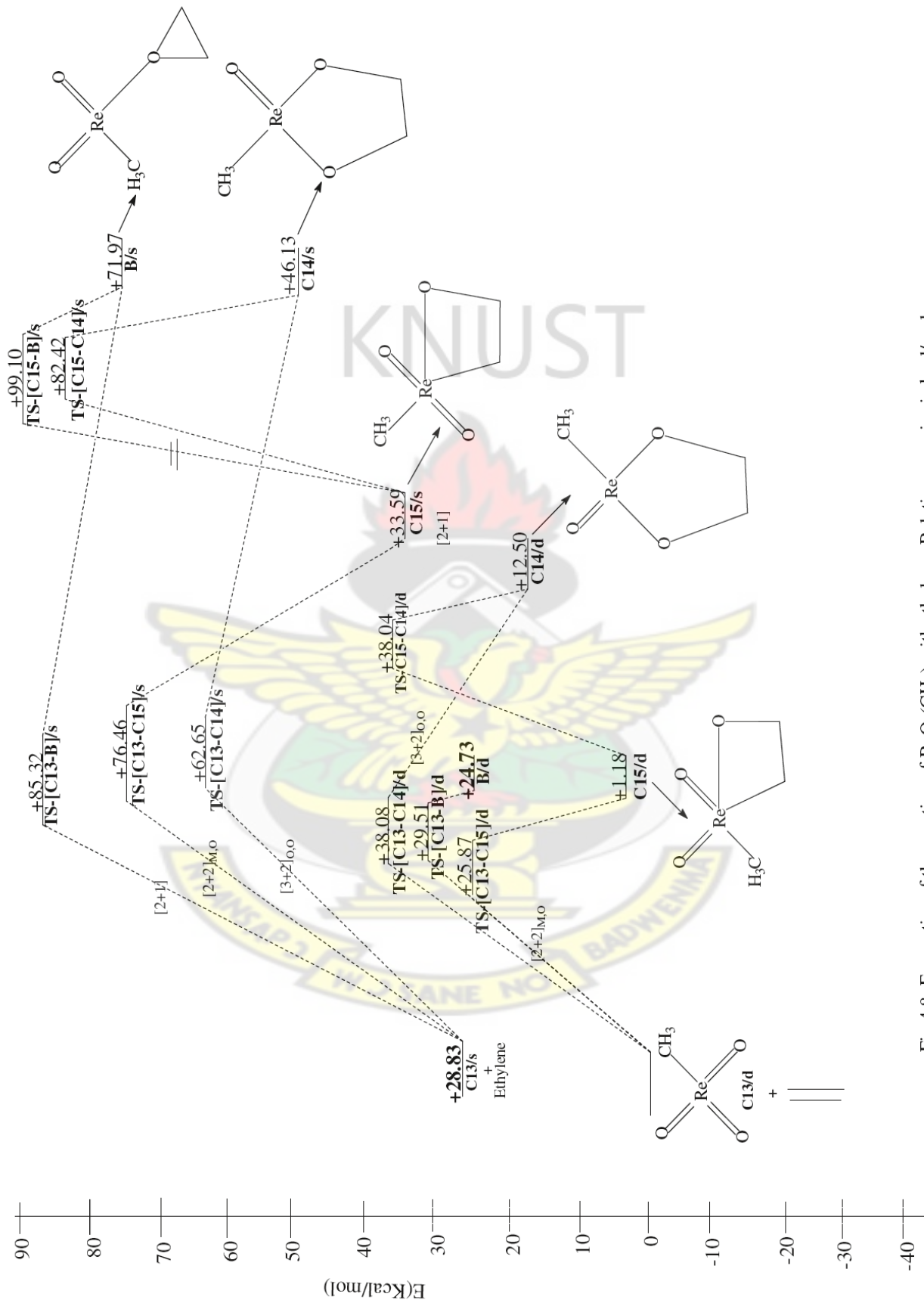


Fig 4.8: Energetics of the reaction of $\text{ReO}_3(\text{CH}_3)$ with ethylene. Relative energies in kcal/mol

4.3.5 Reaction of $\text{ReO}_3(\text{OCH}_3)$ with ethylene

Figure 4.9 and 4.10 show the optimized geometries and relative energies of the main stationary points involved in the reaction between $\text{ReO}_3(\text{OCH}_3)$ and ethylene respectively. The singlet, doublet, triplet and quartet species have been optimized for the reactant $\text{ReO}_3(\text{OCH}_3)$. The singlet reactant **C16/s** on a singlet reactant has the Re=O bonds at 1.71 Å and Re-O bond at 1.86 Å.

A doublet reactant **C16/d** has been computed to be 31.68 kcal/mol more stable than the singlet reactant **C16/s** and 95.82 kcal/mol more stable than the triplet reactant **C16/t**. The Re-O bond is 0.099 Å longer in the singlet reactant, while the O-C bond is 0.026 Å shorter in doublet structure **C16/d**.

A quartet reactant **C16/q** of C_1 symmetry is 60.07 kcal/mol less stable than the doublet **C16/d**. The quartet reactant is 28.39 kcal/mol less stable than singlet reactant **C16/s** and 35.75 kcal/mol more stable than the triplet ground state reactant **C16/t**.

The [3+2] addition of the C=C bond of ethylene across the O=Re=O functionality of doublet $\text{ReO}_3(\text{OCH}_3)$ through a doublet transition state **TS-[C16-C17]/d** to form the doublet dioxylate **C17/d** has an activation barrier of 36.98 kcal/mol and endothermicity of 5.77 kcal/mol.

The [3+2] addition of the C=C bond of ethylene across the O=Re=O functionality of singlet $\text{ReO}_3(\text{OCH}_3)$ through a singlet transition state **TS-[C16-C17]/s** to form the dioxylate **C17/d** has an activation barrier of 26.28 kcal/mol and endothermicity of 3.89 kcal/mol. A triplet five-membered metallacycle **C17/t** has reaction energy of +52.54 kcal/mol. A quartet species **C18/q** has been computed to have reaction energy of -30.07 kcal/mol.

The formation of the rhenaoxetane **C18/s** by [2+2] addition of the C=C bond of ethylene across the Re=O bond of singlet $\text{ReO}_3(\text{OCH}_3)$ through a singlet transition state **TS-[C16-C18]/s** has activation barrier and endothermicity of 30.58 and 6.19 kcal/mol respectively.

The formation of the metallaioxetane **C18/d** through the doublet transition state **TS-[C16-C18]/d** by [2+2] addition of the C=C bond of ethylene across the Re=O bond of doublet $\text{ReO}_3(\text{OCH}_3)$ has an activation barrier of 31.64 kcal/mol and exothermicity of 1.96 kcal/mol. A triplet rhenaoxetane **C18/t** has been computed to have reaction energy of -29.73 kcal/mol. A quartet metallaioxetane species has reaction energy of -12.53 kcal/mol.

The re-arrangement of the doublet metallaioxetane to the dioxylate (**TS-[4-2]** in Scheme 4.1) through transition state **TS-[C18-C17]/d** has a barrier of +36.23 kcal/mol. On the singlet surface, the activation barrier is +42.41 kcal/mol. No triplet and quartet transition state was located for re-arrangement of the metallaioxetane to dioxylate. Thus the re-arrangement of the doublet metallaioxetane to the dioxylate (+36.23 kcal/mol) is comparable to the activation barrier for the initial [3+2] addition of $\text{C}=\text{C}\pi$ of ethylene across $\text{O}=\text{Re}=\text{O}$ of doublet $\text{ReO}_3(\text{OCH}_3)$ (36.98 kcal/mol). Thus on the doublet surface, the formation of the dioxylate will proceed from the metallaioxetane due to the lower activation barrier for the first-step (+31.64 kcal/mol in Fig 4.10). However, on the singlet surface the dioxylate will proceed from the direct [3+2] addition of ethylene across the two oxygen atoms of singlet $\text{ReO}_3(\text{OCH}_3)$ not from the re-arrangement of the metallaioxetane.

An epoxide precursor was optimized from the reaction of $\text{ReO}_3(\text{OCH}_3)$ with ethylene. The transition state **TS-[C18-F]/s** for the rearrangement of the singlet four-membered metallaioxetane to the epoxide precursor have activation barrier and reaction energy of +61.79

and 27.81 kcal/mol. The activation barrier and reaction energy for the formation of the singlet epoxide precursor from direct attack of the C=C bond on the oxygen atom of $\text{ReO}_3(\text{OCH}_3)$ has been computed to be +60.45 and 34.00 kcal/mol. On the doublet surface, the activation barrier is +32.74 kcal/mol and endothermicity of +26.00 kcal/mol.

Therefore, the most plausible pathway for the formation of the epoxide, if it is to form at all, is by direct [2+1] addition on the doublet surface.

The reaction of ethylene with $\text{ReO}_3(\text{OCH}_3)$ is likely to occur on the doublet PES and the [2+2] addition of ethylene across the Re=O bond of $\text{ReO}_3(\text{OCH}_3)$ to form the metallaoxetane and the subsequent re-arrangement of the metallaoxetane to the dioxylate is kinetically and thermodynamically most favorable. The most competitive reaction on the doublet surface is the formation of the epoxide precursor.



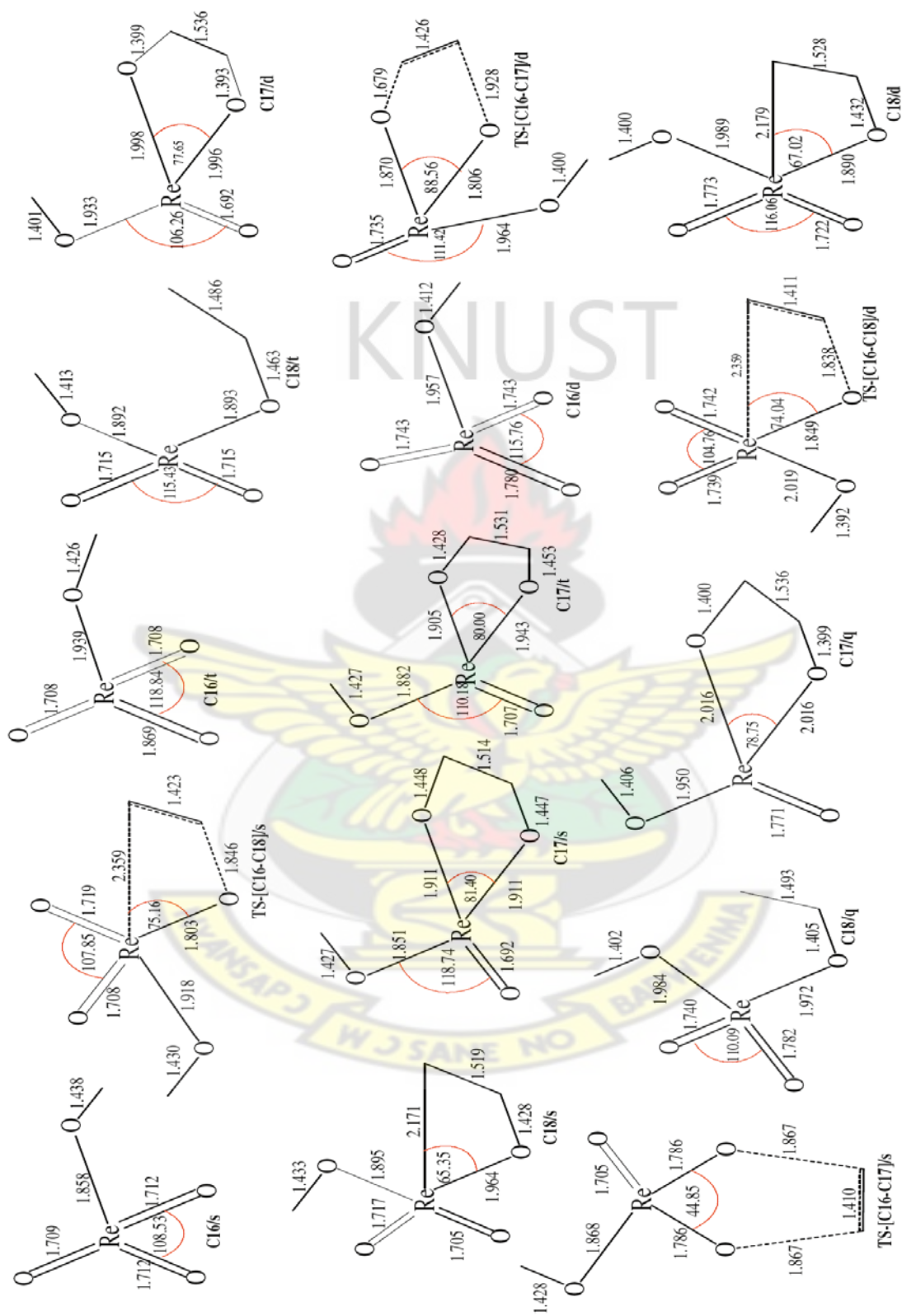


Fig 4.9: Optimized geometrical parameter of the main stationary points involved in the reaction of $\text{ReO}_3(\text{OCH}_3)_3$ with ethylene. Distance in Å and bond angles in degrees.

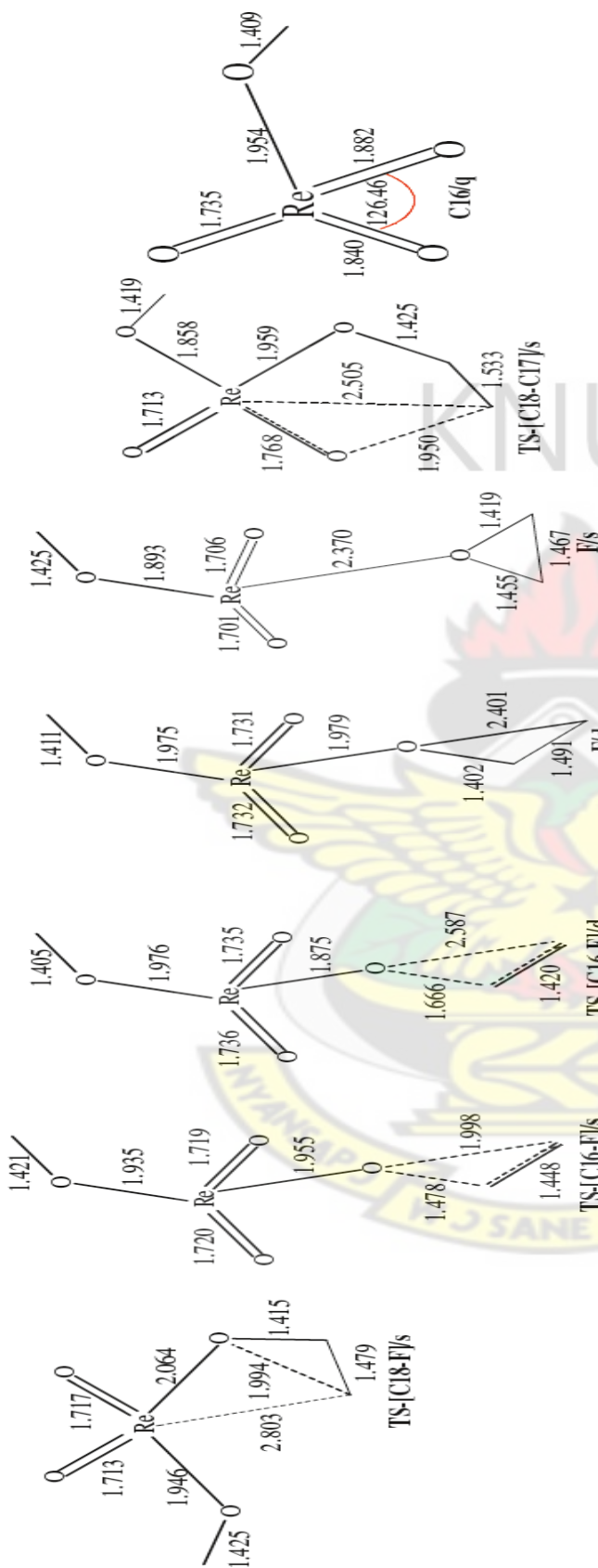


Fig 4.9 cont'd: Optimized geometries of the main stationary points involved in the reaction of $\text{ReO}_3(\text{CH}_3)_3$ with ethylene. Distance in Å and bond angles in degrees.

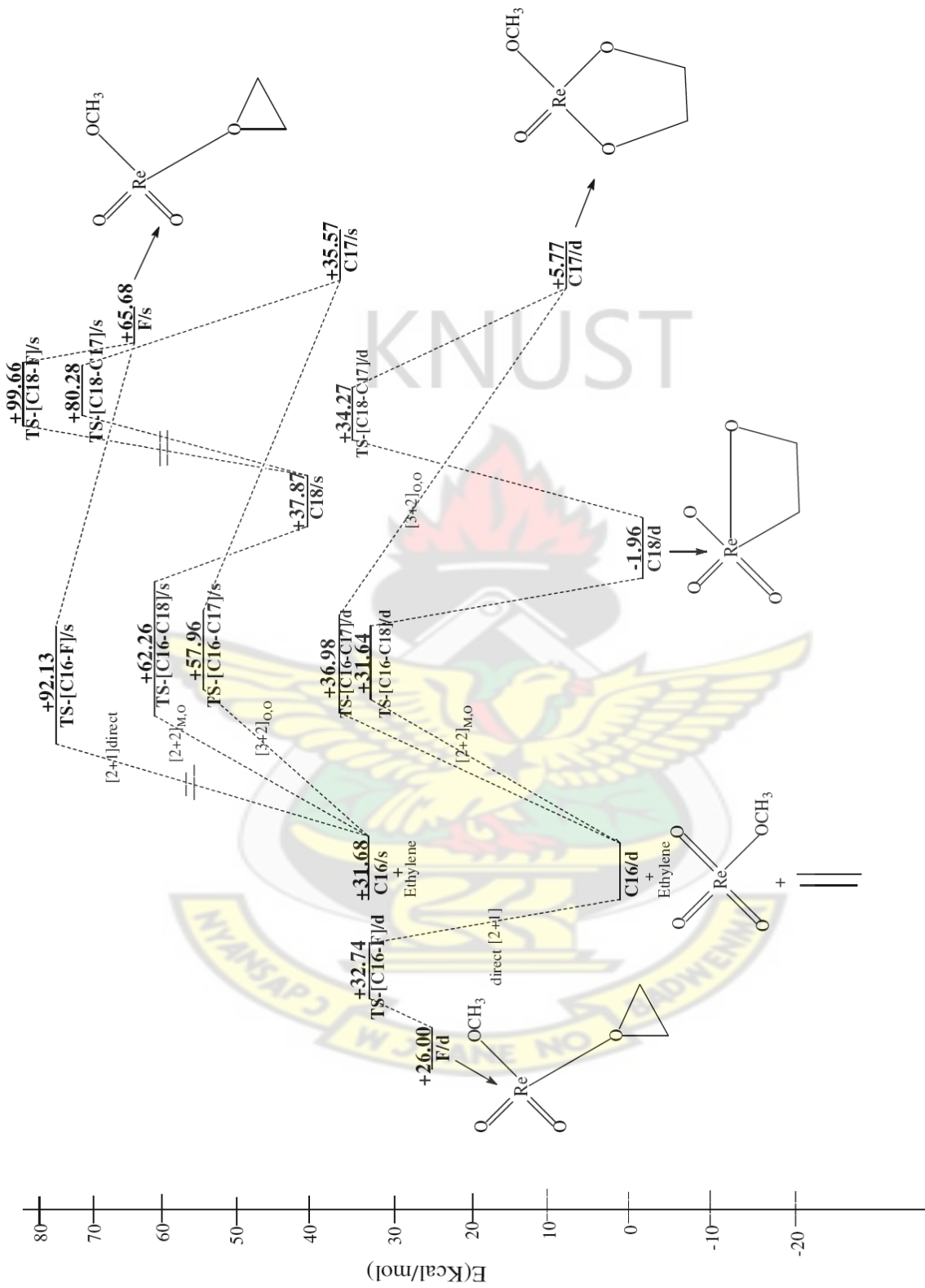


Figure 4.10: Energetics of the reaction of $\text{ReO}_3(\text{OCH}_3)$ with ethylene

4.3.6 Reaction of ReO_3Cp with ethylene

Figure 4.11 and 4.12 respectively show the optimized geometries and relative energies of the main stationary points involved in the reaction between ReO_3Cp and ethylene. The DFT geometry optimization of ReO_3Cp on a singlet potential energy surface gives **C19/s** which has the Re=O bonds at 1.72 Å. The cyclopentadienyl ligand (Cp) is bonded to the metal center in a η^5 fashion i.e. Re-C (Cp) = 2.486, 2.511, 2.518, 2.492 and 2.458 Å, in agreement with work of Deubel and Frenking, 1999; 2003. No doublet, triplet and quartet species could be located for the reactant.

The [3+2] addition of C=C bond of ethylene across the O=Re=O bonds of singlet ReO_3Cp through a singlet transition state **TS-[C19-C20]** to form the metalladioxolane intermediate **C20/s** has an activation barrier of 13.60 kcal/mol and reaction energy of -18.50 kcal/mol in agreement with the activation and reaction energies reported by Deubel and Frenking, (1999) and Gisdakis and Rösch, (2001). The Cp ligand in the singlet [3+2] transition state structure shows η^5 – bonding to the metal centre i.e. (Re-C (Cp) = 2.400, 2.453, 2.447, 2.540, 2.557 Å). The Cp ligand in the singlet ReO_3Cp dioxylate **C20/s** also shows a η^5 – bonding fashion to the Re centre (Re-C (Cp) = 2.336, 2.329, 2.407, 2.519, 2.472 Å) in disagreement with the η^3 – bonding fashion to the metal centre for the ReO_3Cp -dioxylate reported by Deubel and Frenking, (1999).

Even though a doublet TS could not be located for the [3+2] pathway, a doublet metalladioxolane **C20/d** was located and found to be 11.33 kcal/mol less stable than the singlet product **C20/s**. In the doublet dioxylate, the Cp ligand in ReO_3Cp dioxylate **C20/d** also shows η^5 – bonding fashion to the Re centre (Re-C (Cp) = 2.609, 2.294 and 2.167, 2.240, 2.591 Å).

A triplet dioxylate **C20/t** has been computed to have the same reaction energy as the doublet product **C20/d**, indicating equal stability of the doublet and triplet product. The Cp ligand in the triplet ReO_3Cp -dioxylate **C20/t** also shows η^5 -bonding fashion to the Re centre (Re-C (Cp) = 2.386, 2.301, 2.484, 2.528 and 2.437 Å). The quartet metalladioxolane intermediate **C20/q** has reaction energy of -1.65 kcal/mol making it 28.18 kcal/mol less stable than the doublet dioxylate **C20/d**. The Cp ligand in the quartet ReO_3Cp -dioxylate **C20/q** also shows η^5 -bonding fashion to the Re centre (Re-C (Cp) = 2.485, 2.383, 2.306, 2.354, 2.372 Å).

The formation of the rhenaoxetane **C21/s** through the transition state **TS-[C19-C21]/s** on the singlet PES by [2+2] addition of C=C bond of ethylene across Re=O bond of the singlet ReO_3Cp complex, has activation barrier of 33.00 kcal/mol and reaction energy of -5.76 kcal/mol. The Cp ligand in the singlet [2+2] transition state structure shows η^3 -bonding to the metal centre i.e. (Re-C (Cp) = 2.227, 2.744, 2.793 Å). The Cp ligand in the singlet ReO_3Cp -oxetane **C21/s** shows a η^2 -bonding mode to the Re centre, (Re-C (Cp) = 2.174, 2.923 Å) unlike the η^5 -bonding mode in the singlet reactant **C19/s**. This bonding mode is in disagreement with the work of Deubel and Frenking, 1999; 2003 who observed a η^1 -bonding for the ReO_3Cp -oxetane intermediate. No metallaoxetane intermediate were located on the doublet, triplet and quartet PES.

In the thermodynamic study of the reaction of ReO_3Cp with ethylene, Pietsch *et. al.* (1998) asserted that, strong π -bonding ligands such as Cp thermodynamically favor dioxylate formation because of π -bond strain relief. Pietsch *et. al.* (1998) had calculated the dioxylate to be exothermic by 8 kcal/mol while the metallaoxetane was endothermic by 5 kcal/mol.

In this work, the dioxylate and the oxetane products are both exothermic, but the dioxylate is more stable.

The re-arrangement of the singlet metallaoxetane to the singlet dioxylate through transition state **TS-[C21-C20]**/sis +65.05 kcal/mol. No doublet, triplet and quartet transition state was located for re-arrangement of the metallaoxetane to dioxylate. Thus the activation barrier for the re-arrangement of the singlet metallaoxetane to the dioxylate (+70.81 kcal/mol) is higher than the activation barrier for the direct [3+2] addition of C=C π of ethylene across O=Re=O of singlet ReO₃Cp (13.60 kcal/mol). This rule out the formation of the dioxylate from the re-arrangement of the metallaoxetane. The dioxylate is therefore formed from the direct addition of ethylene across the two oxygen atoms of singlet ReO₃Cp

The potential energy surface of the reaction of rhenium tetraoxide with ethylene was further explored in an attempt to locate an epoxide precursor (CpO₂-Re-OC₂H₄) (**3** in Scheme 4.1), but no such minimum was found on these reaction surfaces.

This in agreement with the findings of Burrell *et al.*, 1995; Herrmann *et al.*, 1984; Klahn-olive *et al.*, 1984; Kühn *et al.*, (1994) who reported that CpReO₃ reacts with olefins to predominately form dioxylates (**2** in Scheme 4.1)

The reaction of ethylene with ReO₃Cp is likely to proceed exclusively on the singlet PES and the product formed is the dioxylate from the direct addition of the ethylene to the O=Re=O of the metal complex.

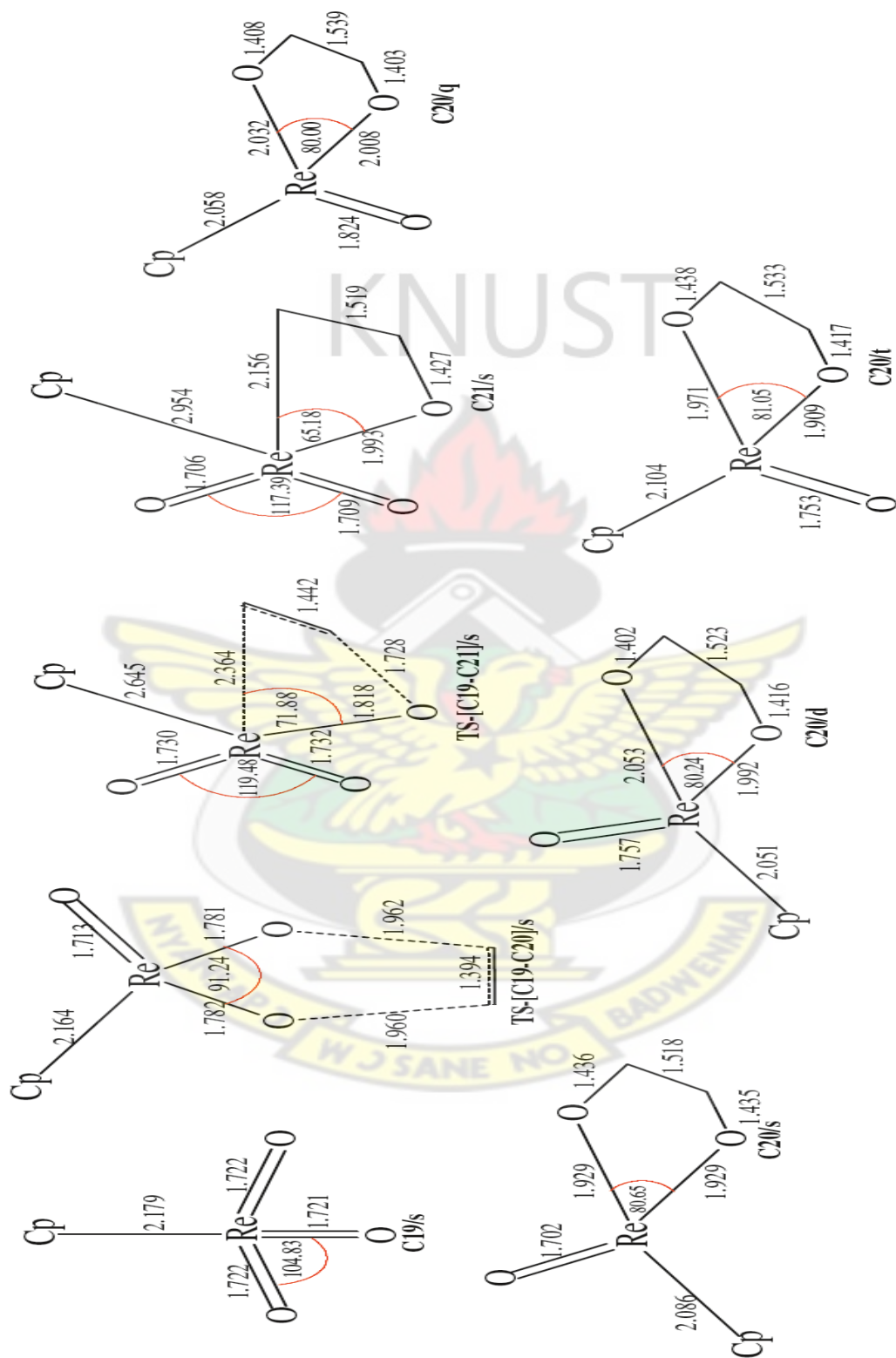


Fig 4.11: Optimized geometries of the main stationary points involved in the reaction of ReO_3Cp with ethylene. Distance in Å and bond angles in degrees.

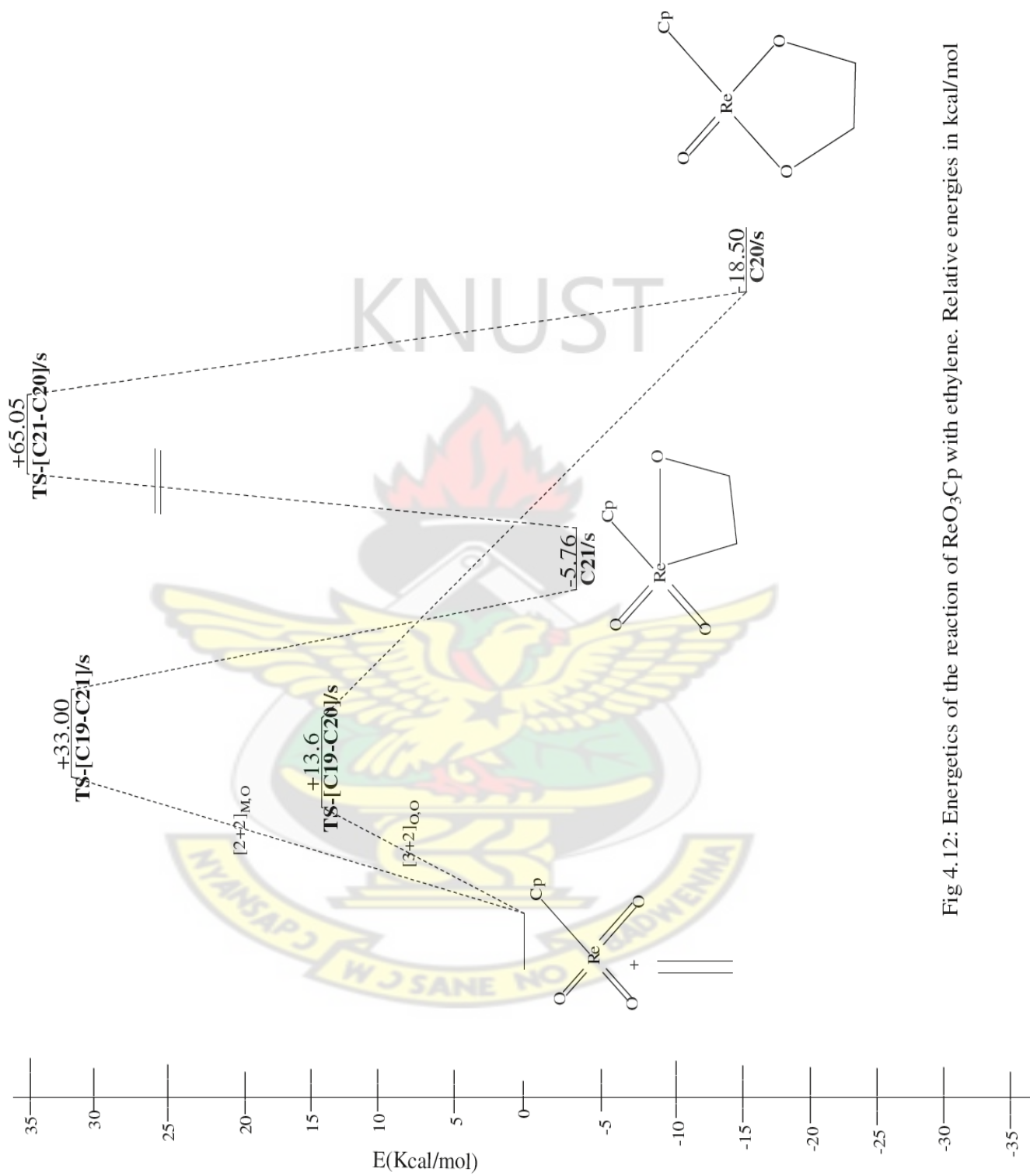


Fig 4.12: Energetics of the reaction of ReO_3Cp with ethylene. Relative energies in kcal/mol

4.4 Conclusion

1. In the reaction between ethylene and the perrhenate (ReO_4^-), the direct [3+2] addition of the C=C bond of ethylene across O=Re=O bond of ReO_4^- to form the dioxylate intermediate on the singlet surface has a lower activation barrier than the two-step process via the [2+2] addition pathway to form the metallaoxetane intermediate and the subsequent re-arrangement of the metallaoxetane to the dioxylate. The dioxylate intermediate is more stable than the metallaoxetane intermediate in agreement with the work of Deubel and Frenking, 1999; Boehme *et. al.* (1999) who computed the [3+2] addition pathway to be kinetically and thermodynamically favorable than the [2+2] addition pathway. The reaction between perrhenate and ethylene would not result in the formation of the epoxide precursor.
2. In the oxidation of ethylene by ReO_3Cl , the direct [2+2] addition of the C=C bond of ethylene across the Re=O bonds of doublet ReO_3Cl to form the metallaoxetane intermediate has a lower activation barrier than the [3+2] addition of the C=C bond of ethylene across O=Re=O bond of singlet and doublet ReO_3Cl to form dioxylate intermediate. The subsequent rearrangement of the metallaoxetane intermediate to the dioxylate has a higher activation barrier. The most plausible pathway that leads to the epoxide precursor is from the organometallic intermediate **X/d** followed by re-arrangement. Thus in the reaction of ReO_3Cl with ethylene, the formation of the metallaoxetane intermediate is kinetically and thermodynamically than the formation of the dioxylate. This work disagrees with earlier works on the subject (Deubel and Frenking, 1999; Boehme *et. al.* 1999) which found the [3+2] addition pathway to be favorable kinetically and the [2+2] addition pathway to be favorable thermodynamically.

3. In the oxidation of ethylene by $\text{ReO}_3(\text{CH}_3)$, the direct [2+2] addition of the C=C bond of ethylene across Re=O bond of doublet $\text{ReO}_3(\text{CH}_3)$ to form the metallaoxetane intermediate has a lower activation barrier than the direct [3+2] addition across the two oxygen atoms of singlet and doublet $\text{ReO}_3(\text{CH}_3)$. However the subsequent rearrangement of the singlet and doublet metallaoxetane to the dioxylate has a higher activation barrier than the direct [3+2] addition across the two oxygen atoms of singlet and doublet $\text{ReO}_3(\text{CH}_3)$. The most plausible pathway to the formation of the epoxide precursor is by direct attack of ethylene on one of the oxo ligand of singlet $\text{ReO}_3(\text{CH}_3)$. Thus the formation of metallaoxetane by the [2+2] addition pathway is kinetically and thermodynamically favorable than the [2+2] addition pathway for ethylene addition to $\text{ReO}_3(\text{CH}_3)$ in agreement with the work of Deubel *et. al.*, (2003).
4. In the reaction of ethylene with (ReO_3Cp) , the direct [3+2] addition of the C=C bond of ethylene across O=Re=O bonds of ReO_3Cp to form the dioxylate has a lower activation barrier than the two-step reaction via, the [2+2] addition across the Re=O bond to form the metallaoxetane intermediate and subsequent rearrangement to the dioxylate. Thus in the reaction of ReO_3Cp with ethylene, the [3+2] addition pathway is more feasible kinetically and thermodynamically than the [2+2] addition pathway in agreement with the works of Deubel *et. al.*, 2003; Deubel and Frenking, (1999). The reaction of ReO_3Cp with ethylene does not result in the formation of an epoxide precursor, in agreement with the works of Burrell *et al.*, 1995; Herrmann *et .al.* 1984; Klahn-olive *et al*, 1984; Kühn *et. al.*, (1994).
5. In the oxidation of ethylene by $\text{ReO}_3(\text{OCH}_3)$, the two-step process via the [2+2] addition of the C=C bond of ethylene across the Re=O bond of doublet $\text{ReO}_3(\text{OCH}_3)$ to form the

metallaioxetane intermediate and subsequent re-arrangement has a lower activation barrier than the direct [3+2] addition of ethylene across the O=Re=O bond of singlet and doublet $\text{ReO}_3(\text{OCH}_3)$. The most plausible pathway to the formation of the epoxide precursor is by direct attack of the ethylene on one of the oxo ligand of doublet $\text{ReO}_3(\text{OCH}_3)$. The [2+2] addition of the C=C bond of ethylene across the Re=O bond of doublet $\text{ReO}_3(\text{OCH}_3)$ to form the metallaioxetane intermediate is kinetically and thermodynamically favorable than the [3+2] addition pathways leading to the dioxylate intermediate for ethylene addition to $\text{ReO}_3(\text{OCH}_3)$.

6. In the reaction between $\text{ReO}_3(\text{NPH}_3)$ and ethylene, the [2+2] addition of the C=C bond of ethylene across the Re=N bond of doublet $\text{ReO}_3(\text{NPH}_3)$ to form the four-membered metallacyclic intermediate has a lower activation barrier than the [3+2] addition of ethylene across the O=Re=O and N=Re=O bonds of $\text{ReO}_3(\text{NPH}_3)$. The most plausible pathway to the formation of the epoxide precursor is by direct attack of the ethylene on one of the oxo- ligand of $\text{ReO}_3(\text{NPH}_3)$. The formation of the epoxide precursor is not a particular feasible reaction. Thus in the oxidation of ethylene by $\text{ReO}_3(\text{NPH}_3)$, the [2+2] addition of ethylene across the Re=N bond of doublet $\text{ReO}_3(\text{NPH}_3)$ is kinetically and thermodynamically favorable than the formation of the metallaioxetane and dioxylate intermediate in disagreement with the works of Deubel *et. al.* 2003; Deubel and Frenking, (2003) who found the [2+2] addition pathway to form the metallaioxetane intermediate to have a higher activation barrier than the [3+2] addition pathway that leads to the formation of the dioxylate

7. In the reaction of ethylene with $LReO_3$, the [3+2] addition pathway is favored kinetically and thermodynamically when ($L= O^-$, Cp) while the [2+2] addition pathway is kinetically and thermodynamically favorable when ($L= CH_3, OCH_3, NPH_3$).

KNUST



REFERENCES

- Becke, D. (1993) Density-Functional Thermochemistry (III).The Role of Exact Exchange.*J. Chem. Phys.* 98: 5648 - 5652.
- Boehme, C.; Dapprich, S.; Deubel, D.; Pidun, U.; Stahl, M.; Stegmann, R.; Frenking, G. (1999) Reaction Mechanisms of Transition Metal Catalyzed Processes. *ACS symposium series.* 721:114–127.
- Burrell, A. K.; Cotton, F. A.; Daniels, L. M.; Petricek, V. (1995) *Inorg.Chem.* 34: 4253
- Clark, M.; Cramer, R. D.; Opdenbosch, N. V. (1989) Validation of the general purpose tripos5.2 force field.*J. Comp. Chem.* 10: 982-1012.
- Corey, E. J.; Noe, M. C. (1997) Kinetic Investigations Provide Additional Evidence That an Enzyme-like Binding Pocket Is Crucial for High Enantioselectivity in the Bis-Cinchona Alkaloid Catalyzed Asymmetric Dihydroxylation of Olefins. *J. Am. Chem. Soc.* 118: 319 - 329.
- Criegee, R. (1936) Osmiumsaeure-ester als Zwischenprodukte bei Oxydationen. *Justus Liebigs Ann. Chem.* 522:75-96.
- Criegee, R.; Marchand, B.; Wannowius, H. (1942) Zur Kenntnis der organischen Osmium-Verbindungen. II. Mitteilung. *Justus Liebigs. Ann. Chem.* 550:99-133
- Dapprich, S.; Ujaque, G.; Maseras, F.; Lledos, A.; Musaev, D.G.; Morokuma, K. (1996) Theory Does Not Support an Osmaoxetane Intermediate in the Osmium-Catalyzed Dihydroxylation of Olefins. *J. Am. Chem. Soc.* 118: 11660 - 11661.

Del Monte, A. J.; J. Haller, J.; Houk, K. N.; Sharpless, K. B.; Singleton, D. A.; Strassner, T.; Thomas, A. A. (1997) Experimental and Theoretical Kinetic Isotope Effects for Asymmetric Dihydroxylation. Evidence Supporting a Rate-Limiting “(3 + 2)” Cycloaddition. *J. Am. Chem. Soc.* 119: 9907 - 9908.

Deubel, D. V.; Schlecht, S.; Frenking, G. (2001) [2+2] versus [3+2] Addition of Metal Oxides across C=C Double Bonds: Toward an Understanding of the Surprising Chemo- and Periselectivity of Transition-Metal-Oxide Additions to Ketene. *J. Am. Chem. Soc.* 123: 10085 - 10094.

Deubel, D. V.; Frenking, G. (1999) Are There Metal Oxides That Prefer a [2 + 2] Addition over a [3 + 2] Addition to Olefins? Theoretical Study of the Reaction Mechanism of $LReO_3$ Addition ($L = O-, Cl, Cp$) to Ethylene. *J. Am. Chem. Soc.* 121: 2021.

Deubel, D. V.; Frenking, G. (2003) [3+2] versus [2+2] Addition of Metal Oxides across C=C Bonds. Reconciliation of Experiment and Theory. *Acc. Chem. Res.* 36: 645–651.

Deubel, D. V.; Muniz, K. (2004) Road maps for nitrogen-transfer catalysis: The challenge of the Osmium (VIII)-catalyzed diamination. *Chem. Eur. Journal.* 10: 2475-2486.

Dunning, T. H. Jr.; Hay, P. J. (1976) In: *Modern Theoretical Chemistry*, H. F. Schaefer, III, Vol.3; Plenum, New York.

Gisdakis, P.; Rösch, N. (2001) [2+3] Cycloaddition of Ethylene to Transition Metal Oxo Compounds. Analysis of Density Functional Results by Marcus Theory. *J. Am. Chem. Soc.* 123: 697 - 701.

Haller, J.; Strassner, T.; Houk, K. N. (1997) Experimental and Theoretical Kinetic Isotope Effects for Asymmetric Dihydroxylation. Evidence Supporting a Rate-Limiting “(3 + 2)” Cycloaddition. *J. Am. Chem. Soc.* 119: 8031.

Herrmann, W. A.; Serrano, R.; Bock, H. (1984) *Angew. Chem., Int. Ed. Engl.* 23: 383.

Houk, K. N.; Strassner, T. (1999) Establishing the (3 + 2) Mechanism for the Permanganate Oxidation of Alkenes by Theory and Kinetic Isotope Effects. *J. Org. Chem.* 64: 800 - 802.

Johnson, R. A.; Sharpless, K. B. (1993) In: *Catalytic Asymmetry Synthesis*, Ojima, J. Ed.; VCH: Weinheim, 227.

Klahn-Oliva, A. H.; Sutton, D. (1984) *Organometallics* 3:1313.

Kolb, H. C.; Van Nieuwenzhe, M. S.; Sharpless, K. B. (1994) Catalytic Asymmetric Dihydroxylation. *Chem. Rev.* 94: 2483 – 2547.

Kühn, F. E.; Herrmann, W. A.; Hahn, R.; Elison, M.; Blumel, J.; Herdtweck, E. (1994) *Organometallics*. 13: 1601.

M. Rouhi, M. (1997) Charting a path for macromolecules, *Chem. Eng. News*. 75: 23.

Nelson, D. W.; Gypser, A.; Ho, P. T.; Kolb, H. C.; Kondo, T.; Kwong, H.; McGrath, D. V.; Rubin, A. E.; Norrby, P.; Gable, K. P.; Sharpless, K. B. (1997) Toward an Understanding of the High Enantioselectivity in the Osmium-Catalyzed Asymmetric Dihydroxylation. Electronic Effects in Amine-Accelerated Osmylations. *J. Am. Chem. Soc.* 119: 1840.

Pidun, U.; Boehme, C.; Frenking, G. (1996) Theory Rules Out a [2 + 2] Addition of Osmium Tetraoxide to Olefins as Initial Step of the Dihydroxylation Reaction. *Angew. Chem. Int. Ed. Engl.* 35: 2817-2820.

Pietsch, M. A.; Russo, T. V.; Murphy, R. B.; Martin, R. L.; Rappe', A. K. (1998) LReO₃ Epoxidizes, cis-Dihydroxylates, and Cleaves Alkenes as Well as Alkenylates Aldehydes: Toward an Understanding of Why. *Organometallics*. 17: 2716.

Schröder, M. (1980) Osmium tetraoxide cis-hydroxylation of unsaturated substrates. *Chem. Rev.* 80: 187 - 213.

Sharpless, K. B.; Teranishi, A. Y.; Bäckvall, J. E. (1977) Chromyl chloride oxidations of olefins. Possible role of organometallic intermediates in the oxidations of olefins by oxo transition metal species. *J. Am. Chem. Soc.* 99: 3120.

Spartan, Waefunction, Inc.; 18401 Von Karman Ave., # 370, Irvine, CA, 92715, USA.

Tia, R.; Adei, E. (2009) Density functional theory study of the mechanism of oxidation of ethylene by chromyl chloride. *Inorg. Chem.* 48: 11434-11443.

Tia, R.; Adei, E. (2011) Computational studies of the mechanistic aspects of olefin metathesis reactions involving metal oxo-alkylidene complexes. *Computational and Theoretical Chemistry*. 971: 8 - 18.

Torrent, M.; Deng, L.; Duran, M.; Sola, M.; Ziegler, T. (1997) Density Functional Study of the [2+2] and [2+3] Cycloaddition Mechanisms for the Osmium-Catalyzed Dihydroxylation of Olefins. *Organometallics*. 16: 13-19.

Torrent, M.; Deng, L.; Duran, M.; Sola, M.; Ziegler, T. (1999) Mechanism for the formation of epoxide and chlorine-containing products in the oxidation of ethylene by chromyl chloride: a density functional study. *Can.J.Chem.* 77: 1476 - 1491.

Torrent, M.; Deng, L.; Ziegler, T. (1998) A Density Functional Study of [2+3] versus [2+2] Addition of Ethylene to Chromium–Oxygen Bonds in Chromyl Chloride. *Inorg. Chem.* 37: 1307.

Wadt, W. R.; Hay, P. J. (1985) Ab initio effective core potentials for molecular calculations. Potentials for main group elements Na to Bi. *J. Chem. Phys.* 82: 284.

Wadt, W. R.; Hay, P. J. (1985) Ab initio effective core potentials for molecular calculations. Potentials for K to Au including the outermost core orbitals. *J. Chem. Phys.* 82: 299.



CHAPTER FIVE

CONCLUDING REMARKS

In the study of the oxidation of ethylene by LMnO_3 ($\text{L} = \text{O}^-$, Cl , Cp , CH_3 , OCH_3 , NPH_3), it was found that the [3+2] addition pathway leading ultimately to the formation of the dioxylate intermediate (structure **2** in Scheme 2.1) is favored kinetically and thermodynamically when ($\text{L} = \text{Cp}$ and CH_3). Also, the suggested re-arrangement of the metallaoxetane intermediate to the dioxylate by Sharpless *et. al.*, (1977) for LMnO_3 reaction with ethylene ($\text{L} = \text{O}^-$, Cp , OCH_3 , CH_3 , NPH_3) has a higher activation barrier than the direct [3+2] addition across the two oxygen atoms to form the dioxylate intermediate. The activation barriers for the epoxide precursor formation are not competitive with the barriers for the formation of the dioxylate intermediate. The reaction of LMnO_3 ($\text{L} = \text{O}^-$, Cp) with ethylene would likely not result in the formation of epoxide precursor.

In the reaction of LTcO_3 ($\text{L} = \text{O}^-$, Cl , Cp , CH_3 , OCH_3 , NPH_3) with ethylene, it was found that the [3+2] addition pathway leading ultimately to the formation of the dioxylate intermediate on the doublet surface (structure **2** in Scheme 2.1) is favored kinetically and thermodynamically over the two-step process involving the formation metallaoxetane intermediate by the [2+2] addition pathway and the subsequent re-arrangement of the metallaoxetane intermediate to the dioxylate for LTcO_3 ($\text{L} = \text{O}^-$, Cl , Cp , OCH_3). The formation of the epoxide precursor is kinetically favorable for CH_3TcO_3 and the [3+2] addition pathway thermodynamically favorable when ($\text{L} = \text{CH}_3$) while the [2+2] addition pathway is kinetically and thermodynamically favorable when ($\text{L} = \text{NPH}_3$). The reaction of LTcO_3 ($\text{L} = \text{O}^-$, Cp) with ethylene would not result in the formation of an epoxide precursor. In conclusion, the [3+2] addition of ethylene across two oxygen atoms of

the complex $LTcO_3$ to form the dioxyate intermediate is not pervasive for all the oxo-complexes of technetium studied in this work. The exceptions are $LTcO_3(L=CH_3, NPH_3)$

In the oxidation of ethylene by $LReO_3$, it was found that the [3+2] addition pathway leading to the formation of the dioxyate intermediate on the doublet PES is favored kinetically and thermodynamically when $(L= Cp, O^-)$ while the [2+2] addition pathway to form the metallaioxetane intermediate is kinetically and thermodynamically favorable when $(L= Cl, CH_3, OCH_3, NPH_3)$. In the case of ethylene addition to $ReO_3(OCH_3)$, the [2+2] addition to form the metallaioxetane and the subsequent re-arrangement to the dioxyate are lower than the direct [3+2] addition leading to the dioxyate intermediate. The reaction of $LReO_3 (L= O^-, Cp)$ with ethylene would likely not result in the formation of an epoxide precursor. In conclusion, the [3+2] addition of ethylene across two oxygen atoms of the complex $LReO_3$ to form the dioxyate intermediate is not pervasive in all the oxo-complexes of rhenium studied in this work. The exceptions are $LReO_3(L= Cl, OCH_3, CH_3 \text{ and } NPH_3)$ where the [2+2] addition pathway to form the metallaioxetane intermediate is preferred.

In the reaction of $LMO_3 (M= Mn, Tc, Re, L= O^-, Cl^-, CH_3O^-, CH_3, Cp, NPH_3)$ with ethylene

- Dioxyate catalyst- $MnO_3(OCH_3) < TcO_3Cp < MnO_3Cp$
- Metallaioxetane catalyst - $ReO_3(CH_3)$
- Epoxidation agent - $TcO_3(CH_3) < ReO_3(OCH_3)$.
- Halohydrin agent - $MnO_3Cl < ReO_3Cl$

Future determination of the activation barriers for the formation of the triplet and quartet species would help to fill in the gap in the knowledge of the kinetics of formation of these species in the present study of the oxidation of ethylene by LMO_3 .

Also work with substituted alkenes could be initiated to explore the influence of steric hindrance on the energetics of the reaction. Future works into the exploration of spin crossover along the reaction coordinates from the reactants to the product to assess their viability should be carried out.

Also, the extent to which atomic properties such as charges and solvation influence the reaction barriers should be explored in future works.

